

**DAMAGE OF BURIED WATER PIPELINES DUE TO AN
EARTHQUAKE IN DHAKA CITY**

K.M.MOSTAFA HASAN



DEPARTMENT OF CIVIL ENGINEERING
BANGLADESH UNIVERSITY OF ENGINEERING AND TECHNOLOGY
DHAKA, BANGLADESH

JANUARY, 2009

**DAMAGE OF BURIED WATER PIPELINES DUE TO AN
EARTHQUAKE IN DHAKA CITY**

A Project

By

K.M.MOSTAFA HASAN

A project submitted to the Department of Civil Engineering,
Bangladesh University of Engineering and Technology, BUET, Dhaka
in partial fulfillment of the requirements for the degree

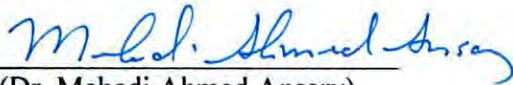
Of

MASTER IN CIVIL ENGINEERING (GEOTECHNICAL)

JANUARY, 2009

The project titled DAMAGE OF BURIED WATER PIPELINES DUE TO AN EARTHQUAKE IN DHAKA CITY, Submitted by K.M. Mostafa Hasan, Roll No.: 040304217 P, Session: April 2003 has been accepted as satisfactory in partial fulfillment of the requirements for the degree of Master in Civil Engineering on January 2009.

BOARD OF EXAMINERS

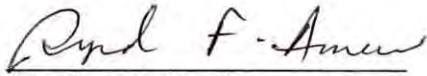


(Dr. Mehedi Ahmed Ansary)

Professor

Department of Civil Engineering
BUET, Dhaka 1000

Chairman
(Supervisor)

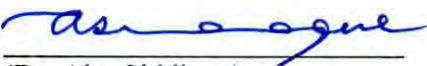


(Dr. Syed Fakhrul Ameen)

Professor

Department of Civil Engineering
BUET, Dhaka 1000

Member



(Dr. Abu Siddique)

Professor

Department of Civil Engineering
BUET, Dhaka 1000

Member

CANDIDATE'S DECLARATION

It is hereby declared that this thesis or any part of it has not been submitted elsewhere for the award of any degree or, diploma.

Signature of the candidate

A handwritten signature in black ink, consisting of several loops and a long horizontal stroke extending to the right.

K.M. Mostafa Hasan

CONTENTS

	PAGE NO
CONTENTS	I
LIST OF TABLES	IV
LIST OF FIGURES	VII
ACKNOWLEDGEMENT	X
ABSTRACT	XI
 CHAPTER ONE INTRODUCTION	
1.1 Background	1
1.2 Objectives of Study	3
1.3 Thesis Outline	4
 CHAPTER TWO LITERATURE REVIEW	
2.0 General	5
2.1 Earthquake Effects	5
2.2 Faulting	7
2.3 Ground Shaking	9
2.3.1 Effects of Surface Topography	12
2.3.2 Effects of Soft Surface Layers	13
2.4 Strong-motion Parameters	14
2.4.1 Macroseismic Intensity	14
2.4.2 Instrumental Parameters	16
2.4.2.1 Amplitude Parameters	16
2.4.2.1 Duration Parameters	17
2.4.2.2 Frequency-content Parameters	17
2.5 Collateral Effects	17
2.5.1 Liquefaction	17

PAGE NO

2.5.2	Densification	19
2.6	Pipeline Response to Ground Shaking	20
2.6.1	Influence of Site Effects on the Seismic Response of Buried Pipelines	20
2.6.2	Factors Affecting Earthquake Vulnerability of Pipelines	22
2.6.2.1	Fragility Relations for Buried Pipes Subject to Ground Shaking	27
2.6.2.2	Katayama <i>et al.</i> (1975)	27
2.6.2.3	Eguchi (1991)	31
2.6.2.4	O'Rourke & Ayala (1993)	32
2.6.2.5	Hwang & Lin (1997)	33
2.6.2.6	O'Rourke <i>et al.</i> (1998)	35
2.6.2.7	Isoyama <i>et al.</i> (2000)	37
2.6.2.8	ALA (2001)	39
2.6.2.9	Findings	41
2.6.2.10	Lessons Learned	42
2.7	Summary	46

CHAPTER THREE SEISMIC MICROZONATION OF DHAKA CITY

3.0	General	47
3.1	Geographical Setting of Dhaka City	47
3.2	Geology of the Study Area	48
3.3	Regional Techtonics	50
3.4	Seismic Zoning Map of Bangladesh	52
3.5	Microtremor Investigation of Site Effects	56
3.6	Geotechnical Characteristics of Dhaka City	60
3.7	Seismic Microzonation Map of Dhaka City	62
3.8	Summary	65

CHAPTER FOUR BURIED WATER PIPELINE DAMAGE ANALYSIS

4.0	General	76
4.1	Pipeline Database Development	77
4.2	Selection of Peak Ground Acceleration (PGA) Values form Intensity	81
4.3	Selection of Damage Analysis Methods	84
4.4	Water pipeline Damage Analysis	86
4.5	Financial Loss Estimation	89
4.6	Summary	91

CHAPTER FIVE CONCLUSIONS AND RECOMMENDATIONS

5.1	Conclusions	92
5.2	Recommendations	94

REFERENCES	95
-------------------	----

APPENDICES

Appendix-A	Modified Marcelli Scale of Felt Intensity	99
Appendix-B	Water pipeline networks of Dhaka city (DWASA, 1993)	102
Appendix-C	Water pipeline networks of Dhaka city (DWASA, 1991)	103

LIST OF TABLES**PAGE NO**

Table 1.1	Break down of damage to the water supply system in Kobe City (after Matsushita et al., 1998)	2
Table 2.1	Damage to water pipelines in the 1999 Ji-Ji (Taiwan) earthquake (Shih et al., 2000; Miyajima and Hashimoto, 2001)	6
Table 2.2	Regression coefficients for different categories of fault slip type for use in equation (2.1) (Wells and Coppersmith, 1994)	9
Table 2.3	Some commonly-used pipeline-related abbreviations, together with typical yield stress and yield strain values for common pipe barrel materials (from O'Rourke and Liu, 1999).	22
Table 2.4	Relative earthquake vulnerability of water pipes (Ballantyne, 1995). Joint types: B&S - bell & spigot; RG - rubber gasket; R - restrained; UR - unrestrained.	24
Table 2.5a	Summary of pipeline fragility studies for ground shaking effects according to earthquake data used.	28
Table 2.5b	Strong-motion parameters considered by each study. Studies highlighted in grey present fragility curves; other studies show the range of data observed but do not define fragility curves (as Table 2.5a).	29
Table 2.5c	Summary of earthquakes used in studies given in Table 2.5a	29
Table 2.6	Correction factors for application to the fragility relations of Isoyama <i>et al.</i> (2000). Values in brackets are less reliable due to small sample size.	39
Table 2.7	Summary of data sources used to develop the ALA (2001) database of pipeline damage caused by ground shaking.	39
Table 2.8	Pipe material and pipe diameter categories included in the dataset for the ALA (2001) fragility relation (percentages subjected to rounding errors).	40

	PAGE NO	
Table 2.9	Pipeline fragility relations for PGA derived by several investigations. R_R denotes repair rate. PGA is measured in cm/s^2 .	43
Table 2.10	Pipeline fragility relations for PGV derived by several investigation. R_R denotes repair rate. PGV is measured in cm/s	44
Table 3.1	Great historical earthquakes in and around Bangladesh	51
Table 3.2	Magnitude, EMS Intensities and distances of some major historical earthquakes around Dhaka (after Ansary, 2001 & 3CD City Profiles Series)	52
Table 3.3	Quantification rules for seismic hazard (after Stephanie and Kiremidjian, 1994)	63
Table 4.1	Pipeline lengths according to intensity	81
Table 4.2	Correlation between peak ground acceleration (PGA) and modified Mercalli intensity (MMI)	82
Table 4.3	PGA values based on different existing empirical relationships for different intensity	83
Table 4.4	Pipeline repair rate from different fragility relations for PGA values based on Trifunac and Brady and Gutenberg and Richter relations	84
Table 4.5	Intensity and number of repairs based on O'Rourke and Trifunac and Brady relation	87
Table 4.6	Intensity and number of repairs based on O'Rourke and Gutenberg and Richter relation	87
Table 4.7	Intensity and number of repairs based on Isoyama and Trifunac and Brady relation	87
Table 4.8	Intensity and number of repairs based on Isoyama and Gutenberg and Richter relation	88
Table 4.9	Pipeline repair rate for different intensity and fragility relation	88

		PAGE NO
Table 4.10	Repair rate calculated for loss estimation	89
Table 4.11	Repair cost for intensity VIII	90
Table 4.12	Repair cost for intensity IX	90
Table 4.13	Repair cost for intensity X	90

LIST OF FIGURES**PAGE NO**

Figure 2.1	Surface expression of different types of faulting (Taylor & Cluff, 1977). FW – foot wall; HW – hanging wall.	8
Figure 2.2	Deformations produced by body waves: (a) p-wave; (b) SV-wave (Bolt, 1993)	10
Figure 2.3	Deformations produced by surface waves: (a) R-wave; (b) L-wave (Bolt, 1993).	11
Figure 2.4	Comparison between various intensity scales. MMI – Modified Mercalli; RI – Rossi-Forel; JMA – Japanese Meteorological Agency; MSK – Medvedev-Spoonheuer-Karnik (Kramer, 1996)	15
Figure 2.5	Lateral spreading caused by liquefaction of subsurface layer (a) before and (b) after an earthquake (Kramer, 1996)	18
Figure 2.6	Field measurements of PGV and peak ground strain at sites in Japan with different ground conditions (Nakajima <i>et al.</i> , 1998)	21
Figure 2.7	Pipeline failure rate for various pipe types from the study by Shirozu <i>et al.</i> (1996). Pipe lengths are given for each category (km)	25
Figure 2.8	Cross-sections of anti-seismic pipe joints (Nakajima <i>et al.</i> , 1998)	26
Figure 2.9	Pipeline fragility data of Katayama <i>et al.</i> (1975) as presented by O'Rourke & Liu (1999). This graph presents the data in a more comprehensive manner than the graph included in the original study and includes trends suggested by Bresko (1980)	30
Figure 2.10	Bilinear pipeline fragility relations of Eguchi (1991). See Table 2.3 for abbreviations. Note that repair rate is given per 1000 ft	31
Figure 2.11	Fragility relations of Barenberg (1988) (derived from data points A – D), and O'Rourke & Ayala (1993) (derived from data points A-K).	32
Figure 2.12	A comparison between the fragility curve of Hwang & Lin (1997) with other fragility curves for PGA (1993)	34
Figure 2.13	Damage rate ratio for different pipe diameters (Hwang & Lin, 1997)	35
Figure 2.14	Pipeline repair rate contours for CI pipe vs. PGV for the Northridge earthquake (O'Rourke & Toprak, 1997)	36

Figure 2.15	Pipeline repair rate correlation with PGV for steel, CI, DI and AC distribution lines: (a) CI distribution lines; and (b) steel, CI, DI and AC distribution lines (O'Rourke <i>et al.</i> , 2001)	37
Figure 2.16	Data set used by ALA (2001) to derive pipeline vulnerability function for PGV. Median repair rate (RR) line defines standard "backbone" curve. Lines defining the 16 th and 84 th percentiles are included to illustrate the scatter.	41
Figure 2.17	Comparison of the pipeline fragility relations for PGA expressed in Table 2.9.	43
Figure 2.18	Comparison of the pipeline fragility relations for PGV expressed in Table 2.10.	44
Figure 3.1	Geological map of Dhaka metropolitan area (after GSB, 1991)	49
Figure 3.2	Seismo-tectonic lineaments capable of producing damaging earthquakes (after Banglapedia, 2004)	50
Figure 3.3	Seismic zoning map of Bangladesh (after BNBC, 1993)	54
Figure 3.4	Seismic zoning map of Bangladesh (after Sharfuddin, 2001)	55
Figure 3.5	Map of 1.8 and 2.5 times amplified areas	57
Figure 3.6	Map showing liquefied areas and non-liquefied areas	59
Figure 3.7	Map of Dhaka City Showing Borehole Locations (GRIDS ARE EXPRESSED IN KILOMETER, after Bashar, 2004)	66
Figure 3.8	Soil Profile through grid A-A' (after Bashar, 2004)	67
Figure 3.9	Soil Profile through grid B-B' (after Bashar, 2004)	68
Figure 3.10	Soil Profile through grid C-C' (after Bashar, 2004)	69
Figure 3.11	Soil Profile through grid D-D' (after Bashar, 2004)	70
Figure 3.12	Soil Profile through grid 1-1' (after Bashar, 2004)	71
Figure 3.13	Soil Profile through grid 2-2' (after Bashar, 2004)	72
Figure 3.14	Soil Profile through grid 3-3' (after Bashar, 2004)	73
Figure 3.15	Soil Profile through grid 4-4' (after Bashar, 2004)	74
Figure 3.16	Soil Profile through grid 5-5' (after Bashar, 2004)	75

	PAGE NO
Figure 3.17 Combined hazard intensity	64
Figure 4.1 Full digitized map of whole pipeline networks of DWASA (1993)	78
Figure 4.2 Lay-out of 100mm, 200mm, 300mm and 450mm diameter pipe on Microzonation map of intensity 8	79
Figure 4.3 Lay-out of 100mm, 200mm, 300mm and 450mm diameter pipe on Microzonation map of intensity 9	80
Figure 4.4 Lay-out of 100mm, 200mm, 300mm and 450mm diameter pipe on Microzonation map of intensity 10	80
Figure 4.5 Comparison of PGA values derived from different modified Mercalli intensity (PGA-MMI) empirical relationships	83
Figure 4.6 Comparison of the pipeline repair rate for different PGA values obtained from Trifunac and Brady PGA-MMI relation	85
Figure 4.7 Comparison of the pipeline repair rate for different intensity and fragility relation	88

ACKNOWLEDGEMENTS

All praises to Allah, the merciful and the kind.

The author expresses his heartiest gratitude to his supervisor, Dr. Mehedi Ahmed Ansary, Professor of Civil Engineering Department, BUET for his guidance, invaluable suggestions and affectionate and continuing encouragement at different stages of the study.

The author is also extends his gratefulness to Dr. Syed Fakhru Ameen, Professor, Department of Civil Engineering, BUET and to Dr. Abu Siddique, Professor, Department of Civil Engineering, BUET for their constructive suggestions.

ABSTRACT

Earthquakes can cause extensive damage to buried water supply pipelines which is one of six categories of infrastructure grouped under the heading 'lifelines', resulting in disruption of essential services for the whole community. This thesis focuses on the damage analysis of buried water supply pipelines of Dhaka city subject to earthquake effects.

The water pipeline network is essential for daily life. It provides household using as well as industry and firefighting using. Damage prediction of water supply pipelines due to earthquake involves seismic microzonation of Dhaka city and determination of the length of water supply pipeline. In this process already developed seismic microzonation map of Dhaka city is used and the available map of water supply pipeline network of Dhaka WASA is digitized to get the length of pipelines with the help of GIS software.

On the basis of intensity the whole Dhaka city has been divided into three different zones. Out of total area of 135 sq.km 88 sq.km is (65%) of intensity VIII, 39 sq.km is (29%) of intensity IX and remaining 9 sq.km is (6%) of intensity X.

From the digitized pipeline network, based on 1993 DWASA data, the length of 100mm, 200mm, 300mm and 450mm diameter pipe is found to be 916 km, 259 km, 170 km and 53 km respectively. But these lengths according to DWASA 2008 data are 1693 km, 419 km, 190 km and 54 km for 100mm, 200mm, 300mm and 450mm diameter pipe respectively. Again from the intensity based pipeline network it is found that 1043 km pipe falls in the zone of intensity VIII, 274 km falls in the zone of intensity IX and 81 km falls in the zone of intensity X irrespective of pipe diameter.

A selection step is followed to estimate peak ground acceleration (PGA) to determine the pipeline damage rate. Existing empirical relations such as Katayama (1975), O'Rourke (1982), Isoyama and Katayama (1998) and Isoyama (2000) for the prediction of earthquake-induced pipeline damage are reviewed. Finally using above four relations and selected peak ground acceleration damage rate of pipelines is determined and an estimation of financial loss is presented.

Pipeline damage rate is expressed in number of repairs per unit length of pipe. Total number of repairs for all intensities are 587 within a total pipe length of 2356 km. Out of which 421 number of repairs required for 1693 km pipelines of 100mm diameter, 109 number of repairs required for 419 km pipelines of 200mm diameter, 42 number of repairs for 190 km pipeline of 300mm diameter and 15 number of repairs for 54 km pipeline of 450mm diameter.

CHAPTER ONE

INTRODUCTION



1.1 BACKGROUND

Lifelines are those systems that relate to daily life needs. Water distribution systems are one of six broad categories of infrastructure grouped under the heading 'lifelines' (O'Rourke, 1998). Together with electric power, gas and liquid fuels, telecommunications, transportation and wastewater facilities, they provide the basic services and resources upon which modern communities have come to rely, particularly in the urban context. Disruption of these lifelines through earthquake damage can therefore have a devastating impact, threatening life in the short term and a region's economic and social stability in the long term.

Like other fields of earthquake engineering lifeline earthquake engineering is not so old. Its formal recognition came in the 1970's with the establishment in the United States of ASCE's Technical Council on Lifeline Earthquake Engineering (Duke & Matthiesen, 1973). In 1975, Council Members, C.M. Duke and D.F. Moran commented that the state-of-the-art for lifeline earthquake engineering was 10 to 20 years behind that of buildings (Duke & Moran, 1975). A concerted research effort since then has made up much of the lost ground, but many challenges remain.

The whole post-earthquake operation may be jeopardized due to damage of city's water distribution system. Lack of clean piped mains supply for basic drinking and sanitation needs in the immediate aftermath of an earthquake constitutes a fresh threat to the lives of those who have survived the initial devastation.

The concern is that many pipelines get broken causing water loss from storage reservoirs eventually results in shortage of water for fire suppression. Fire losses, in particular, can be greater than the losses directly due to the earthquake. The fire that followed the 1906 San Francisco earthquake is perhaps the most striking example. Reduced fire-fighting capabilities as a result of rupture of the city's three principal water transmission pipelines and breaks in

the trunk line system contributed to the destruction by fire of almost 500 blocks of the city, resulting in the worst fire loss in US history (O'Rourke et al., 1992).

Table 1.1 gives an overview of water supply system damage in Kobe City following the 1995 Hyogoken-Nanbu earthquake in Japan. The total cost of damage caused by this earthquake approached US\$100bn and a significant proportion of this (5%) was lifelines-related. Of the damage caused to lifelines in Kobe and its surrounding area, around one tenth was damage to water distribution facilities (Katayama, 1996). The cost of damage to distribution mains alone accounted for almost half of the total system damage.

Table 1.1 Break down of damage to the water supply system in Kobe City (after Matsushita et al., 1998)

Facility	Total system composition	Damage level	Repair cost (US\$m)
Dams	3	1	70
Purification plants	7	2	
Trunk mains	43 km	2 lines	
Principal feeder mains	260 km	6 lines	
Distribution reservoirs	119	1	19
Distribution mains	4002 km	1757 failures	135
Service connections	650 000 lines	89 584 failures	25
Miscellaneous	Various components	Several buildings including Waterworks Bureau Head Office	41
Total			290

The primary earthquake hazards of concern for water pipes are transient and permanent ground movements. Transient ground deformation is caused by the passage of seismic waves (ground shaking). Permanent ground deformation is caused by surface faulting or secondary effects which give rise to localized ground failure (liquefaction, landslides and densification of surface soil layers).

The impact of different effects on buried pipelines is relative as it varies from earthquake to earthquake. Transient effects are common to all earthquakes and are felt over a wide geographical area and associated pipeline damage tends to be spread over the whole of a water supply system. Resulting damage rates (in terms of breaks per unit length of pipe) are relatively low but the total number of pipe breaks can be high. Surface faulting or secondary

earthquake effects can give rise to very high ground strains. Where these phenomena coincide with buried pipelines, relatively high pipeline damage rates are observed but in localized areas. In the current study, key factors affecting transient ground motion and pipeline vulnerability due to earthquake have been reviewed.

1.2 OBJECTIVE OF THE STUDY

It has been proved that the greater risk for the lifeline systems is the earthquake disaster. According to the statistical report from a lot of earthquake surveys, the damage or malfunctions of lifeline systems is the key factor for huge economic loss during earthquake invading. The major objectives of study are as follows:

1. to develop a database of buried water supply pipelines of Dhaka WASA based on GIS.
2. to assess the vulnerability of the buried water supply pipelines for the earthquakes.

1.3 THESIS OUTLINE

In **Chapter Two** different earthquake effects, seismic response of buried pipelines, factors affecting earthquake vulnerability of pipelines are studied. Different existing empirical fragility relations for buried pipelines are also reviewed in this chapter.

Chapter Three reviews background information of the seismic environment prevailing in Bangladesh as a part of the evaluation of seismic hazard. Important tectonic features of Bangladesh, seismic zoning map, geotechnical characteristics and seismic microzonation map of Dhaka city are described.

Chapter Four deals with the development of pipeline damage database with the GIS software, selection of peak ground acceleration (PGA) values from intensity. Estimation of damage based on existing methods was done and presented in this chapter. Monetary loss estimation is also presented in this chapter.

In **Chapter Five** conclusions from this study and recommendations for further areas of study are made.

CHAPTER TWO

LITERATURE REVIEW

2.0 GENERAL

Earthquake is the trembling or shaking movement of the earth's surface. Most earthquakes are minor tremors, while larger earthquakes usually begin with slight tremors, rapidly take the form of one or more violent shocks, and end in vibrations of gradually diminishing force called aftershocks. Earthquake is a form of energy of wave motion, which originates in a limited region and then spreads out in all directions from the source of disturbance. It usually lasts for a few seconds to a minute. The point within the earth where earthquake waves originate is called the focus, from where the vibrations spread in all directions. They reach the surface first at the point immediately above the focus and this point is called the epicentre. It is at the epicentre where the shock of the earthquake is first experienced. On the basis of the depth of focus, an earthquake may be termed as shallow focus (0-70 km), intermediate focus (70-300 km), and deep focus (>300 km). The most common measure of earthquake size is the Richter's magnitude. The Richter scale uses the maximum surface wave amplitude in the seismogram and the difference in the arrival times of primary and secondary waves for determining magnitude. The magnitude is related to roughly logarithm of energy. Earthquakes originate due to various reasons, which fall into two major categories viz non-tectonic and tectonic. The origin of tectonic earthquakes is explained with the help of 'elastic rebound theory'. Earthquakes are distributed unevenly on the globe. However, it has been observed that most of the destructive earthquakes originate within two well-defined zones or belts namely, 'the circum-Pacific belt' and 'the Mediterranean-Himalayan seismic belt' (Banglapedia, 2004).

2.1 EARTHQUAKE EFFECTS

The direct effects of earthquakes are surface faulting and ground shaking. Secondary or "collateral" effects include liquefaction, landslides, densification and tsunami.

Earthquake effects on buried pipelines are best understood by considering the displacements induced in the surrounding soil. Damage may be caused by transient ground deformation (GDt), or permanent ground deformation (GDp), or a combination of the two. O'Rourke (1998) defines the distinction between these two effects, "*GDp involves the irrecoverable movement of the ground that often is the result of ground failure, but also may result from modest levels of volumetric strain and shear distortion. GDt involves ground waves and soil strains associated with strong shaking. Although ground cracks and fissures may result from GDt, the magnitude of this residual deformation will normally be less than the maximum GDt during strong shaking.*" All of the collateral earthquake effects, plus faulting, can give rise to permanent ground deformation.

The relative impact of different effects on buried pipelines varies from earthquake to earthquake. Transient effects are common to all earthquakes and are felt over a wide geographical area and associated pipeline damage tends to be spread over the whole of a water supply system. Resulting damage rates (in terms of breaks per unit length of pipe) are relatively low but the total number of pipe breaks can be high. Surface fault rupture and collateral earthquake effects can give rise to very high ground strains.

Water pipeline damage data from the 1999 Ji-Ji (Taiwan) earthquake reveals the relative impact of different earthquake effects (Table 2.1). In this case, ground shaking was directly responsible for almost half of the total damage. The proportion of fault-induced damage was also high, due to the extensive faulting and large fault displacements that characterized this earthquake. Liquefaction induced damage was relatively insignificant. However, because the earthquake-affected area was mountainous, landslide-induced damage was significant.

Table 2.1 Damage to water pipelines in the 1999 Ji-Ji (Taiwan) earthquake (Shih et al., 2000; Miyajima and Hashimoto, 2001)

Cause of damage to water pipelines	% of total damage
Ground shaking	48
Faulting	35
Landslides	11
Liquefaction	2
Other (unspecified)	4

The relative impact of the various earthquake effects on buried pipelines depends on the geological conditions in which surface faulting and collateral effects occur and the coincidence of these regions with the buried infrastructure. Even in the absence of surface faulting, landslides, liquefaction or ground settlement, pipeline damage can be severe, as observed in the 1985 Michoacan (Mexico) earthquake (Ayala and O'Rourke, 1989).

2.2 FAULTING

Most earthquakes occur as a result of the build up of stresses at tectonic plate boundaries. When these stresses exceed the rock's ability to resist them, rupture occurs along a fault, releasing the stored strain energy in the form of seismic waves and heat. The fault rupture usually coincides with pre-existing discontinuity in the Earth's crust. The extent of faulting is linked closely with earthquake magnitude. Large earthquakes can produce faults of several hundred kilometres length with widths of tens of kilometres and offsets of several metres.

In most earthquakes, the fault rupture plane does not have a surface expression (*blind faulting*) (Reiter, 1990). A surface fault trace is usually only observed for large earthquakes occurring at shallow depth. The extent of surface faulting depends chiefly on the length and amount of offset of the subsurface faulting, the attitude of the fault plane, the direction of the fault movement and the type and thickness of the surficial geology (Taylor and Cluff, 1977). Faults can be classified according to the movement of the two sides of the fault relative to each other (Figure 2.1). Faulting is termed *strike-slip* when the movement is predominantly horizontal. It is known as *dip-slip* when the movement is predominantly in the direction of dip of the fault plane. Dip-slip movement where the horizontal component is compressional is called *reverse faulting*. Where the horizontal component is extensional, the faulting is termed *normal*. A combination of dip-slip and strike-slip movement is referred to as *oblique faulting*.

Not all fault-like features observed at the surface are related to tectonic rupture. Fractures may be formed by ground shaking, landslides. As illustrated in Figure 2.1, fault-induced ground-strain is most severe at the intersection between the fault plane and the ground surface. However, the crustal deformation that accompanies earthquake faulting can be significant at considerable distances from the surface rupture.

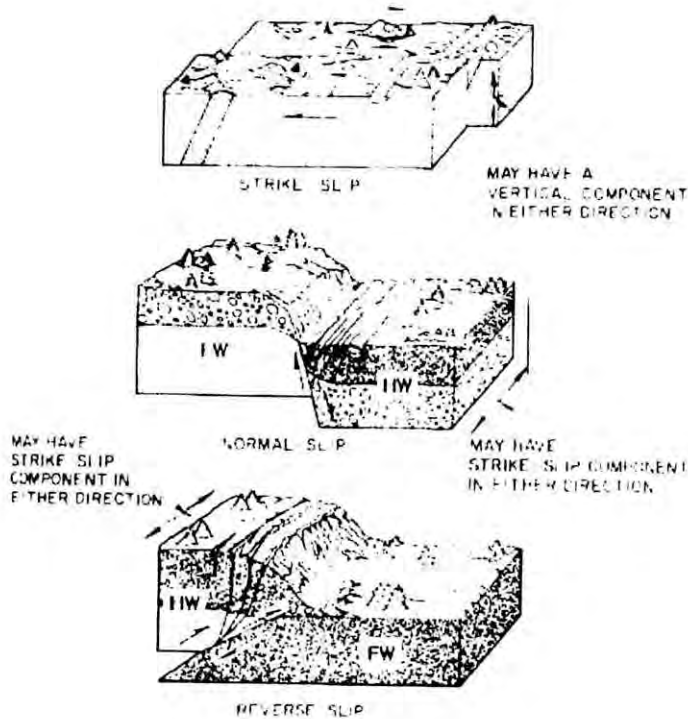


**Figure 2.1 Surface expression of different types of faulting (Taylor & Cluff, 1977).
 FW – foot wall; HW – hanging wall.**

The large permanent ground deformations associated with faulting can present a very severe hazard to structures on or near to active faults. Where potentially active faults can be identified, “nobuild” zones can be designated, to avoid unnecessary damage in the event of an earthquake. In the case of water pipelines, crossing active faults is often unavoidable, since pipeline location is dictated by the locations of supply and demand areas. It is therefore useful to be able to estimate the amount of permanent ground displacement that might occur in the event of an earthquake of a given magnitude on a particular fault.

Numerous studies have been carried out to investigate the connection between earthquake magnitude and various characteristics of the fault rupture. Wells and Coppersmith (1994) compiled a worldwide database of 244 earthquakes covering the moment magnitude range $5.6 \leq M_w \leq 8.1$. Observed fault displacements ranged from 0.05 - 8.0 m for strike-slip faults, 0.08 - 2.1 m for normal faults and 0.06 - 1.5 m for reverse faults. From this database, empirical relationships were derived among magnitude, rupture length, rupture width, rupture area and surface displacement. These expressions can be used to predict likely fault rupture characteristics given a specific magnitude of event. Of most interest for the prediction of

pipeline damage are expressions for expected surface fault displacement as a function of magnitude:

$$\text{Log } D = C_1 + C_2 M_w \quad 2.1$$

Where: D is the average surface fault displacement (m),
 M_w is the moment magnitude,
 C_1 and C_2 are coefficients derived from the regression, Values for different categories of fault slip type are presented in Table 2.2.

Table 2.2 Regression coefficients for different categories of fault slip type for use in Equation (2.1) (Wells and Coppersmith, 1994)

Fault slip type	C_1	C_2	Standard deviation	Correlation coefficient	Magnitude range
Strike-slip	-6.32	0.90	0.28	0.89	5.6 – 8.1
Reverse	-0.74	0.08	0.38	1.10	5.8 – 7.4
Normal	-4.45	0.63	0.33	0.64	6.0 – 7.3
All	-4.80	0.69	0.36	0.75	5.6 – 8.1

Even for earthquakes without a surface fault expression, coseismic strains induced in the epicentral region may still be large enough to cause damage to buried pipelines. The response of a buried pipe to surface faulting depends to a large extent on its orientation with respect to the fault. Bending, buckling due to axial compression or pull-out due to axial extension are all possible responses.

2.3 GROUND SHAKING

Ground shaking is caused by two different kinds of seismic waves: *body waves* and *surface waves*. Body waves are generated by earthquake faulting and are responsible for the radiation of seismic energy from the rupture zone at depth to the surface of the Earth. Body wave disturbances are of two types: *P-waves* (primary waves) and *S-waves* (secondary) (Figure 2.2). P-waves (compression waves) are characterized by disturbance parallel to the direction of wave propagation whereas waves (shear waves) cause a disturbance perpendicular to the direction of travel. The direction of particle movement can be used to divide S-waves into two components: SV (vertical) and SH (horizontal).

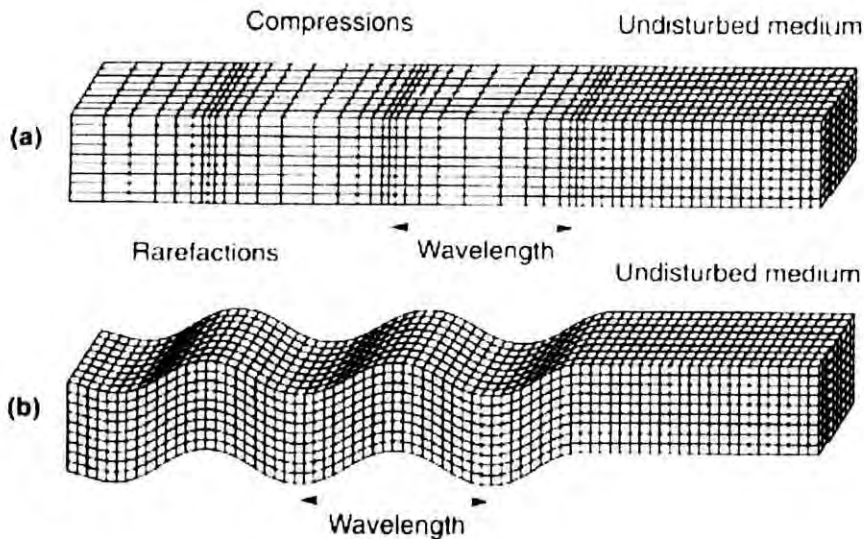


Figure 2.2 Deformations produced by body waves: (a) p-wave; (b) SV-wave (Bolt, 1993)

The interaction of body waves with the surface of the Earth causes surface waves, the most important of which, for engineering purposes, are *R-waves* (Rayleigh waves) and *L-waves* (Love waves) (Figure 2.3). For R-waves, the particle motion traces an ellipse in a vertical plane, the size of the ellipse decreasing with depth below the ground surface. R-waves also have a horizontal component, which is parallel to the direction of propagation. For L-waves, the particle motion is in the horizontal plane, perpendicular to the direction of propagation, with the amplitude decreasing with depth below the ground.

Both types of waves are of interest when considering the response of buried pipelines to seismic ground shaking. For body waves, only S-waves are normally considered as they carry more energy than P-waves. In the case of surface waves, it is R-waves which are most important, inducing axial strains in buried pipelines of much more significance than the bending strains induced by L-waves (O'Rourke & Liu, 1999). Seismic wave propagation theory indicates significant differences between the transient ground motions associated with body waves and those associated with surface waves.

In order to predict earthquake damage to pipeline systems or design a new pipeline for earthquake resistance, it is therefore important to define the predominant effects at the site or region of interest.

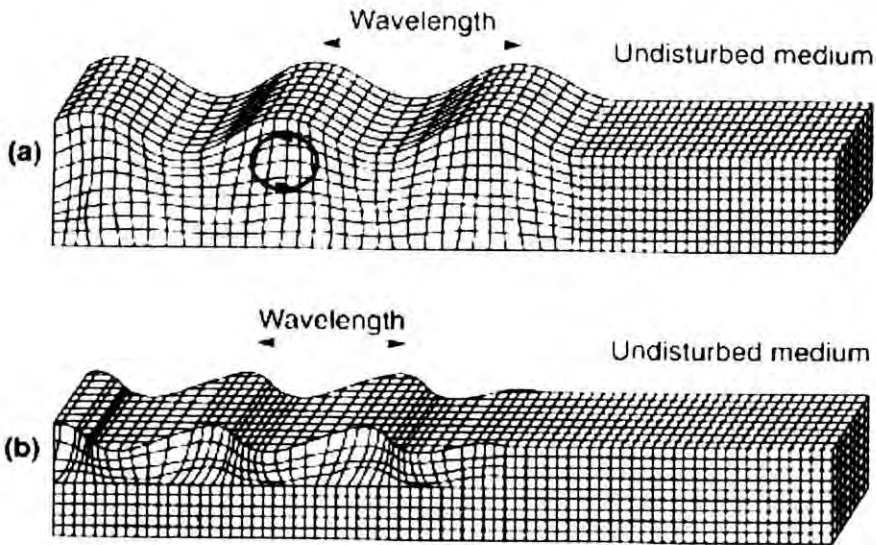


Figure 2.3 Deformations produced by surface waves: (a) R-wave; (b) L-wave (Bolt, 1993)

The ground shaking felt at a given location will be made up of a combination of body waves and surface waves. In the immediate locality of the fault rupture, body waves will dominate the motion. The amplitude of ground motion reduces with distance from the source of seismic energy release. This is due to a combination of geometric attenuation, which accounts for the spread of the wave front as it moves away from the source, and anelastic attenuation, which is caused by material damping. Geometric attenuation is different for body waves than for surface waves. Assuming that the earthquake rupture zone can be represented as a point source and R is the distance from the rupture zone, the amplitude of body waves decreases in proportion to $1/R$, while the amplitude of surface waves decreases in proportion to $1/\sqrt{R}$. This explains why ground motion at large epicentral distances is generally dominated by surface waves.

The response of buried pipelines to seismic waves differs substantially from that of most aboveground structures. For a building, the ratio of its weight (inertia) to the restoring forces (stiffness) in the structural elements is high, causing significant relative motion between the building and the ground on which it stands. A fluid-filled pipeline typically has less weight than the soil it replaces. Inertial forces are therefore low with respect to the stiffness of the surrounding soil. The response of the pipeline to ground shaking depends on the level of strain induced in the ground, the stiffness of the soil, the stiffness of the pipeline and the frictional resistance at the pipeline-soil interface.

O'Rourke (1998) identifies four distinct categories of transient ground shaking effects of relevance to pipelines and other lifelines:

a) *Travelling ground waves.*

b) *Surface-wave generation in large sedimentary basins* (typically several kilometres wide with depths less than 1 km). Significant long-period motions are caused by surface waves generated by the trapping and focussing of obliquely incident S-waves in large sedimentary basins.

c) *Vibration of sediments in relatively narrow valleys* (several hundreds of metres wide by several tens of metres deep). For smaller basins, mass shear deformation in the valley sediments is more important than wave scattering effects. In such cases, large strains are induced near valley margins.

d) *Liquefaction-induced ground oscillation* The last three phenomena are examples of long-period ground motion. It is only large earthquakes, with extended fault ruptures that give sufficiently strong excitation in the long-period range to be of engineering interest.

2.3.1 EFFECTS OF SURFACE TOPOGRAPHY

Destructive earthquakes have often caused higher concentrations of building damage on the tops of hills than at their bases. Instrumental and theoretical evidence supports the hypothesis that surface topography can significantly modify the amplitude and frequency content of ground motion. However, few systematic investigations have been conducted into this phenomenon and there is, as yet, no general consensus.

Geli *et al.* (1988) made a compilation of eleven individual studies of topographic effects, including both instrumental and theoretical results. Their conclusions are summarised below:

a) The amplification of ground motions on a hilltop and its de-amplification at the foot of a hill is supported, at least qualitatively, by observations and theory. In general, amplification is more pronounced for the horizontal components of ground motion than for the vertical component.

b) Amplification on a hilltop is roughly related to the sharpness of the topography. The steeper the terrain, the greater the amplification at the peak.

c) The frequencies most significantly modified by surface topography are those which correspond to wavelengths comparable to the horizontal dimension of the topographic feature.

In view of the current lack of understanding of topographic modification of earthquake ground motion, Bard & Riepl-Thomas (2000) suggest the need for more detailed studies of this phenomenon involving dense arrays of strong-motion instruments and detailed geotechnical characterization of the study area.

2.3.2 Effects of Soft Surface Layers

It is well recognized that earthquake-induced ground motions are strongly influenced by the nature of near-surface geological materials. Earthquake damage to structures situated on soft soil is consistently greater than damage to structures on firm soil or bedrock outcrops.

The amplification of ground motion in soft soils is caused by the trapping of seismic waves within the soft layers because of the contrast in properties between the soft overlying material and the firmer underlying bedrock. In the simplest case of horizontally layered sediments, this trapping affects only the vertical propagation of body waves. However, any real soil structure will also have lateral heterogeneities which trap horizontally propagating surface waves. The trapped waves interfere with each other, giving rise to resonance effects whose spatial distribution and frequency content depend on the characteristics of the incident seismic wave form and the geometrical and mechanical characteristics of the geological structure.

Resonance effects at a given strong-motion measurement location can be identified by considering frequency domain representation of the ground motion. Fourier or response spectral plots will peak at resonant frequencies. The location of these peaks will depend on the thickness and seismic velocities of the soil layers. For a simplified single layer 1-D structure, the fundamental frequency, f_0 and its harmonics, f_n are given by the expressions below:

$$f_o = v_s / 4H \quad 2.2$$

$$fn = (2n+1)f_o \quad 2.3$$

where: v_s is the shear-wave velocity of the surface soil layer,

H is the layer thickness, and

n is an integer.

Very thick deposits or very soft soils (of low-shear wave velocity) are therefore characterized by low fundamental frequencies ($\sim 0.2\text{Hz}$), whereas very thin or stiff layers have much higher fundamental frequencies ($\sim 10\text{Hz}$).

The amplitude of resonant peaks depends mainly on the contrast between the soil layers and the underlying bedrock, on the material damping in the sediments and, to a lesser extent, on the characteristics of the incident wave field (type of waves, incidence angle, and distance from fault rupture). In the case of a single homogeneous layer impinged by vertically propagating plane S-waves, the amplification, A_0 of the fundamental peak is given by:

$$A_0 = \frac{1}{(1/C) + 0.5\pi\xi_1} \quad 2.4$$

with:

$$C = \rho_2 v_{s2} / \rho_1 v_{s1} \quad 2.5$$

where: C is the impedance contrast.

ρ_i is the density of the i th medium ($i = 1$ for sediments; $i = 2$ for bedrock), and

ξ_1 is the material damping of the sediments

For very low damping values ($\xi_1 \approx 0$), the amplification is simply equal to the impedance contrast.

2.4 STRONG-MOTION PARAMETERS

2.4.1 MACROSEISMIC INTENSITY

Macroseismic intensity is a subjective measure of the severity of earthquake effects at a particular location. It is defined according to an index scale, each level having a qualitative

description of earthquake effects based on human perceptions, effects on construction and effects on natural surroundings. A widely used scale, the Modified Mercalli Intensity (MMI) scale alludes specifically to the level of response of various aspects of water supply systems (see Appendix A).

At the lower intensity levels (up to VI), the effects are unlikely to be damaging to intact components of the water supply system, although sloshing effects can disrupt water treatment processes and cause structural damage to water storage tanks. Significant damage is associated with levels of VII or more.

Estimates of intensity at individual locations are combined to create isoseismal maps where contours delineate regions within which the intensity is approximately the same. The level of correlation between macroseismic intensity and damage to the water supply system depends on the weighting given to water supply system-related criteria and the level of smoothing applied when defining the isoseismals.

Various different intensity scales exist, each with its own qualitative descriptions of earthquake effects at different intensity levels. Approximate conversions can be made between different scales, as illustrated in Figure 2.4.

MMI	I	II	III	IV	V	VI	VII	VIII	IX	X	XI	XII
RF	I	II	III	IV	V	VI	VII	VIII	IX	X		
JMA	I			II	III	IV	V		VI	VII		
MSK	I	II	III	IV	V	VI	VII	VIII	IX	X	XI	XII

Figure 2.4 Comparison between various intensity scales. MMI – Modified Mercalli; RI – Rossi-Forel; JMA – Japanese Meteorological Agency; MSK – Medvedev-Spoonheuer-Karnik (Kramer, 1996)

2.4.2 INSTRUMENTAL PARAMETERS

To completely characterise earthquake ground motion at a point, time histories would be required of the amplitude of oscillation in three mutually perpendicular directions plus torsional movements about each of the three axes. However, in order to be of use to the engineer, the severity of ground motion must be quantified concisely whilst retaining the important damage-inducing characteristics of the earthquake record. There are many ways of doing this, based on time histories of ground motion, although no single parameter is considered sufficient to accurately describe all of the key ground-motion characteristics (Kramer, 1996; Bommer & Martinez-Pereira, 2000). For earthquake engineering applications, amplitude, duration, frequency content and energy are the strong-motion characteristics of most interest.

2.4.2.1 AMPLITUDE PARAMETERS

The commonest measure of the amplitude of earthquake motion is the peak ground acceleration, PGA. Although accelerations are related directly to inertial forces, PGA itself is not a particularly good measure of damage to structures, except in certain special cases (i.e. very stiff structures). Relatively small magnitude earthquakes, for example, can give rise to large peak accelerations but have very little impact on structures because the duration of ground shaking is so transient and the peak accelerations are at frequencies too high to be of engineering interest. As far as pipelines are concerned, regions of high PGA have been seen to correlate with pipeline damage where this damage has been due to permanent ground deformations (O'Rourke & Toprak, 1997).

Velocity is a parameter less sensitive to high frequency components of the ground motion. As such, the peak ground velocity, PGV is a useful indicator of the effect of ground motion on structures such as tall or flexible buildings, which are sensitive to intermediate frequencies. It is a very useful parameter for understanding the seismic behavior of buried pipelines.

Peak ground displacements (PGD) are related more to the low-frequency content of strong ground motion. Where displacements are calculated from the integration of acceleration time-histories, their reliability in characterizing aspects of the true ground motion is significantly limited by inaccuracies in processing the raw data.

2.4.2.2 DURATION PARAMETERS

The level of earthquake damage is often strongly influenced by the duration of strong ground motion. In the presence of certain ground conditions (e.g. liquefiable deposits), repeated stress or load cycles of moderate amplitude, over an extended period, can cause more damage than higher amplitude motion over a shorter period.

2.4.2.3 FREQUENCY-CONTENT PARAMETERS

The earthquake response of structures and the ground is highly influenced by the frequency content of the input motion. Frequency content is significant for buried structures in as much as the response of the soil layers in which they are embedded is sensitive to frequency content. It is therefore important to consider how the amplitude of ground motion is distributed among the range of frequencies.

The maximum system response values are referred to as the spectral displacement (SD), spectral velocity (SV) and spectral acceleration (SA) respectively. The spectral acceleration at zero natural period (which corresponds to an infinite natural frequency) is equal to PGA.

The peak velocity and the peak acceleration values are related to the high and intermediate frequency components of strong ground-motion respectively. The ratio PGV/PGA is therefore a measure of the relative importance of these frequency ranges in the motion.

2.5 COLLATERAL EFFECTS

2.5.1 LIQUEFACTION

Liquefaction is a term used to describe a variety of complex phenomena involving soil deformations characterized by the generation of excess pore-water pressure under undrained loading conditions. The term *liquefaction* has been used to describe a number of different, though related phenomena. For engineering purposes, Kramer (1996) divides liquefaction phenomena into two main groups: *flow liquefaction* and *cyclic mobility*.

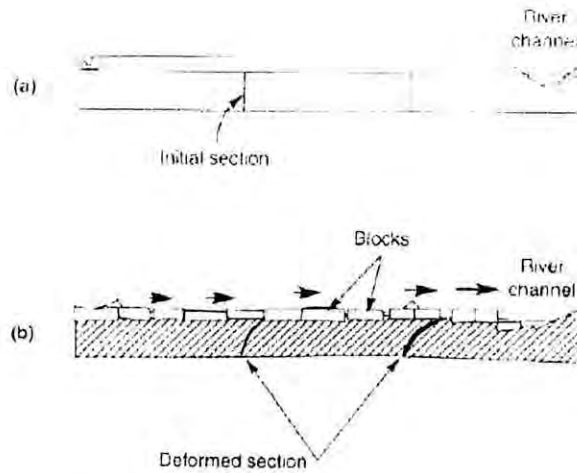


Figure 2.5 Lateral spreading caused by liquefaction of subsurface layer (a) before and (b) after an earthquake (Kramer, 1996)

Flow liquefaction failures are characterized by their sudden, catastrophic nature and the speed and extent of movement of the liquefied materials. The occurrence of flow liquefaction requires an undrained disturbance to bring the soil to an unstable state. Once initiated, it is actually the static shear stresses that drive the failure and give rise to the often large deformations observed.

Cyclic mobility occurs under a broader range of soil and site conditions than flow liquefaction. As a result, it is observed in the field much more frequently although its effects are generally less severe. Cyclic mobility occurs when the static shear stress is smaller than the shear strength of the liquefied soil. Deformations are not sudden as in the case of flow liquefaction, but develop incrementally over the duration of ground shaking. The deformations to which it gives rise are termed *lateral spreads* and can be up to several meters if the earthquake is large enough or of sufficient duration. Lateral spreading can occur on very gently sloping ground or even on flat ground adjacent to a free face, as illustrated in Figure 2.5. In this case, lateral movement of the liquefied subsurface soil has broken the surface layer into distinct blocks which move differentially both horizontally and vertically. A pipeline embedded in the non-liquefied surface layer may be pulled apart or sheared. A pipeline passing through the liquefied layer would be subject to horizontal and vertical forces due to the flow of soil around it, plus an uplift force due to buoyancy.

Soil liquefaction has caused significant damage to buried lifelines in past earthquakes. Zonation of liquefaction hazard is therefore of particular importance to lifeline earthquake engineers. Not all soils are susceptible to liquefaction, so the first stage of liquefaction hazard evaluation must be determination of liquefaction susceptibility. For any given soil, liquefaction susceptibility can be judged according to various historical, geological, compositional or soil state criteria.

Given that liquefaction is likely at a particular location, of most importance from an engineering perspective is to predict the amount of permanent ground displacement associated with the liquefaction. Hamada *et al.* (1986), for example, proposed a formula to predict the horizontal ground displacement caused by liquefaction-induced lateral spreads, based on failures observed in the 1964 Niigata and 1983 Nihonkai-Chubu earthquakes. The amount of horizontal displacement, the thickness of the inferred liquefied layer and the severity of ground slope were then averaged within each block to give the following expression:

$$D_H = 0.75 \sqrt{H_{liq}} \sqrt[3]{\theta} \quad 2.6$$

where: D_H is the horizontal ground displacement (m).

H_{liq} is the thickness of the liquefied layer (m)

θ is the maximum of slope of base of liquefied layer and slope of ground surface ($^\circ$)

H_{liq} is a parameter which indirectly accounts for the amount of ground shaking (a function of earthquake magnitude and distance) as well as the soil conditions at the site.

2.5.2 DENSIFICATION

Earthquake-induced strong ground-shaking can cause densification of both cohesive and cohesionless soils (O'Rourke & Liu, 1999). This process manifests itself as settlement at the ground surface and is therefore potentially damaging to buried infrastructure. Seismic densification of clays has been observed, but it is the densification of sands, either saturated or dry, which is of greater consequence.

Settlement of dry sands is normally complete by the end of strong ground-shaking. However, the process in saturated sands occurs only as earthquake-induced excess pore water pressures

dissipate. This will depend on the permeability and compressibility of the soil and on the drainage path length and therefore may not be complete until some hours after the earthquake. Following the 1995 Hyogoken-Nanbu (Kobe) earthquake, post-liquefaction settlements of up to 1 m were observed in the loose artificial fill materials on reclaimed land in the Osaka Bay area.

2.6. PIPELINE RESPONSE TO GROUND SHAKING

In this part the influence of ground condition on pipeline response and factors affecting the earthquake vulnerability of buried pipelines are discussed including a detailed review of empirical relations for the estimation of pipeline damage caused by seismic ground shaking.

2.6.1 INFLUENCE OF SITE EFFECTS ON THE SEISMIC RESPONSE OF BURIED PIPELINES

The influence of site conditions on the seismic response of buried pipelines is related to the shear-wave velocity of the ground. For both body waves and surface waves, for a fixed value of PGV, ground strain will generally be greater in soft soils (i.e. low v_s value) than stiffer soils. As shown in Figure 2.6, for the same value of PGV, maximum ground strain observed in soft ground (Shimonaga) is on average 3 to 4 times that observed in hard ground (Kansen). In this case, the predominant period of the soft ground was 1.3 s whilst the predominant period of the hard ground was around 0.4 s.

One of the earliest investigations into the effect of geological environment on pipeline damage was by Kachadoorian (1976). Using data mainly from the 1964 Alaska and 1971 San Fernando earthquakes, he considered three broad geological categories: bedrock, fine-grained sediments and coarse-grained sediments. For each category, he identified the relative occurrence of various potentially damaging earthquake effects. He then assigned relative pipeline damage intensities to each earthquake effect for all three geological categories. For the earthquakes studied, across all earthquake effects (which included ground shaking, landslides, faulting, seismic settlement and others), pipeline damage intensity was greatest in fine-grained soils, and least in bedrock. Kachadoorian (1976) suggested that this reflected the greater abundance of damaging earthquake effects in fine-grained soils compared to the other

two geological environments. For ground shaking alone, slightly more pipeline damage was observed in fine-grained soils than coarse-grained soils.

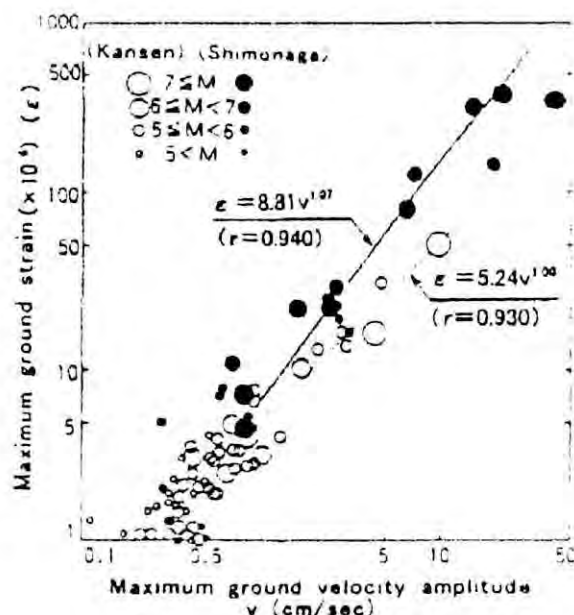


Figure 2.6 Field measurements of PGV and peak ground strain at sites in Japan with different ground conditions (Nakajima *et al.*, 1998)

In the preceding discussion, earthquake-induced pipe strains are shown to be strongly influenced by the average properties of the soil in which they are laid, whether that be characterised by the shear wave velocity or the natural period. Many field observations and theoretical studies have shown, however, that for transient earthquake effects, the level of non-uniformity of ground conditions is also extremely important in the seismic behaviour of buried pipelines (Liang & Sun, 2000). Lateral variation of ground conditions has been shown to cause strain concentrations during ground shaking due to significant differences in ground-motion characteristics even over short distances. Strong-motion array measurements have shown variations by a factor of five in velocity over a distance of 200 m and by a factor of two in acceleration over the same distance, all caused by variable site conditions (Zerva, 2000). Ground non-uniformity significant to the seismic behaviour of buried pipelines includes lateral variation in surface soil type, variation in surface topography and sloping subsurface strata. The features responsible for ground non-uniformity can be large scale, as in the case of major geological boundaries between surface soil types or small scale such as man-made cut-and-fill boundaries.

Nishio *et al.* (1988) investigated the effect of lateral variations in ground conditions on earthquake induced ground and pipe strain using an instrumented arc-welded steel pipeline at Tama New Town in a western suburb of Tokyo. The pipeline under observation passed through a boundary between stiffer cut ground and softer fill material. Observations made during twelve earthquakes, with magnitude values $4.2 \leq M_{JMA} \leq 6.7$, always showed greater peak accelerations in the filled ground than the cut ground. Maximum pipe strains, as measured using an array of strain gauges, were also much greater where the pipe was embedded in the fill material. Maximum strains generally coincided with the shoulder of the embankment, which was assumed to be a topographic effect. Other than this, an additional strain concentration was observed at the cut-and-fill boundary due to lateral variation in ground stiffness.

2.6.2 FACTORS AFFECTING EARTHQUAKE VULNERABILITY OF PIPELINES

For succinctness (conciseness) in the discussion which follows, a few useful abbreviations are defined in Table 2.3.

Table 2.3 Some commonly-used pipeline-related abbreviations, together with typical yield stress and yield strain values for common pipe barrel materials (from O'Rourke and Liu, 1999)

Abbreviation	Term	Typical yield stress, σ_y (Mpa)	Typical yield strain, e_y
AC	asbestos cement	†	†
C	concrete	2 - 28	0.0001 - 0.0013
CI	cast iron	97 - 290	0.001 - 0.003
DI	ductile iron	293 - 360	0.0018 - 0.0022
PE	polyethylene	15 - 17	0.022 - 0.025
PVC	polyvinyl chloride	35 - 45	0.017 - 0.022
S	steel	227, 289, 358, 448, 517*	0.00134, 0.00231**
SG	steel (threade joint)	-	-
WS	welded steel	-	-
WSAWJ(A,B)	welded steel arc-welded joints (Grades A & B steel)	-	-
WSAWJ(X)	welded steel arc-welded joints (Grade X steel)	-	-
WSCJ	welded steel caulked joints	-	-
WSGWJ	welded steel gas welded joints	-	-

† AC does not have yield values due to its brittleness. Its strength is normally characterized using transverse crushing strength or beam strength.

* Values are quoted for five different grades of steel: B, X-42, X-52, X-65 & X-70 respectively.

** Values are given for X-42 and X-65 grades of steel.

Many studies have been done on the factors affecting pipeline vulnerability under non-catastrophic (aseismic) operating conditions. Due to the difficulty in characterizing the condition of buried pipelines, much of the work has been inconclusive. However, several important factors influencing pipe leakage and break rates (per unit length of pipe) have been identified. In a literature review covering the period 1948 to 1991, Wengstrom (1993) investigated the influence of pipe age, installation method, material type, pipe dimensions (diameter and thickness), joint type, previous damage history, operating pressure, soil conditions, land use and seasonal variations of external environment. Many of these factors are important in understanding pipeline vulnerability under seismic conditions.

Three of these factors (pipe type, joint type and pipe diameter) have been considered in a rating scheme developed by Ballantyne (1995) for earthquake vulnerability of pipelines. Ballantyne (1995) assessed the seismic performance of pipelines based on four qualitative parameters: *ruggedness* - a function of pipe material strength and ductility; *bending* - a measure of resistance of the pipe barrel to bending failure; *joint flexibility* - a measure of the pipe's ability to extend, compress or bend and rotate around the joint without breaking the joint's water-tight seal; *restraint* - a measure of the ability of the pipe-joint system to hold together in extension.

The scheme highlights the influence of joint type on the overall pipeline vulnerability. A pipe-joint system is only as strong as its weakest element. A gas-welded joint renders a steel pipe as vulnerable to damage as a CI or AC pipe, even though the tensile strength of a steel barrel is much greater than that of CI or AC (Table 2.3). For a given joint type, however, steel and ductile iron (DI) pipes are less vulnerable than more brittle pipe types (eg. PVC, AC, CI).

Table 2.4 Relative earthquake vulnerability of water pipes (Ballantyne, 1995). Joint types: B&S - bell & spigot; RG - rubber gasket; R – restrained; UR – unrestrained

Material type/diameter	Joint type	Ruggedness	Bending	Joint flexibility	Restraint	Total
LOW VULNERABILITY						
ductile iron	B&S, RG, R	5	5	4	4	18
polyethylene	Fused	4	5	5	5	19
steel	arc welded	5	5	4	5	19
steel	Riveted	5	5	4	4	18
steel	B&S, RG, R	5	5	4	4	18
LOW/MODERATE VULNERABILITY						
concrete cylinder	B&S, R	3	4	4	3	14
ductile iron	B&S, RG, UR	5	5	4	1	15
PVC	B&S, R	3	3	4	3	13
steel	B&S, RG, UR	5	5	4	1	15
MODERATE VULNERABILITY						
AC > 200mm ϕ	Coupled	2	4	5	1	12
cast iron > 200mm ϕ	B&S, RG	2	4	4	1	11
PVC	B&S, UR	3	3	4	1	11
concrete cylinder	B&S, UR	3	4	4	1	12
MODERATE/HIGH VULNERABILITY						
AC < 200mm ϕ	Coupled	2	1	5	1	9
cast iron < 200mm ϕ	B&S, RG	2	1	4	1	8
steel	gas welded	3	3	1	2	9
HIGH VULNERABILITY						
cast iron	B&S, rigid	2	2	1	1	6

Observations of pipeline damage in Kobe, Ashiya and Nishinomiya cities, caused by the 1995 Hyogoken-nanbu earthquake are consistent with the rating scheme given in Table 2.4. A summary of data collected by Shirozu *et al.* (1996) is given in Figure 2.7. The worst affected category of pipes was steel with threaded joints (SG). However, this failure rate is unrealistically high, representing localised damage averaged over a very short length of pipe. The highest reliable damage rate was observed in AC pipes, followed by CI, PVC and DI, with steel pipes showing the best overall performance.

The importance of joint type is illustrated with reference to the performance of pipes having “Stype” or “S II type” joints. DI pipes having these specially-designed anti-seismic joints (not included in Table 2.4), suffered no damage as a result of the Hyogoken-nanbu earthquake. These types of pipe-joint systems constituted about 270 km of the total water distribution

network, 100 km of which coincided with areas experiencing significant liquefaction-induced permanent ground deformation (Shirozu *et al.*, 1996). In the Ashiyama District, for example, a 500mm diameter pipe with S type joints remained intact after a lateral ground movement of about 2m. A 300 mm diameter pipeline with SII type joints at the Egeyama distribution reservoir also suffered no damage, in spite of subsidence of around 1.3 m (Inada, 2000).

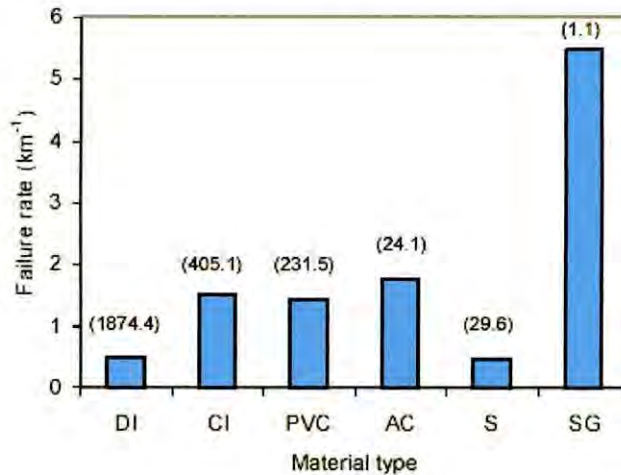


Figure 2.7 Pipeline failure rate for various pipe types from the study by Shirozu et al. (1996). Pipe lengths are given for each category (km)

These S and S II type anti-seismic joints are illustrated in Figure 2.8. S II type joints are for smaller diameter pipes (in the range 75 - 450 mm), whilst S type joints are for larger diameter pipes (500 -600 mm). Both joint types allow for expansion and contraction at the joint equal to 1% of pipe length. A run of several anti-seismic pipe lengths can therefore tolerate significant permanent ground deformations. Due to the high costs involved, installation of anti-seismic joints is only warranted in locations likely to experience significant permanent ground deformation as a result of liquefaction, landslides or faulting.

Seismic loading of pipelines can cause a number of different failure modes. The principal failure modes for corrosion-free continuous pipelines (e.g. steel pipe with welded joints) are rupture due to axial tension, local buckling due to axial compression and flexural failure. For shallow burial depths, continuous pipelines in compression can also fail by beam buckling. For corrosion-free segmented pipelines with bell and spigot type joints, the main failure modes are axial pull-out at the joints, crushing at the joints and round flexural cracks in pipe segments away from the joints.

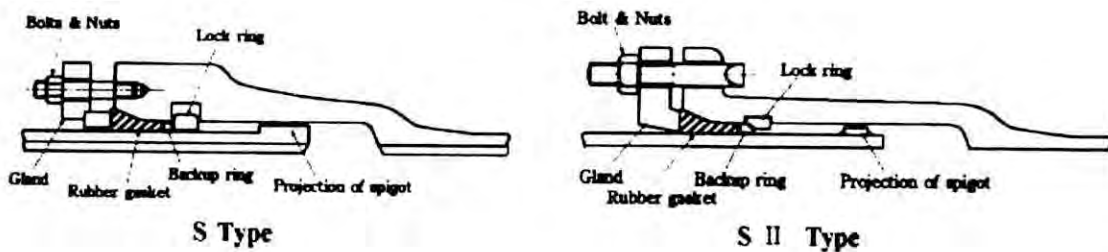


Figure 2.8 Cross-sections of anti-seismic pipe joints (Nakajima *et al.*, 1998)

The presence of corrosion in CI, DI or steel pipes increases the likelihood of failure by decreasing pipe wall thickness. The occurrence of corrosion is linked to pipeline age but is significantly influenced by the prevailing soil conditions.

AC pipes are weakened due to softening caused by leaching of lime (decalcification) and PVC pipes are weakened by fatigue. The influence of pipe age, however is also connected to environmental changes and the changes over time of pipe installation and material specification and selection practices.

Certain elements of a pipeline network have increased vulnerability to earthquake damage due to stress concentrations induced by the passage of seismic waves. Stresses at pipeline elbows and at pipe intersections can significantly exceed stresses in adjacent portions of straight pipe (Stuart *et al.*, 1996; Datta, 1999). Portions of pipe connecting to manholes, tanks or buildings can be vulnerable due to their propensity for differential movements.

For seismic risk analysis of water distribution systems, pipeline repair rates need to be related to earthquake effects as well as factors affecting pipeline vulnerability. Since the 1970's, attempts have been made to correlate earthquake intensity and various peak ground motion parameters with pipeline damage rates (given in terms of numbers of repairs per unit length of pipe). The resulting *fragility* relations can then be used for predictive purposes in estimating likely damage in the event of a future earthquake.

2.6.2.1 FRAGILITY RELATIONS FOR BURIED PIPES SUBJECTED TO GROUND SHAKING

Separate pipeline fragility relations exist for permanent ground deformation and ground shaking effects. The focus of the current review is on ground shaking effects.

A total of seventeen studies have been found relating pipeline damage to ground shaking effects from data culled from past earthquakes. A summary of these studies, fifteen of which present fragility relationships, is given in Table 2.5a. The strong-motion parameter(s) used to define the level of ground shaking/earthquake effects for each study are summarized in Table 2.5b. The table also indicates the earthquakes from which data have been obtained in each study, and wherever known, the number of data points used. Fragility curves, including the datasets from which they are derived are included wherever available. The dependent variable is given variously as “repair rate”, “damage rate” or “damage ratio”; other studies use the term “failure rate”. These terms are used interchangeably in the literature. In the following sections, specific emphasis is placed on identifying the size, origin and reliability of the data for each study.

2.6.2.2 Katayama *et al.* (1975)

One of the first attempts to correlate observed seismic damage in pipelines with any strong-motion parameter was when Katayama *et al.* (1975) considered damage rate in terms of PGA. The study is based on pipeline failure rates obtained for six earthquakes, as indicated in Table 2.5a. Figure 2.9 shows the data of Katayama *et al.* (1975) as presented by Bresko (1980). This figure has been reproduced in several publications (e.g. O’Rourke & Liu, 1999) although the original report (Bresko, 1980) was not available. Numbers of data points indicated in Table 2.5a refer to the original dataset of Katayama *et al.* (1975). Where the numbers of data points presented by Bresko (1980) differ, these are given in brackets. The small differences are due to different ways of aggregating the pipeline damage statistics.

PGA values in the vicinity of each damaged pipeline system were estimated from the few strongmotion records available for these earthquakes. For the 1923 Kanto (Tokyo) and 1948 Fukui earthquakes, no records were available so ranges of values were assigned from

Table 2.5a Summary of pipeline fragility studies for ground shaking effects according to earthquake data used

Event ID	Date	Earthquake Name	Country	Magnitude	Katayama et al (1975)	Iaoyama & Katayama (1982)	Eguchi (1983)	Barenberg (1988)	Ballantyne et al (1990)	Eguchi (1991)	ASCE/TCLL (1991)	O'Rourke et al (1991)	Hamada (1991)	Tiiedemann (1992)	O'Rourke & Ayala (1993) [HAZUS]	Eidinger (1995, 1998)	Kitaura & Miyajima (1996)	Hwang & Lin (1997)	O'Rourke et al. (1998)	Isoyama et al. (2000)	ALA (2001)
1	18-Apr-06	San Francisco	US	7.9																	
2	1-Sep-23	Kanto	Japan	7.9 (MJMA)	2						2			1							2
3	11-Mar-33	Long Beach	US	6.5																	1
4	28-Jun-48	Fukui	Japan	7.1 (MJMA)	1						1										GDp
5	13-Apr-49	S Puget Sound	US	6.7																	2
6	16-Jun-64	Nigita	Japan	7.5 (MJMA)	1						1			1			1				1
7	29-Apr-65	Puget Sound	US	6.5 (ML)				1							1	1					2
8	16-May-68	Tokachi-*oki	Japan	7.9 (MJMA)	11 (9)						8										GDp
9	1-Oct-69	Santa Rosa	US	5.6 [5.7] (ML)			1	1	1	1		1			1	1					a-s
10	9-Feb-71	San Fernando	US	6.6	19			3			19			2	2	2			2		13
11	23-Dec-72	Managua	Nicaragua	6.3	3 (1)		1			1	1										GDp
12	28-Jul-76	Tangshan	China	7.6 (Ms)										2							
13	12-Jun-78	Miyagiken-oki	Japan	7.4 (MJMA)									1								
14	15-Oct-79	Imperial Valley	US	6.5																	1
15	2-May-83	Coalinga	US	6.4							1	1			2	1					1
16	26-May-83	Nihonkai-chubu	Japan	7.7 (MJMA)									3								
17	19-Sep-85	Michoacan	Mexico	8[7.5]											3	5					a-s
18	1-Oct-87	Whittier	US	5.9[5.3]															1		a-s
19	25-Apr-89	Tiahuac	Mexico	6.9 (Ms)											2	1					1
20	18-Oct-89	Loma Prieta	US	7										1		9	5		1		13
21	28-Dec-94	Sanriku Haruka-oki	Japan	7.7													1				
22	17-Jan-94	Northridge	US	6.7															7		35
23	16-Jan-95	Hyogoken-nanbu	Japan	6.9													3			19	9
TOTAL NO. EARTHQUAKES					6	1	4	3	6	4	7	7	2	7	6	7	5	15	4	1	12

Notes for Table 2.5a Magnitudes are M_w unless otherwise stated and are mostly taken from ISESD (Ambraseys *et al.*, 2002) or TMG (1995). Studies highlighted in grey present fragility curves; other studies show the range of data observed but do not define fragility curves. Shaded boxes in the main table indicate the use of data from a given earthquake. For each study, the number of separate data points from a given earthquake is given where known. For the ALA (2001) study, GDP refers to data points considered but excluded due to likely effects of permanent ground deformation; a-s refers to data points considered in the study but excluded due to the occurrence of an aftershock of similar magnitude to the main event, leading to difficulties in associating damage to a single event. Aftershock magnitudes are indicated in square brackets. For this study, PGD refers to the transient peak ground displacement, rather than permanent ground displacement.

Table 2.5b Strong-motion parameters considered by each study. Studies highlighted in grey present fragility curves; other studies show the range of data observed but do not define fragility curves (as Table 2.5a)

Strong-motion parameter	Katayama <i>et al.</i> (1975)	Iaoyama & Katayama (1982)	Eguchi (1983)	Barenberg (1988)	Ballantyne <i>et al.</i> (1990)	Eguchi (1991)	ASCE/TCLÉE (1991)	O'Rourke <i>et al.</i> (1991)	Hamada (1991)	Tiedemann (1992)	O'Rourke & Ayala (1993) [HAZUS]	Eidinger (1995, 1998)	Kitaura & Miyajima (1996)	Hwang & Lin (1997)	O'Rourke <i>et al.</i> (1998)	Isoyama <i>et al.</i> (2000)	ALA (2001)
I_a																	
I_{MM}																	
PGA																	
PGV																	
PGD																	
SA																	
SI																	

Table 2.5c Summary of earthquakes used in studies given in Table 2.5a

Location	No. of earthquakes
US	11
Japan	8
Mexico/Central America	3
China	1

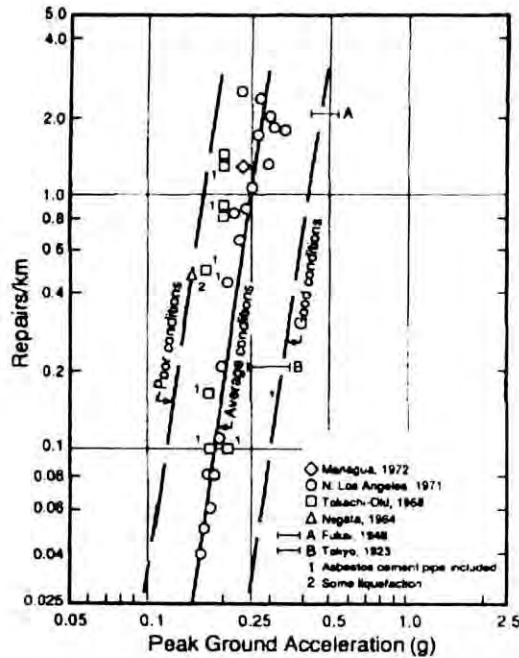


Figure 2.9 Pipeline fragility data of Katayama et al. (1975) as presented by O'Rourke & Liu (1999). This graph presents the data in a more comprehensive manner than the graph included in the original study and includes trends suggested by Bresko (1980)

earthquake effects, as shown in Figure 2.9. Eight separate data points are shown for different localities affected by the 1968 Tokachi-oki earthquake. PGA values appear to have been estimated from values of JMA intensity given for each locality although the conversion method used is not known. Nineteen separate data points were obtained for the 1971 San Fernando earthquake by dividing a map of pipeline failures in Northern Los Angeles into 19 strips, each of width 0.48 km. A PGA value for each strip was found by estimating PGA at the northern and southern extremities of the mapped area (probably based on strong-motion recorded nearby, although details are not specified) and interpolating values using a strong-motion attenuation relationship. The PGA values given in Figure 2.9 for the San Fernando earthquake cover the range 0.18 – 0.34 g whereas those in Katayama *et al.* (1975) for the same earthquake cover the range 0.27 – 0.50 g. This represents a discrepancy between the Bresko (1980) and Katayama *et al.* (1975) studies. Another discrepancy is found in the PGA value for the 1972 Managua earthquake, which Katayama *et al.* (1975) estimate at 0.41 g \pm 0.05 g but which Bresko (1980) plots below 0.25 g. PGA for the 1964 Niigata earthquake is not specified by Katayama *et al.* (1975) and may be an addition from Bresko (1980) based on either intensity or strong-motion values. The scatter in the dataset presented by Bresko (1980) is considerable, although it would be greater if the original PGA values of Katayama *et al.*

(1975) had been used. Such large scatter is typical of pipeline fragility relations, although in this case is undoubtedly influenced by heightened damage rates due to permanent ground deformation in certain cases (eg. liquefaction-induced damage during the Niigata earthquake and damage due to faulting in the case of the Managua earthquake). Most of the data presented in Figure 2.9 is for CI pipes although the data from the 1968 Tokachi-oki earthquake includes damage to AC pipes. The fragility relationship makes no distinction between different pipe diameters or joint types, both of which are known to influence damage rates. However, Katayama *et al.* (1975) do comment on the tendency for damage to increase with increasing pipe diameter. The fragility relations indicated in Figure 2.9 are those suggested by Bresko (1980) and expressed in Equation (2.9) (Table 2.9). b is a parameter which depends on a range of factors including soil conditions and pipe age. It has a value of 4.75, 3.65 or 2.20 for “poor”, “average” or “good” conditions respectively (Ayala & O’Rourke, 1989).

2.6.2.3 Eguchi (1991)

The work of Eguchi (1991) was a modification of an earlier study (Eguchi, 1983) in the light of data from more recent (unspecified) earthquakes. Both sets of fragility relations give pipeline repair rate as a function of IMM (see Appendix B).

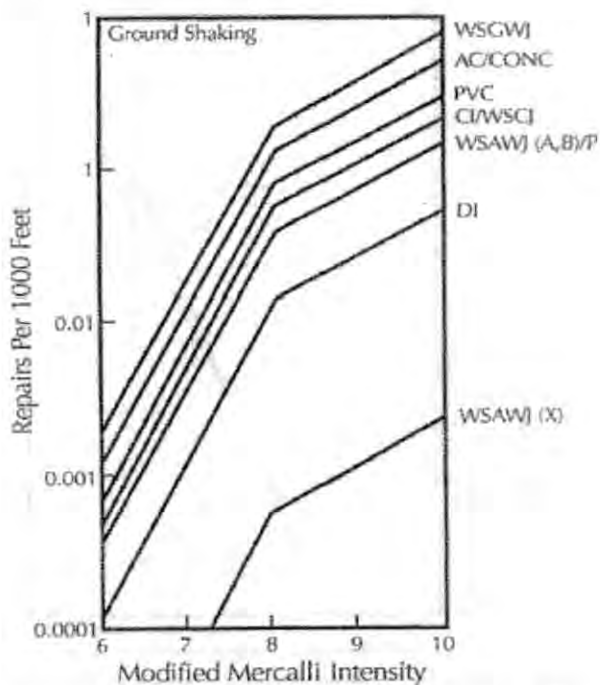


Figure 2.10 Bilinear pipeline fragility relations of Eguchi (1991). See Table 2.3 for abbreviations. Note that repair rate is given per 1000 ft.

The modified relations are shown in Figure 2.10. The amount of scatter associated with these relations is not possible to determine as individual data points are not presented. Distinction is made between different pipe and joint types, with greatest damage rates observed in steel pipes with gas-welded joints. AC and concrete pipes were found to be more vulnerable than PVC pipes, which in turn were more vulnerable than CI pipes and welded steel pipes with caulked joints. DI pipes experienced on average about ten times fewer repairs per unit length than the worst performing pipes.

2.6.2.4 O'Rourke and Ayala (1993)

Barenberg (1988) plotted the damage rate for CI pipe against PGV using data from three US earthquakes (Table 3.4a). O'Rourke & Ayala (1993) subsequently added data from the 1983 Coalinga and two Mexican earthquakes (1985 Michoacan and 1989 Tlahuac). The fragility relations defined by both investigations are shown in Figure 2.11.

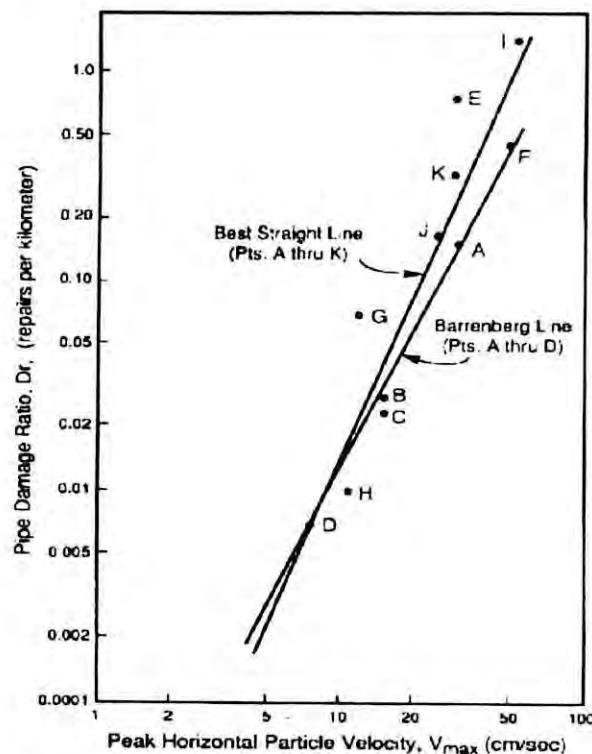


Figure 2.11 Fragility relations of Barenberg (1988) (derived from data points A – D), and O'Rourke & Ayala (1993) (derived from data points A-K).

The fragility relationship of Barenberg (1988) suggests that a doubling of PGV will lead to an increase in the pipeline damage rate by a factor of about 4.5. The same increase in PGV for

the modified relationship results in a 6-fold increase in pipeline damage rate. Two outlying points, E and G are largely responsible for this change. It is suggested that the relatively high damage level in this case is largely due to abrupt changes in the subsurface conditions which characterise this region (O'Rourke & Ayala, 1993). Pipeline failures are not influenced by permanent ground deformation effects and PGV values are more reliable due to greater availability of strong-motion records for these later earthquakes. Katayama *et al.* (1975) and Barenberg (1988) both comment on the inadequacy of PGA for determining ground shaking intensity.

The fragility relationship of O'Rourke & Ayala (1993) has been incorporated into the national loss estimation methodology used in the US, HAZUS (FEMA, 1999). The relationship, given in Equation (2.13) (Table 2.10) is used for brittle pipes only as it is based on data from AC, concrete and CI pipes. For more ductile pipe types (steel, DI or PVC), HAZUS (FEMA, 1999) suggests this relation be multiplied by 0.3. Steel pipes with arc-welded joints are classified as ductile whereas steel pipes with gas-welded joints are classified as brittle. In the absence of joint information, pre- 1935 steel pipes are classified as brittle pipes. The HAZUS methodology does not consider pipe diameter as a factor.

2.6.2.5 Hwang and Lin (1997)

The fragility relation of Hwang & Lin (1997) gives pipeline failure rate as a function of PGA and is based on a review of data drawn from six studies (Katayama *et al.*, 1975; Eguchi, 1991; ASCE/TCLEE, 1991; O'Rourke *et al.*, 1991; Hamada, 1991; Kitaura & Miyajima, 1996). The fragility curve of Hwang & Lin (1997) is shown in Figure 2.12 along with the relations upon which it is based.

Figure 2.12 highlights how great the differences are between different fragility relationships. The basic curve established by Hwang & Liu (1997) is for CI pipes with diameters of around 300 mm. The pipe diameter factor, RD , which is defined based on data from the 1995 Hyogoken-nanbu earthquake (Kitaura & Miyajima, 1996; Shirozu *et al.*, 1996), is shown in Figure 2.13.

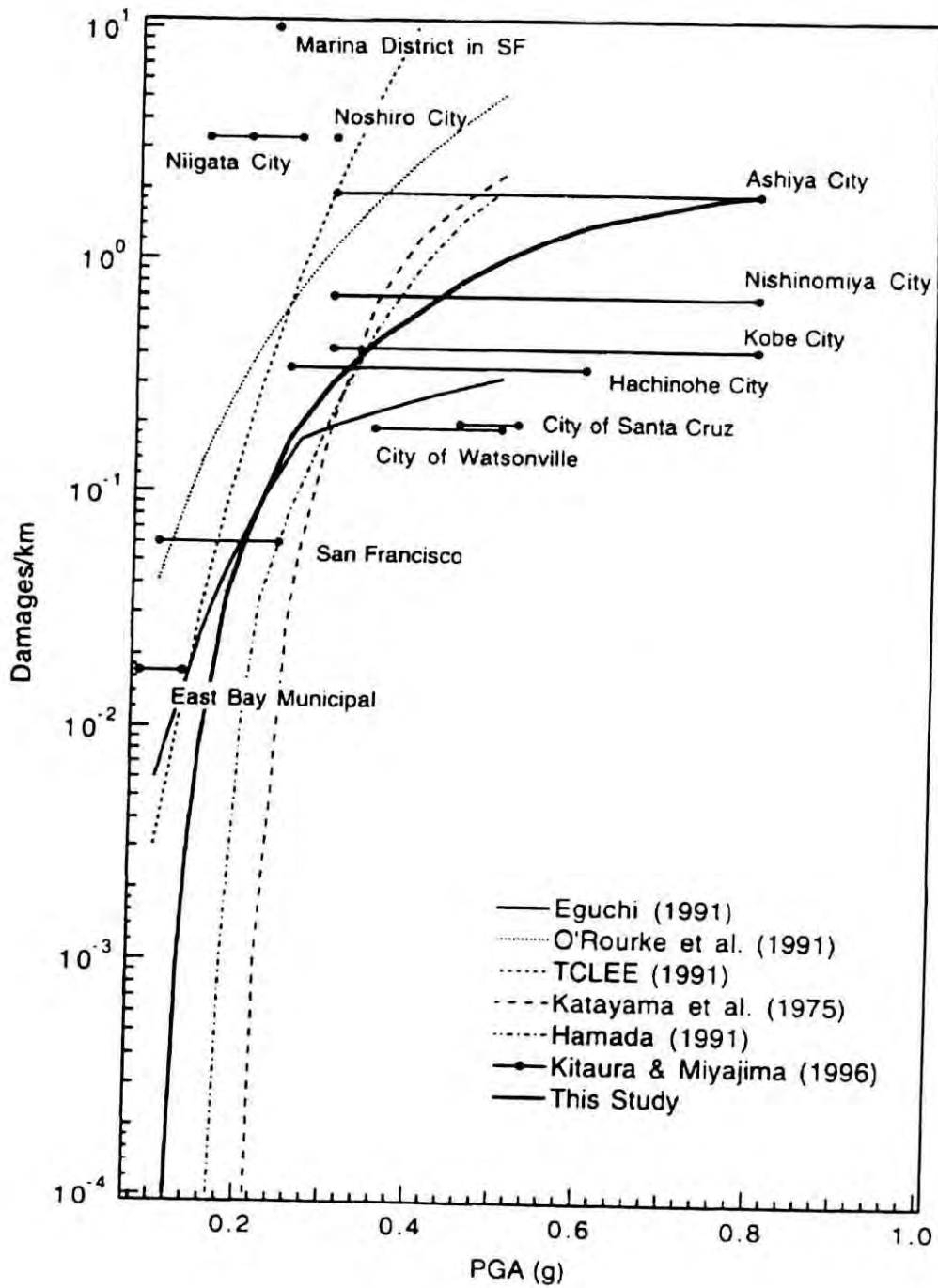


Figure 2.12 A comparison between the fragility curve of Hwang & Lin (1997) (*This Study) with other fragility curves for PGA (1993)

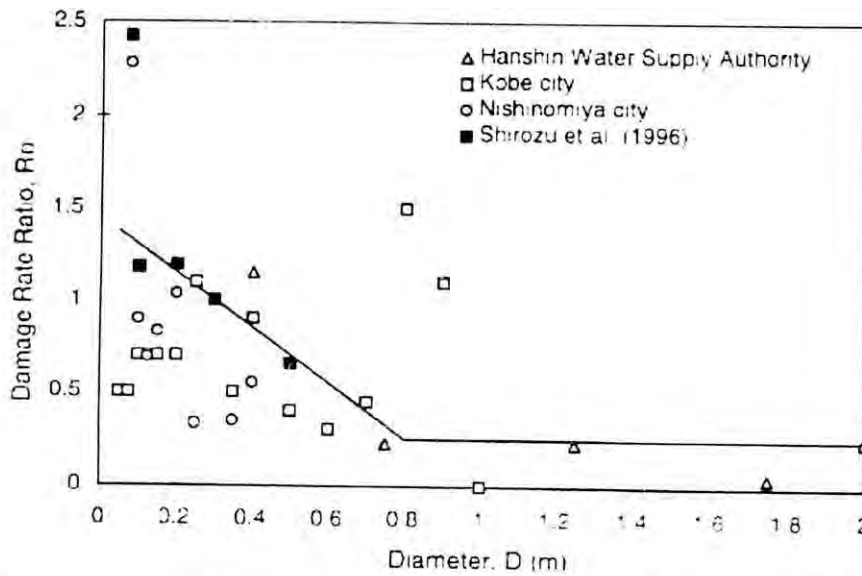


Figure 2.13 Damage rate ratio for different pipe diameters (Hwang & Lin, 1997)

2.6.2.6 O'Rourke *et al.* (1998)

O'Rourke *et al.* (1998) used a GIS database to investigate factors affecting water supply system damage caused by the 1994 Northridge earthquake. All Los Angeles Department of Water and Power (LADWP) and Metropolitan Water District (MWD) trunk lines within the LADWP system were digitised from 1:12,000 maps provided by LADWP. The trunk line repair database was assembled from statistics provided by LADWP and MWD and the distribution line repair database came from statistics developed for the State of California Office of Emergency Services (OES). Of 1,405 original OES repair records, 1,013 were deemed valid for investigation into damage to distribution mains and hydrants. Of these, reliable information about pipe composition could be found for 964 repairs, most of which (944) also had information concerning pipe diameter. An extensive strong-motion dataset allowed reliable contour maps to be drawn for various different strong-motion parameters, including PGA, PGV, PGD, SA, I_a and SI.

Pipeline repair rate contours were calculated for CI pipes, which constituted approximately 76% of the distribution network. The contours were found by dividing the Northridge area into a grid of 2 x 2 km squares and determining the length of CI pipe and number of CI pipeline repairs in each square. Figure 2.14 shows the repair rate contours for CI pipes

superimposed on a contour map of PGV. No pipeline damage was observed in regions with $PGV < 10$ cm/s. Highest repair rates were shown to coincide reasonably well with zones of highest PGV. Similar correlations were found for other strong-motion parameters. Concentrated areas of damage were generally found to coincide with occurrences of ground failure due to liquefaction or landslides.

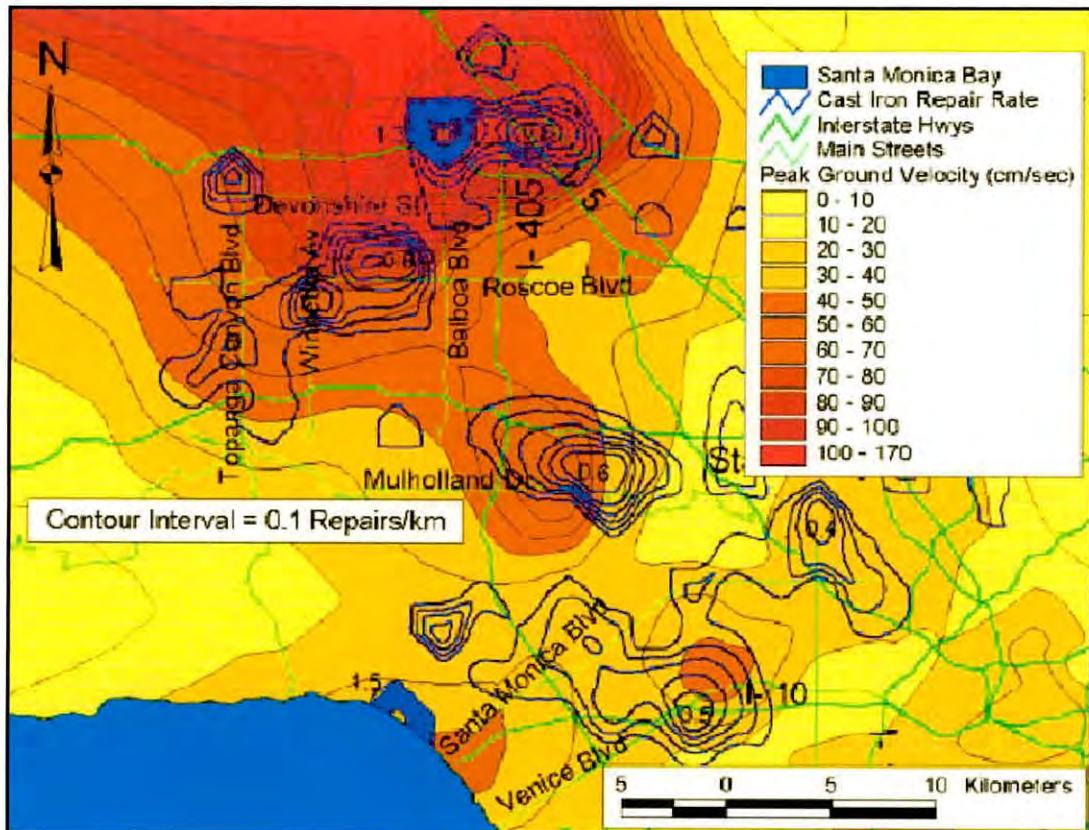


Figure 2.14 Pipeline repair rate contours for CI pipe vs. PGV for the Northridge earthquake (O'Rourke & Toprak, 1997)

The study by O'Rourke *et al.* (1998) includes pipeline fragility relations for IMM and SI based only on Northridge data and relations for PGA and PGV which also use data from three other US earthquakes. The relation shown in Figure 2.15 (a) is for PGV for CI pipes of all diameters. The trend of O'Rourke *et al.* (2001) is expressed in Equation (2.16) and has been plotted in Figure 2.18 for subsequent comparison with fragility relations by other investigators. The PGA fragility relation of O'Rourke *et al.* (1998) is expressed in Equation (2.11) and plotted in Figure 2.18.

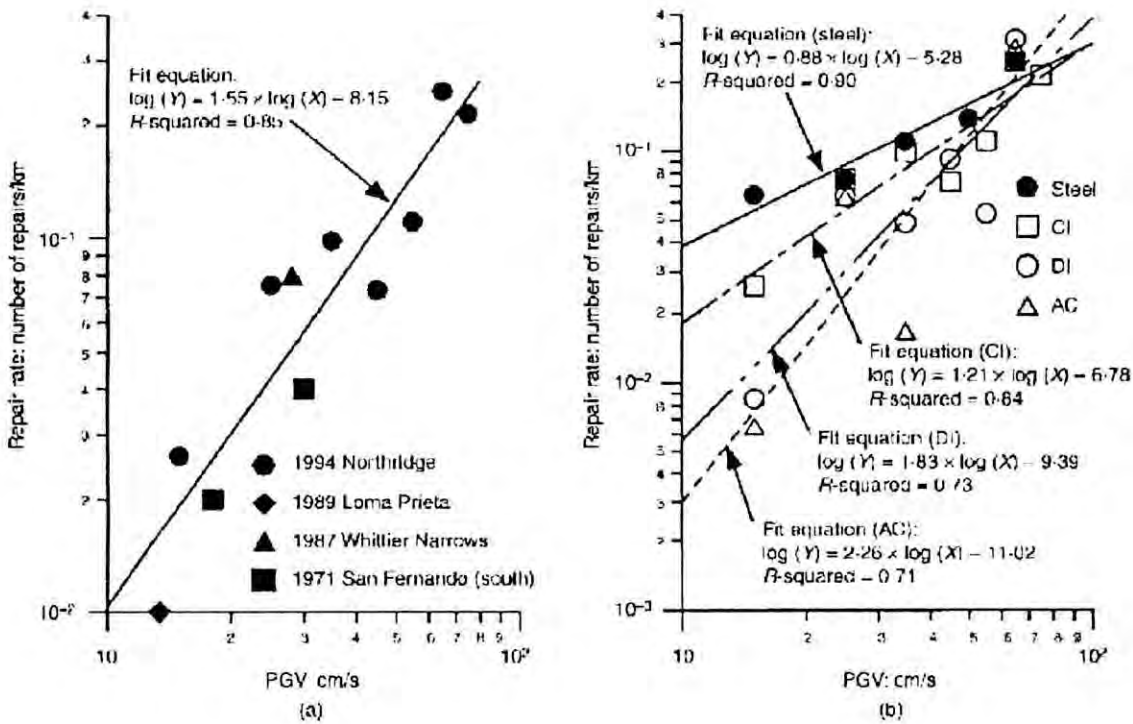


Figure 2.15 Pipeline repair rate correlation with PGV for steel, CI, DI and AC distribution lines: (a) CI distribution lines; and (b) steel, CI, DI and AC distribution lines (O'Rourke *et al.*, 2001)

Figure 2.15 (b) shows repair rate correlations for steel, CI, DI and AC pipes, all obtained from GIS analysis of the Northridge data. The relative vulnerabilities of CI and DI pipes implied by these trends confirm the findings of previous studies. The low damage rates observed for AC pipes and the high damage rates observed for steel pipes are, however, surprising.

2.6.2.7 Isoyama *et al.* (2000)

Isoyama *et al.* (2000) extended the GIS-based investigation of the Japan Water Works Association (JWWA) (Shirozu *et al.*, 1996) to establish pipeline fragility relations for PGA and PGV. Shirozu *et al.* (1996) established a GIS database to analyse factors influencing water pipeline damage caused by the 1995 Hyogoken-nanbu earthquake. This database consisted of distribution pipes digitised from 1:5000 or 1:6000 maps for the whole of Kobe City and neighbouring Ashiya City (except for Okuyama and Okuike Districts) and Nishinomiya City, all of which suffered extensive earthquake damage. The location of each

pipeline repair, including data on pipe material, pipe diameter, failure mode and year of installation, was entered into the database. Isoyama *et al.* (2000) carried out a more detailed investigation focusing on Ashiya and Nishinomiya Cities. For this region, 50 m grid cells were defined in order to better represent “narrow valleys” and other topography types. A multivariate analysis was carried out to quantify the influence of the various factors on pipeline damage rate, establishing empirical correction factors to account for pipe material, pipe diameter, ground topography and liquefaction (Table 2.6).

A separate analysis was performed using strong-motion data from across the whole Kobe-Osaka region to establish standard damage rate curves, to which the correction factors could be applied. The pipeline fragility relationships were derived according to the form given in Equations (2.7) and (2.8).

$$R_R(X) = B_p B_d B_g B_L R_o(X) \quad 2.7$$

$$R_o = a(X - X_{min})^b \quad 2.8$$

where: $R_R(X)$ is the pipeline repair rate per km of pipe as a function of the strong-motion parameter, X . Fragility relations have been derived for PGA and PGV.

B_L are modification factors defined in Table 2.6,

R_o is the standard pipeline damage rate, defined for CI pipe of diameter range 100 - 150 mm located in alluvial soil with no liquefaction (coefficients $B_L = 1.0$ in Table 2.6) a and b are regression coefficients, X_{min} is the minimum value of strong ground-motion for which damage is considered to occur (100cm/s^2 in the case of PGA and 15cm/s in the case of PGV).

In this case the fragility relations were based on 19 data points and 16 data points. In each case, several additional outlying points were excluded due to extreme instances of liquefaction or topographic effects. As a result of the size and quality of the data set, the work of Isoyama *et al.* (2000) represents a major improvement on a previous pipeline fragility relation for PGA developed by Isoyama & Katayama (1982); both relations are plotted in Figure 2.17 for comparison. The algorithms are expressed in Equations (2.10) and (2.12) respectively. The basic repair rate algorithm of Isoyama *et al.* (2000) for PGV is given by Equation (2.15) and plotted in Figure 2.18.

Table 2.6 Correction factors for application to the fragility relations of Isoyama *et al.* (2000). Values in brackets are less reliable due to small sample size.

Pipe material correction factor, Bp		Pipe diameter correction factor, Bd		Ground topography correction factor, Bg		Ground liquefaction correction factor, BL	
DI	0.3	75mm	1.6	Disturbed hill	1.1	No liquefaction	1.0
CI	1.0	100-150mm	1.0	Terrace	1.5	Partial liquefaction	2.0
PVC	1.0	200-400mm	0.8	Narrow valley	3.2	Total liquefaction	2.4
Steel	(0.3)	>500	(0.5)	Alluvial	1.0		
AC	(1.2)			Stiff alluvial	0.4		

2.6.2.8 ALA (2001)

In 2001 the American Lifelines Alliance (ALA), published a set of detailed procedures to evaluate the probability of damage from earthquake effects to various components of water supply systems (ALA, 2001). For buried pipelines, fragility relations were developed separately for permanent ground deformation effects and ground shaking effects.

The database developed for ground shaking effects included pipeline damage rates from 18 earthquakes spanning the period 1923-1995. Data were obtained from a number of sources, as detailed in Table 2.7. The full ALA (2001) database was homogenized as much as possible. Where data were based on IMM or PGA.

Table 2.7 Summary of data sources used to develop the ALA (2001) database of pipeline damage caused by ground shaking.

Source	1923 Kanto	1933 Long Beach	1948 Fukui	1949 S Puget Sound	1964 Nigita	1965 Puget Sound	1968 Tikachi oki	1969 Santa Rosa	1971 San Fernando	1972 Managua	1979 Imperial Valley	1983 Coalinga	1985 Michoacan	1987 Whittier Narrows	1989 Tiahuac	1989 Loma Prieta	1994 Northridge	1995 Hyogoken-nanbu
ALA report (unspecified)																		
Eidinger et al. (1995)																		
Katayama et al. (1975)																		
O'Rourke and Ayala (1993)																		
Shirozu et al. (1996)																		
Toprak (1998)																		

ALA (2001) has published its full dataset as an appendix along with its report. For each data point, pipe material, pipe repair rate (R_R), pipe diameter, PGV and any adjustments made are specified. Where available, the numbers of repairs and length of pipe used to calculate R_R are given. Pipe material and pipe diameter categories are summarized in Table 2.8.

Table 2.8 Pipe material and pipe diameter categories included in the dataset for the ALA (2001) fragility relation (percentages subjected to rounding errors)

Pipeline characteristic	Category	Description	Percentage of total database
Material type	AC	Asbestos cement	12.3
	CI	Cast iron	46.9
	CP	Concrete	2.5
	DI	Ductile iron	11.1
	MX	Mixed (CI & DI combined)	11.1
	S	Steel	16.0
Diameter	DS	Distribution system (mainly small diameter)	70.3
	LG	Large diameter (> 30.48cm)	9.9
	SM	Small diameter (\leq 30.48cm)	19.8

The distribution of data for different pipeline categories is summarized in Table 2.8. The full ALA (2001) dataset is plotted in Figure 2.16.

This includes the standard “backbone” fragility relationship based on a single-parameter linear model and lines representing the 16th and 84th percentiles of the data set. The “backbone” line defines the median slope of all 81 data points and has the property of having equal numbers of points above and below it. The line of median slope is a description of central tendency less sensitive to data outliers. The “backbone” fragility relation is expressed in Equation (2.17) and plotted in Figure 2.18.

Additional analyses were performed to assess the influence of earthquake magnitude, pipe material and pipe diameter on the pipe failure rate. Earthquake magnitude was taken as a surrogate measure for duration of ground shaking, with the implication that for a given value of PGV, pipe damage rate would be higher in regions experiencing longer duration of ground shaking. However, no meaningful relationship was identified from the available data.

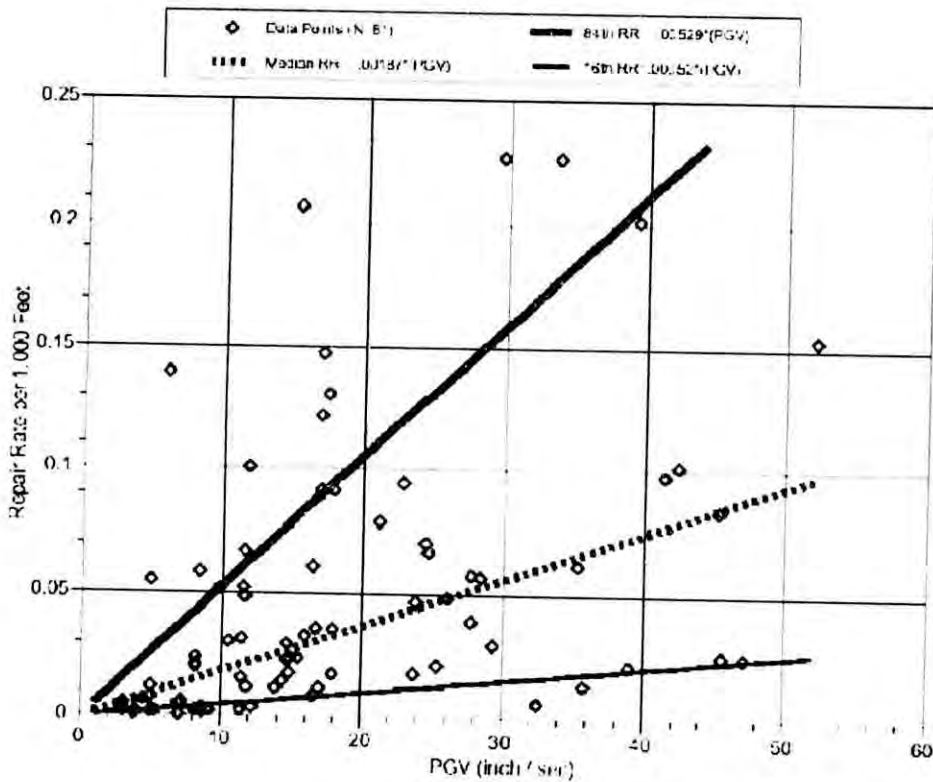


Figure 2.16 Data set used by ALA (2001) to derive pipeline vulnerability function for PGV. Median repair rate (RR) line defines standard “backbone” curve. Lines defining the 16th and 84th percentiles are included to illustrate the scatter.

The ALA (2001) investigation included details on application of the fragility relations for different pipe-joint-diameter-soil types and a discussion of scatter in the dataset, which is considerable.

2.6.2.9 Findings

For seismic risk analysis of water distribution systems, pipeline repair rates need to be related to earthquake effects as well as factors affecting pipeline vulnerability. Since the 1970's, attempts have been made to correlate earthquake intensity and various peak ground motion parameters with pipeline damage rates (given in terms of numbers of repairs per unit length of pipe). The resulting *fragility* relations can then be used for predictive purposes in estimating likely damage in the event of a future earthquake.

The earthquake performance of buried pipelines has been investigated by means of a detailed review of existing pipeline fragility relations. Specific emphasis is placed by Lain Tromans on identifying the size, origin and reliability of the datasets used. Results are presented of a post-earthquake investigation into water pipeline damage in the town of Düzce, Turkey, caused by two destructive earthquakes in 1999. The influence of various factors on the spatial distribution of water pipeline damage was examined using a Geographical Information System.

It is found that most of the fragility relations investigated did not consider the possible categories of pipe material and pipe diameter whereas these parameters play important role in the vulnerability of pipelines. It is also found that no new fragility relation is developed in the case of Duzce earthquake.

2.6.2.10 Lessons learned

The majority of pipeline fragility relations use either PGA or PGV as the predictor parameter. A selection of available relations for PGA are given in Table 2.9 and are plotted for comparison purposes in Figure 2.17, along with an indication of the range of applicability of each relation, where this could be estimated.

The predictions of Bresko (1980), based on the data of Katayama *et al.* (1975) are significantly greater than any of the other predictions for PGA above about 200 cm/s². The high values predicted reflect both the influence of permanent ground deformation effects and large uncertainties in the derivation of repair rates. The curves of Isoyama & Katayama (1982) and Isoyama *et al.* (2000) give similar predictions to each other in the range 120 - 300 cm/s². Much beyond this, the earlier study predicts significantly larger values of repair rate. The Isoyama & Katayama (1982) study is based on data from the San Fernando earthquake (Table 2.5a), which according to Bresko (1980), yielded pipeline repair rate data for the PGA range 170-330 cm/s² (Figure 2.17). Data from the Hyogoken-nanbu earthquake used by Isoyama *et al.* (2000) included data for PGA up to about 800 cm/s² and so is more reliable in the range 330 < PGA < 800 cm/s². In any case, the Isoyama *et al.* (2000) study is based on a much more reliable and comprehensive database than that of the earlier study.

Table 2.9 Pipeline fragility relations for PGA derived by several investigations. R_R denotes repair rate. PGA is measured in cm/s^2 .

Investigators	$RR = f(PGV)$	Notes
Katayama et al. (1975)	$10^{b+6.39 \log \text{PGA}}$ (2.9)	Mainly CI pipes. Data is from Katayama et al. (1975) for "average condition" ($b=3.65$)
Isoyama and Katayama (1982)	$1.698 \times 10^{-16} \text{PGA}^{6.06}$ (2.10)	CI pipes
O'Rourke et al. (1998)	$10^{1.25 \log \text{PGA} - 0.63}$ (2.11)	CI pipes
Isoyama et al. (2001)	$2.88 \times 10^{-6} (\text{PGA} - 100)^{1.97}$ (2.12)	CI pipes

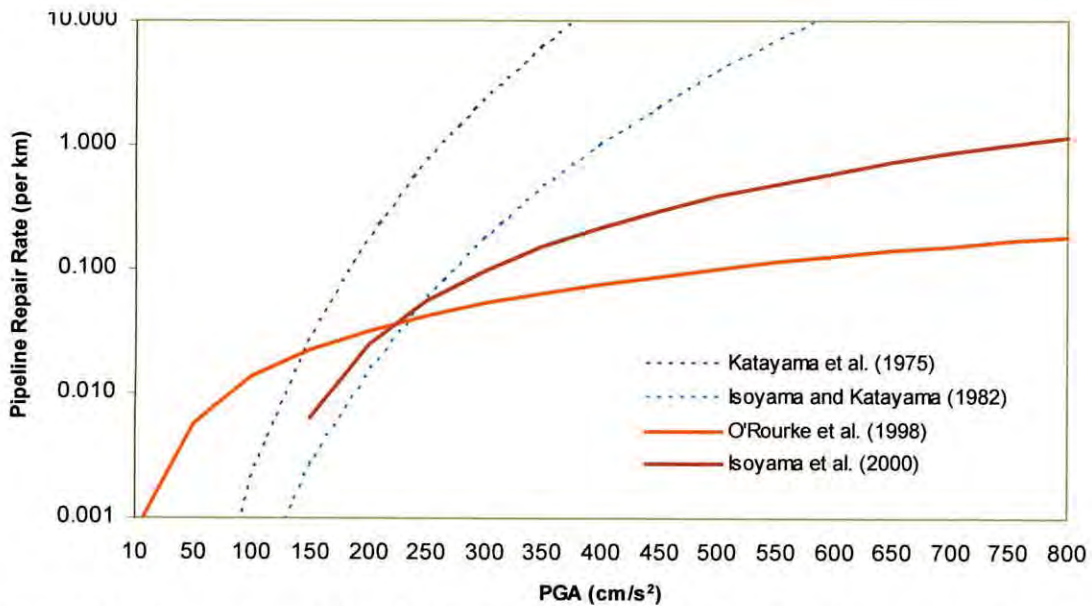


Figure 2.17 Comparison of the pipeline fragility relations for PGA expressed in Table 2.9.

The relation derived by O'Rourke *et al.* (1998) predicts high repair rates for low values of PGA. However, application of the relation to PGA values below about 90 cm/s^2 requires extrapolation beyond the limits of the dataset. For PGA greater than around 220 cm/s^2 , the O'Rourke *et al.* (1998) relation predicts lower repair rate values than the Japanese study. The two curves diverge significantly: the ratio of repair rates for the two relations at 400 and 800 cm/s^2 are 2.9 and 6.4 respectively. The reasons for this difference are not clear without more information on how the relations were derived.

Various PGV fragility relations are expressed in Table 2.10 and compared graphically in Figure 2.18.

Table 2.10 Pipeline fragility relations for PGV derived by several investigation. RR denotes repair rate. PGV is measured in cm/s.

Investigators	$R_R = f(PGV)$	Notes
Eidinger et al. (1995, 1998)	$K_1 0.0001658 PGV^{1.98}$ (2.13)	"best-fit" fragility relation ($K_1=1$), converted from imperial units to SI units
HAZUS (FEMA, 1999)	$0.0001 PGV^{2.25}$ (2.14)	"brittle pipes" fragility relation
Isoyama et al. (2000)	$3.11 \times 10^{-3} (PGV-15)^{1.3}$ (2.15)	CI pipes "standard curve"
O'Rourke et al. (2001)	$e^{1.55 \ln PGV - 8.15}$ (2.16)	CI pipes
ALA (2001)	$K_{1ALA} 0.002416 PGV$ (2.17)	"backbone" fragility relation ($K_{1ALA}=1$), converted from imperial units to SI units

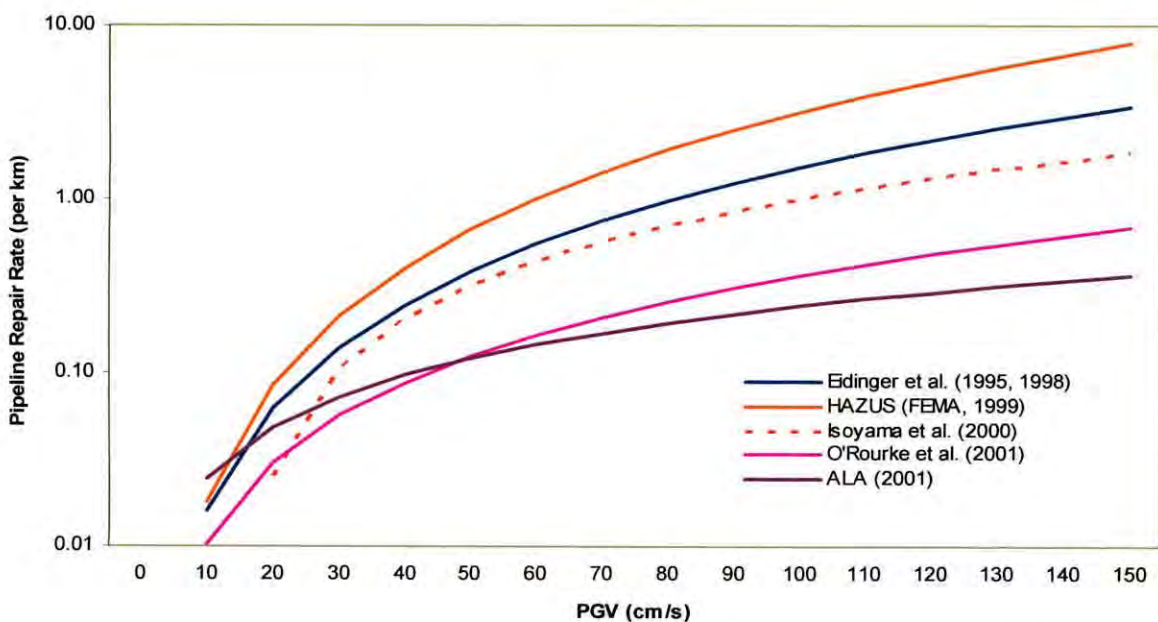


Figure 2.18 Comparison of the pipeline fragility relations for PGV expressed in Table 2.10.

The HAZUS curve, based on the data of O'Rourke & Ayala (1993) gives the highest predictions of pipeline repair rate for PGV greater than 15 cm/s. O'Rourke (1999) considers this fragility relation to be over-conservative, with pipeline repair rates being unduly affected by the long durations of ground shaking experienced during the Michoacan earthquake.

The Eidinger *et al.* (1995, 1998) and Isoyama (2000) relations predict repair rates within about a third of each other over the range $35 < PGV < 70$ cm/s. These predictions are

remarkably close for fragility relations, especially considering the fact that completely different data sets were used in each case. The disagreement at lower levels of PGV is largely

due to the assumption by Isoyama *et al.* (2000) of a lower PGV threshold for pipeline damage. The Eiding *et al.* (1995, 1998) relation has a much more limited range than that of Isoyama *et al.* (2000) and probably should not be extrapolated much beyond about 55 cm/s. The HAZUS relation is based on a dataset with a similarly restricted range. The curves of O'Rourke *et al.* (2001) and ALA (2001) are remarkably similar over a wide range of PGV values.

For the range of strong-motion values typically associated with destructive earthquakes, the variation in repair rate obtainable using different fragility relations is generally less for PGV than PGA (Figures 2.9 and 2.10). This suggests that PGV may be a better predictor of earthquake-induced pipeline damage than PGA. However, many factors have contributed to the scatter observed among the various fragility relations and a more quantitative investigation is required to draw more firm conclusions.

The investigations of O'Rourke *et al.* (1998, 2001) and Isoyama *et al.* (2000) suggest that PGV is more effective than PGA for the prediction of pipeline damage caused by earthquake-induced ground shaking. That this should be the case has been suspected for a long time. Newmark (1967) highlighted the close connection between ground strain and PGV and this served as the motivation for the first PGV fragility relation (Barenberg, 1983). Measures of ground acceleration (although not necessarily the *peak* ground acceleration) are of more relevance in predicting damage to aboveground structures, for which inertial forces are much more important.

Pipeline fragility relations have improved considerably over recent years and are useful for damage prediction. For general application, the PGV relation of ALA (2001) is recommended as it is derived from a global database.

Although it has been shown that PGV is a better predictor parameter for pipeline damage than PGA, it is nevertheless useful to have PGA fragility relations because of the widespread use of this parameter in earthquake risk assessment. It should be stressed, however, that wherever possible, predictions of pipeline damage should be made from PGV estimates.

2.7 SUMMARY

The purpose of this chapter was to review the response of buried water supply pipeline due to ground shaking and site effects. Factors affecting earthquake vulnerability is also reviewed. A thorough review work is done on existing empirical relations such as Katayama (1975), O'Rourke (1982), Isoyama & Katayama (1998) and Isoyama (2000) for the prediction of earthquake-induced pipeline damage and finally a comparison is made among the selected fragility relationships.

CHAPTER THREE

MICROZONATION OF DHAKA CITY

3.0 GENERAL

Seismic microzonation is important for hazard assessment of an area due to earthquake. Seismic hazards due to local site effects such as soil amplification and liquefaction can be estimated by combining the available soil parameter data with the current hazard models or by making use of existing maps showing estimated models of levels of these collateral hazards. Due to recent improvement in the availability and quality of GIS technology, tabular database software, as well as computer hardware, a significant amount of current research is devoted incorporating GIS technology in seismic microzonation for Dhaka city. In this chapter geotechnical characteristics of Dhaka city (Bashar, 2004) is reviewed and by reviewing the outcome of an extensive research work done by Rahman, Gazi Md. Ferooz (2000) a seismic microzonation map of Dhaka city is adopted.

3.1 GEOGRAPHICAL SETTING OF THE CITY

Dhaka the capital city of Bangladesh, was founded about 400 years ago by the side of the river Buriganga. The earliest available map shows Dhaka extending over an area of about 1.5 sq km near the junction of the Dholai Khal and Buriganga river. Large scale urbanization was initiated by the British Raj in 1904 when Dhaka was made the capital of East Bengal, a newly created province of British India. Dhaka gained city status in 1947 when it was made the capital of East Pakistan and by that time stretched over an area of about 40 sq km. The importance of Dhaka increased exponentially after 1971, phenomenally and according to the census of 1991 the area and population of Dhaka Megacity or Dhaka Statistical Metropolitan Area (DSMA) were 1,600 sq km and 6.83 million respectively. According to the same census the area under the Dhaka city corporation was 360 sq km, with a population of 3.39 million. The present population of DSMA is about 9.0 million (2001)

Dhaka is situated between latitudes 23°42' and 23°54'N and longitudes 90°20' and 90°28'E. The city is bounded by the rivers Buriganga to the south, Turag to the west, Balu to the east,

and Tongi Khal to the north. The city has three distinct seasons: winter (November-February), dry with temperatures ranging from 10° to 20°C; the pre-monsoon season (March-May), with some rain and hot temperature reaching up to 40°C; and the monsoon (June-October), which is very wet with temperatures around 30°C. Dhaka experiences about 2,000 mm of rain annually, of which about 80% falls during the monsoon.

Urbanization in Dhaka is restricted mostly to the north bank of the river Buriganga. The four-hundred-year history of Dhaka city can be divided into five different stages of development: Pre-Mughal period, Mughal period, British period, Pakistan period, and Bangladesh period.

3.2 GEOLOGY OF THE STUDY AREA

Quaternary sediments consisting of deltaic and alluvial deposits of the Ganges, Brahmaputra and Meghna rivers and their numerous tributaries underlie more than 80% of Bangladesh. According to the study of Morgan and McIntire (1959), there are two major areas of Pleistocene sediments, commonly known as Madhupur tract and Barind tract. The Madhupur block lies between the Jamuna and Old Brahmaputra rivers and 6 to 30 m above the mean sea level. Madhupur tract is bounded by faults; they appear to be uplifted and structurally complex; the Madhupur block has been tilted eastward (Morgan and McIntire, 1959). The study area is situated on the southern tip of the Madhupur tract. Two characteristic units cover the city and its surroundings, i.e., the Madhupur clay of Pleistocene age and alluvial deposits of recent age. The Madhupur clay is the oldest sediment exposed in and around the city area. The alluvial deposits are characterised by flood plains, depression and abandoned channels. The geological map of Dhaka metropolitan area is presented in Figure 3.1.

The subsurface sedimentary sequence, up to the explored depth of 300m, shows three distinct entities; one is the Madhupur clay formation of Pleistocene age and is characterized by reddish plastic clay with silt and very fine sand particles. This Madhupur clay formation uncomfortably overlies the Dupi Tila formation of Pleistocene age composed of medium to coarse yellowish brown sand and occasional gravel. The incised channels and depression within the city are floored by recent alluvial flood plain deposits and is further subdivided into lowland Alluvium and high land Alluvium (WASA 1991)

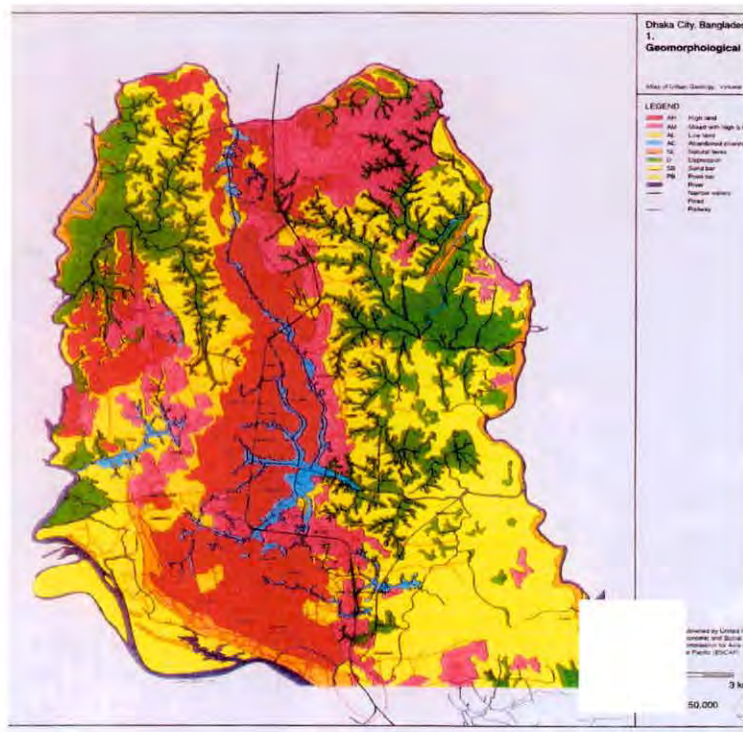


Figure 3.1: Geological map of Dhaka metropolitan area (after GSB, 1991)

Geotechnical Characteristics of the Madhupur Clay in Dhaka city and its surroundings vary significantly both aerially and vertically. The evaluated parameters, particularly its low strength and high compressibility values indicate that the clay, to some extent, is problematic for engineering construction. The moisture content and plastic limit results show that Madhupur Clay is normally consolidated to overconsolidate. The clay is normal to active and has intermediate to high plasticity. The compressibility values suggest that the clay ranges from very low to highly compressible at different locations.

The Dupi Tila sands aquifer is the main source of water in Dhaka city. Madhupur Clay overlies the aquifer with a thickness of 8 to 45 m (averaging 10 m). The aquifer varies in thickness from 100 to 200 m (averaging 140 m). Groundwater occurs at a depth of 25 to 30 m in the central part of the city. In the periphery the ground water lies at a depth of 15 to 20 m. Under the present conditions the peripheral rivers act as sources of recharge where the Dupi Tila sands are exposed along the riverbeds. Other sources of recharge are vertical percolation of rain and flood water, leakage from water mains and the sewer system, and seepage from standing water bodies within the city.

3.3 REGIONAL TECTONICS

Bangladesh lies in the Burma basin, which was formed by the continent-continent collision of India to the north, and subduction of ocean crust beneath the Burma continental crust to the east. Bangladesh is surrounded by regions of high seismicity, which include the Himalayan Arc and Shillong Plateau in the north, the Burmese Arc, Arakan Yoma anticlinorium in the east, and complex Naga-Disang-Haflong thrust zone in the northeast shown in Figure 3.2.

The Dhaka city area does not show any surface folding. However, a large number of faults and lineaments have N-S, E-W, NE-SW, NW-SE trends recognized from air photo interpretation and the nature of the stream courses. All four sides of the city are bounded by major faults.

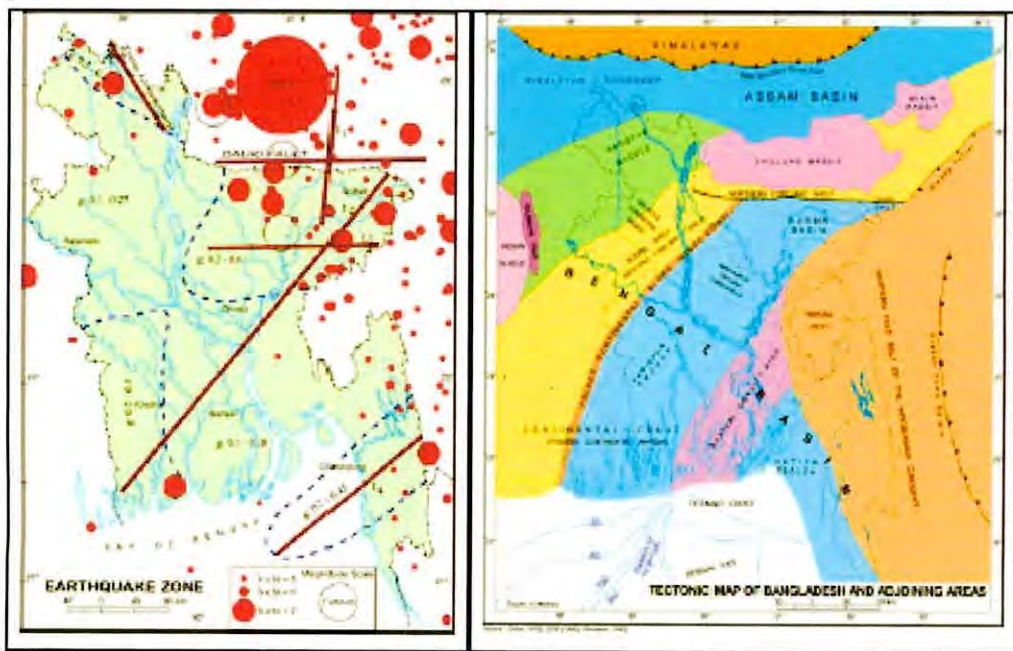


Figure 3.2 : Seismo-tectonic lineaments capable of producing damaging earthquakes (after Banglapedia, 2004)

The country has a long history of seismic activity related to its proximity to the Himalayas. Three great earthquakes of magnitudes exceeding 8 were felt in 1897, 1934, and 1950, and another four earthquakes exceeding magnitude 7 were felt between 1869 and 1950. Major seismic sources are the Meghalaya (8.0), Tripura (7.0), Sub-Dauki (7.3), and Bogra (7.0), all of them with associated earthquakes of expected magnitudes higher or equal to 7.0.

The major earthquakes that have affected Bangladesh since the middle of the last century is presented in Table 3.1.

Table 3.1: Great historical earthquakes in and around Bangladesh

Date	Name	Epicentre	Magnitude (M)
10-01-1869	Cachar Earthquake	Jantia Hill, Assam	7.5
14-07-1885	Bengal Earthquake	Sirajgonj, Bangladesh	7.0
12-06-1897	Great Indian Earthquake	Shillong Plateau	8.7*
18-07-1918	Srimangal Earthquake	Srimangal, Sylhet	7.6
02-07-1930	Dhubri Earthquake	Dhubri, Assam	7.1
15-01-1934	Bihar-Nepal Earthquake	Bihar, India	8.3

* Recently modified as 8.1(M) (Ambraseys, 2001)

Bolt (1987) analyzed different seismic sources in and around Bangladesh and arrived at conclusions related to maximum likely earthquake magnitude (Bolt, 1987). Bolt identified the following four major sources:

- (i) *Assam fault zone*
- (ii) *Tripura fault zone*
- (iii) *Sub- Dauki fault zone*
- (iv) *Bogra fault zone*

Reliable historical data for seismic activity affecting Indian subcontinent is available only for the last 450 years (Gupta et al., 1982). Recently developed earthquake catalogue for Bangladesh and surrounding area (Sharfuddin, 2001) showed that 66 earthquakes with $M_s \geq 4.0$ occurred from 1885 to 1995 within a 200 km radius of Dhaka City. The most prominent historical earthquakes affecting Dhaka is listed in Table 3.2.

Table 3.2 Magnitude, EMS Intensities and distances of some major historical earthquakes around Dhaka (after Ansary, 2001 & 3CD City Profiles Series)

Date	Name of Earthquake	Magnitude (Richter)	Intensity at Dhaka (EMS)	Epicentral Distance from Dhaka(km)
10 January, 1869	Cachar Earthquake	7.5	V	250
14 July, 1885	Benbal Earthquake	7.0	VII	170
12 June, 1897	Great Indian Earthquake	8.7	VIII+	230
8 July, 1918	Srimangal Earthquake	7.6	VI	150
2 July, 1930	Dhubri Earthquake	7.1	V+	250
15 January, 1934	Bihar-Nepal Earthquake	8.3	IV	510
15 August, 1950	Assam Earthquake	8.5	IV	780

3.4 SEISMIC ZONING MAP OF BANGLADESH

The seismic zones and zone coefficients may be determined from the earthquake magnitude for the various return periods and the acceleration attenuation relationship. It is required that for the design or ordinary structures, seismic ground motion having 10% probability of being exceeded in design life of a structure (50 years) is considered critical. An earthquake having 200 years return period originating in Sub-Dauki zone have epicentral acceleration of more than 1.0g but at 50 kilometers the acceleration shall be reduced to as low as 0.3g. In the Bogra fault system, earthquakes having 200 year return period have a value of only 7.3 and at 50 kilometer distance, the acceleration shall be reduced to a value of less than 0.1g. Ali (1998) presented the earthquake base and seismic zoning map of Bangladesh. Tectonic framework of Bangladesh and adjoining areas indicate that Bangladesh is situated adjacent to the plate margins of India and Eurasia where devastating earthquakes have occurred in the past. Non-availability of earthquake, geologic and tectonic data posed great problem in earthquake hazard mapping of Bangladesh in the past. The first seismic map which was prepared in 1979 was developed considering only the epicentral location of past earthquakes and isoseismal

map of very few of them. During preparation of National Building Code of Bangladesh in 1993, substantial effort was given in revising the existing seismic zoning map using geophysical and tectonic data, earthquake data, ground motion attenuation data and strong motion data available from within as well as outside of the country. Geophysical and tectonic data were available from Geological Survey of Bangladesh. Earthquake data were collected from NOAA data files and Geodetic Survey, U.S. Dept. of Commerce.

Seismic zoning map for Bangladesh has been presented in Bangladesh National Building Code (BNBC) published in 1993. The pattern of ground surface acceleration contours having 200 year return period from the basis of this seismic zoning map. There are three zones in the map — Zone 1, Zone 2 and Zone 3. The seismic coefficients of the zones are 0.075g, 0.15g and 0.25g for Zone 1, Zone 2 and Zone 3, respectively. Bangladesh National Building Code (1993) placed Dhaka City area in Seismic Zone 2 as shown in Figure 3.3. The seismic zones in the code are not based on the analytical assessment of seismic hazard and are mainly based on the location of historical data. An updated seismic zoning map as shown in Figure 3.4 based on analytical studies was recently developed by Sharfuddin, (2001). This zoning was based on consistent ground motion criterion such as equal peak ground acceleration levels. In this map also Dhaka City has been placed Zone 2. This map also has been three zones namely — Zone 1, Zone 2 and Zone 3. The seismic coefficients are also the same as in the map presented by BNBC (1993). The only modifications are is the zone areas. From both maps, it is seen that Dhaka city belongs to Zone 2 where the seismic coefficient is 0.15g.

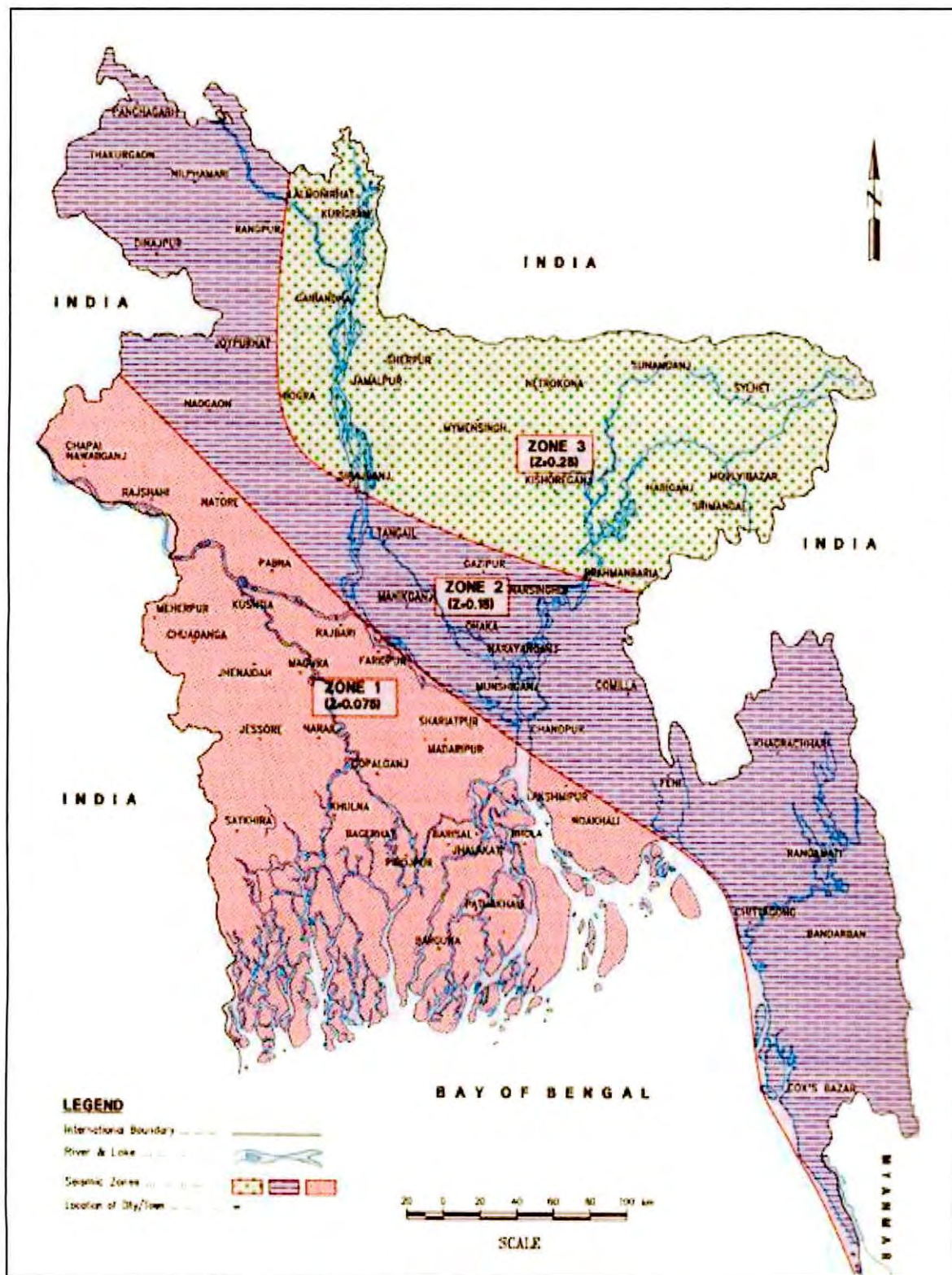


Figure 3.3 Seismic zoning map of Bangladesh (after BNBC, 1993)

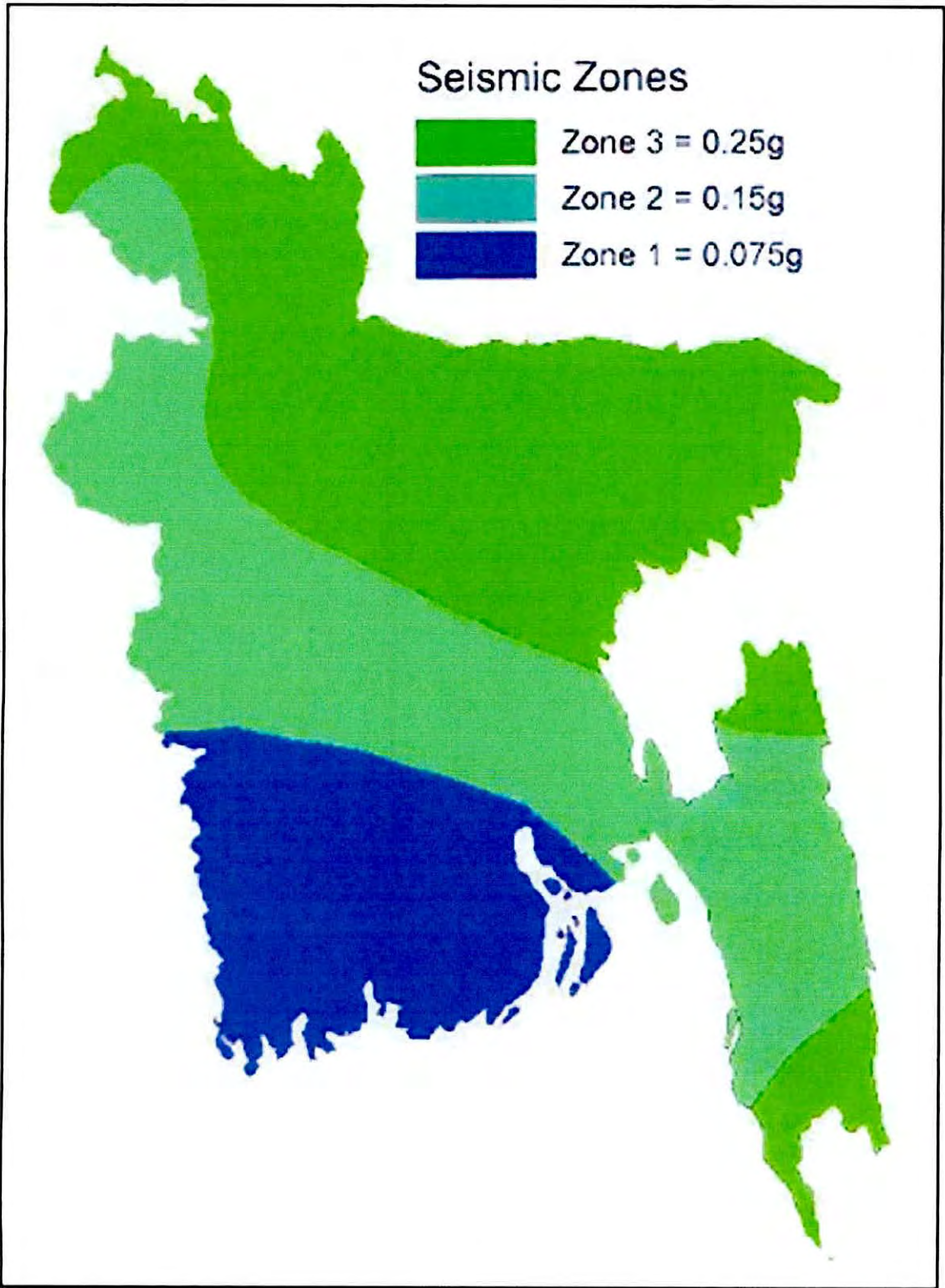


Figure 3.4 Seismic zoning map of Bangladesh (after Sharfuddin, 2001)

3.5 MICROTREMOR INVESTIGATION OF SITE EFFECTS

Microtremor observation was carried out at different locations (120 in all) in Dhaka city during 2002 (Ansary, 2003). The equipment used was Tokyo Buttan Services GEODAS-10-24DS system connected to a triaxial accelerometer with a natural period of 1 second. In that experiment, the recording system operated continuously for about 6 minutes, with a sampling rate of 100 Hz. For the analysis of microtremors, base line corrections were done and then a Butterworth band pass filter (0.40 to 25 Hz) was applied to the data. From the processed data sixteen 2048 point windows were selected and Fourier Spectra for NS, EW and UD components were computed with a Parzen window. Then the mean curve for sixteen spectra both for NS and EW components were calculated. Finally, the Nakamura spectral ratio as suggested by Equation (3.1) was obtained as follows:

$$HV = \frac{\sqrt{NS} \sqrt{EW}}{UD} \quad (3.1)$$

To validate the results obtained from microtremor observations, *H/V* spectral ratios were compared with the transfer functions obtained from a one-dimensional numerical simulation using the computer program SHAKE, which consists of the response analysis of horizontally layered soils under seismic excitation, with linear equivalent soil behavior. Similar transfer functions from soil column using SHAKE were also estimated for areas where no microtremor observations were made.

Use of geotechnical data for each of the sites and a synthesis of drilling data extracted from the existing subsurface database of Dhaka enabled to determine soil columns representative of each site. In most of the soil columns, a dense sand layer was encountered at a depth of 30 m and in some cases, silty clay layer was found. Soil columns of eight sites, for which *H/V* spectral ratio and SHAKE transfer functions were compared.

Using the soil configurations a transfer function was calculated for each site using the SHAKE numerical code. In addition, recordings of background noise by microtremor observations for each site were used to calculate average *H/V* spectral ratios. The amplification and the fundamental frequency obtained by the two methods are almost similar for all sites studied. Figure 3.5 shows map of amplification at fundamental frequencies of Dhaka City.

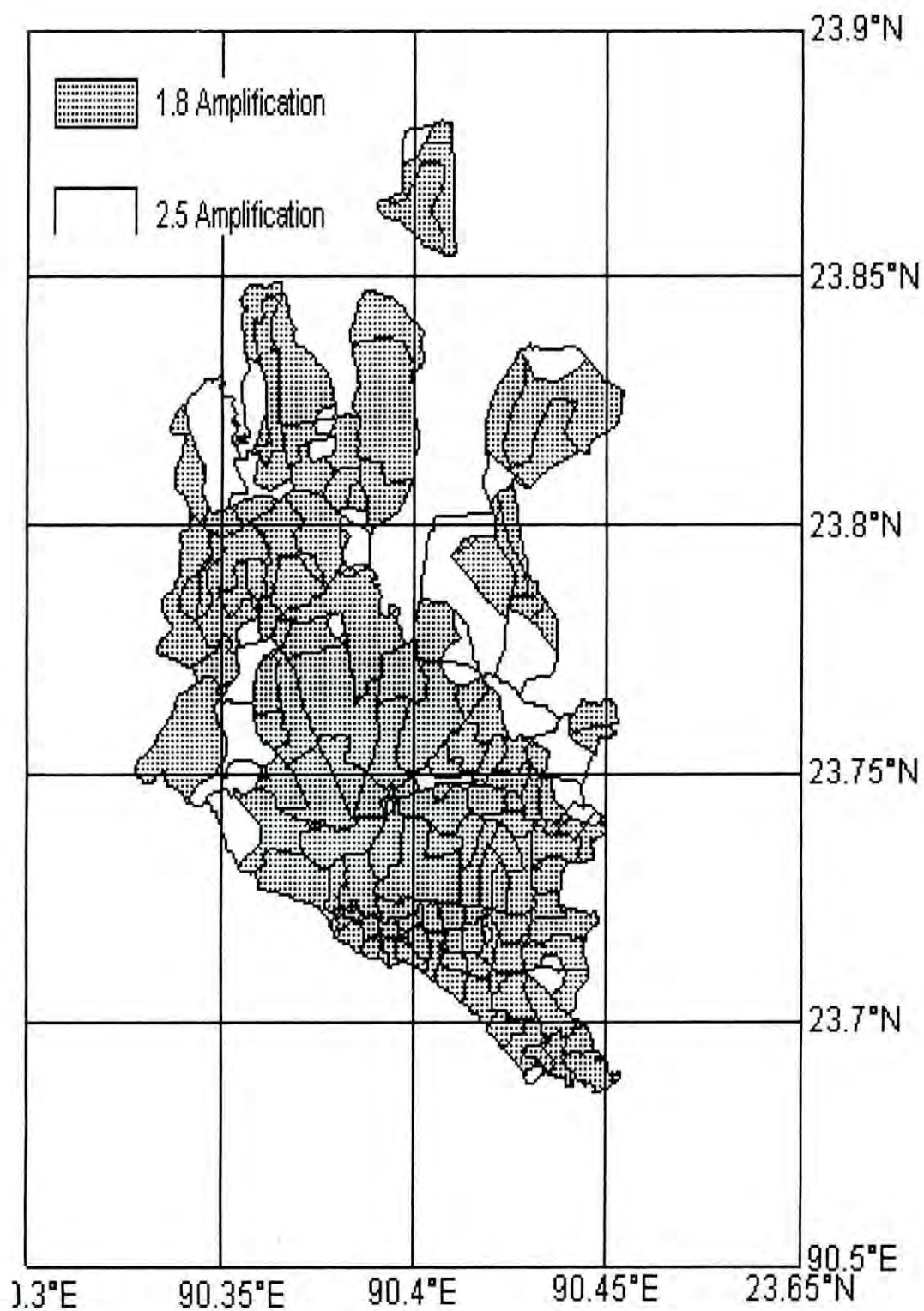


Figure 3.5: Map of 1.8 and 2.5 times amplified areas (after Rahman, 2004)

Bangladesh including Dhaka is largely an alluvial plain consisting of loose fine sand and silt deposits. Although the older alluvium consisting of mainly silty clay with deeper ground water table is less susceptible to liquefaction, the recent deposits consisting of loose fine sand with shallower water table along the river flood plains may liquefy during a severe earthquake. The ground water table is quite deep (20 to 25 m) in most places except the areas near the rivers. Clearly liquefaction is a serious component of the earthquake hazard in certain parts of Dhaka as indicated by Ansary and Rashid (2000) and needs to be considered.

The total area of Dhaka city are classed into two categories, one is liquefiable area and another is non-liquefiable. Figure 3.6 shows the map of liquefied areas and not liquefied areas.

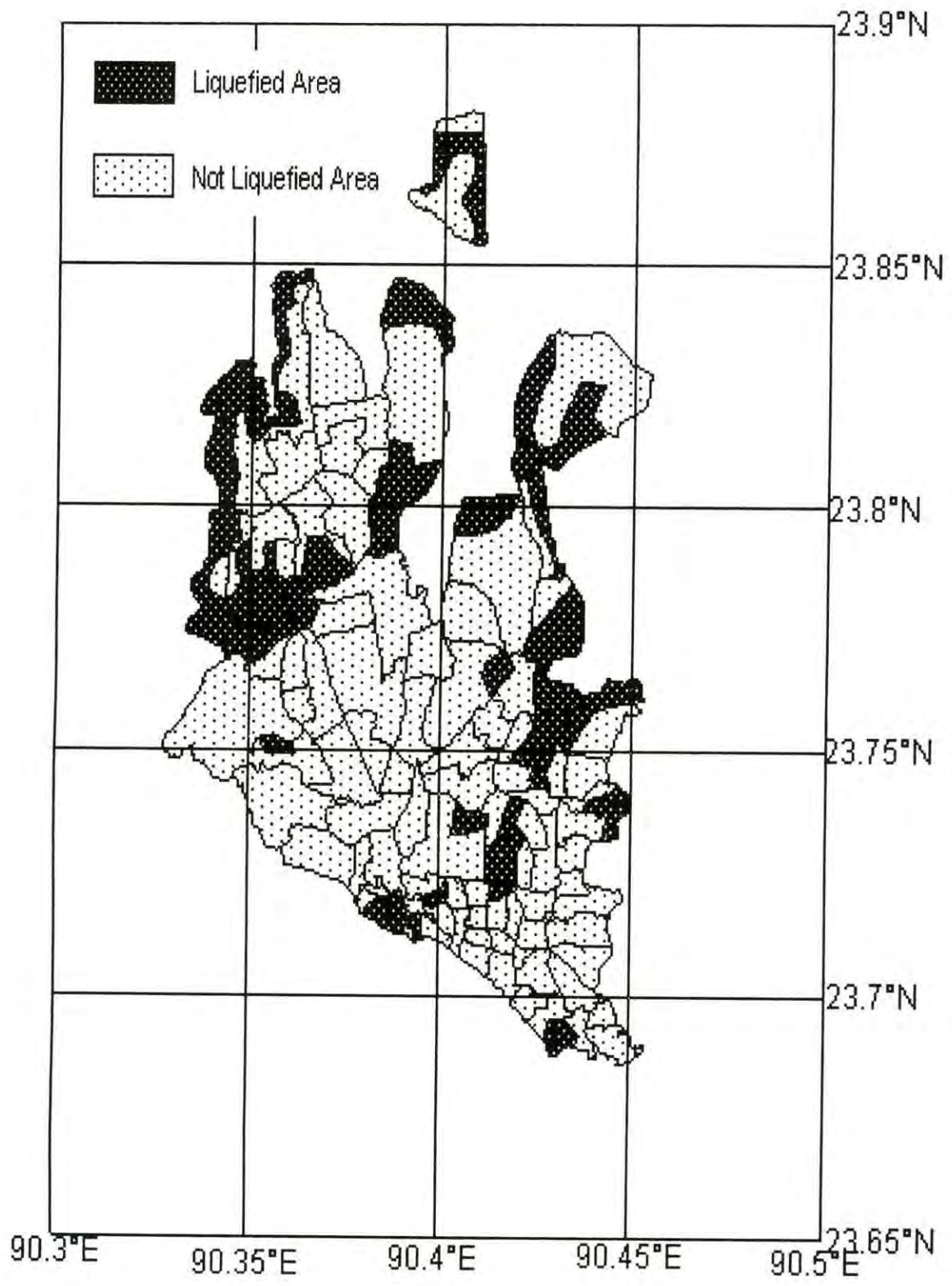


Figure 3.6: Map showing liquefied areas and non-liquefied areas (after Rahman, 2004)

3.6 GEOTECHNICAL CHARACTERISTICS OF DHAKA CITY

Geotechnical characterization is important for understanding the soil behavior. A rigorous study was carried out (Bashar 2004) to develop generalized soil profiles of Dhaka Metropolitan area. Attempt was made to investigate the variation of the soil properties with depth and to establish approximate correlation among different geotechnical properties of the sub-soil of the Dhaka M.

About 300 sub-soil investigation reports consisting of data of 674 boreholes were collected from different drilling companies, civil consulting firms and other organizations of different places of DMP area. Majority of the borings were drilled up to depth of 50 ft to 60 ft and a few borings were drilled up to 100 ft. Dhaka city map, bounded by longitude 90 deg 20' to 90deg 27'E and 23deg41' to 23deg53'N, has been divided into grids by four longitudinal grid lines A-A', B-B', C-C' and D-D' along North-South direction and five cross grid lines 1-1', 2-2', 3-3', 4-4' and 5-5' along East-West direction to establish soil profiles along these grid lines which are shown if Figure 3.7. These grid lines were spaced at 2 minutes interval. All borehole site location points were inserted on the Dhaka city map. One site location point consists of multiple numbers of boreholes. Under the scheme of research, seven test borings of 100 ft depth were drilled in the vicinity of the grid points.

The longitudinal soil profile along grid line A-A' include the area Digun, Agunda, Rupnagar Housing(part), Mirpur Section-1, Jahurabad, Harirampur, Gabtoli, Adabar, Baitulaman, Mohammadpur (partly), Northern part of Mirpur such as Digun and Agunda are low land used as agriculture land. Longitudinal soil profile along grid A-A' is shown in Fig. 3.8

The longitudinal soil profile along grid line B-B', staring from north include the areas such as Uttara, Sector 12, Sector-14, then low land Bhasantek, Baunia, Mipur (Sector-10, Sector-11, Sector-12, Sector-13, Sector-14), Senpara, Ibrahimpur, Sewrapara, Sher-e-Bangla Nagar, Tejgoan, Mohammadpur Lalmatia, Raja Bazar, Kalabhagan, Dhanmondhi, Azimpur, Bhakhshibazar, Lalbagh and Charkamrangi soil profiles have been established. as shown Fig. 3.9.

The longitudinal soil profile along grid line C-C' line passes through the area of Uttarkhan, Dakhin Khan Uttara, Sector 4, Sector-6, Khikhet, Joar Shahara, Nadda kalachandpur, Bharidhara, Gulshan, Badda, Rampura, Tejgoan, Maghbazar, Malibagh, Siddeswari, Segunbaghicha, Motijheel, Gulistan, Wari, Sutrapur and Postaghola Fig 3.10 shows soil profile through C-C' grid line.

The longitudinal soil profile along grid line D-D', starting from north include the areas such as Satarkul, Kajla and Mothertak. soil profiles have been established as shown Fig 3.11.

The cross profile along grid line 1-1', starting from west include the areas such as Nawabchar, Char Kamrangi, Lalbagh, Couul Bazar, Wari, Jatrabari and Kajla. soil profiles have been drawn as shown Fig 3.12.

The cross profile along grid line 2-2', starting from west cover the areas such as Basila, Lalmatia, Kalabaghan, Kaoran Bazar, Malibagh, Khilgaon and Mathertak. The soil profile along grid line 2-2' is shown in Fig. 3.13.

The cross profile along grid line 3-3', starting from west include the areas such as Gabtali, Kallyanpur, Kafrul, Moakhali, Gulshan, Badda and Satarkul. The soil profile along grid line 3-3' is shown in Fig. 3.14.

The cross profile along grid line 4-4', starting from west include the areas such as Botanical Garden, Mirpur-7, Mirpur-11, Bashantek, Joar Sahara and Bashundhara. Fig. 3.15 presents the soil profile along grid line 4-4'.

The cross profile along grid line 5-5', starting from west mainly include the areas Uttara. Gaor and Dhakinkhan. Fig. 3.16 presents the soil profile along grid line 5-5'.

Soil profiles established for Dhaka M area, in general, showed soft to very stiff cohesive layers at the top strata up to depth of 20ft to 60 ft. at large depths, the soil layers have been found to consist of loose to very dense sand soils. In some areas of the eastern region of DMP, however, cohesive layers up to depth of 100ft have been encountered. Range of the values of different soil parameters near the locations of sixteen grid points of DMP area has

been summarized. The soil parameters considered are N-value, liquid limit, plasticity index, natural moisture content, grain size fractions (percentages of sand, silt and clay), unconfined compressive strength, compression index and initial void ratio.

Geotechnical properties of the sub-soil of DMP area were found to vary with depth. In general, water content, liquid limit and plasticity index decrease with the increase in soil depth. The percentage of coarser material increases with the increase in soil depth.

3.7 SEISMIC MICROZONATION MAP OF DHAKA CITY

To mitigate/understand the seismic hazard a map of hazard assessment is required in which locations or zones with different level of hazard potential are identified. Seismic hazards due to local site effects such as soil amplification and liquefaction can be estimated by combining the available soil parameter data with the current hazard models or by making use of existing maps showing estimated models of levels of these collateral hazards. In order to establish such seismic microzonation map an extensive work was carried out by Rahman, Md. Gazi Ferooz (2000) where a soil database of 253 boreholes is developed. The soil data are used to develop site amplification and soil liquefaction potential assessment. Both of these site effects are integrated in Geographical Information System (GIS) platform for combined hazard assessment. Three past historical earthquakes are used as scenario events namely 1885 Bengal earthquake, 1897 Great Indian earthquake and 1918 Srimangal earthquake. Intensity value obtained for these events is calibrated against attenuation laws to check the applicability of the laws for this study. Using these laws, bedrock Peak Ground Acceleration (PGA) values are obtained. Finally, a bedrock PGA value for the scenario events is selected. PGA values are also converted into intensity values to integrate the effect of site amplification as well as liquefaction.

Every analysis region is different; therefore the quantification of the secondary site effects and the weighting scheme for combining the various seismic hazards is heuristic, based on judgment and expert opinion about the influence of local site conditions in the region and the exactness of the available geologic and geotechnical information.

At first the bedrock-level ground shaking in the region was ascertained. The shaking was depicted in terms of peak ground motion values.

It is decided that the final combined seismic hazard would be quantified in terms of Modified Marcelli Intensity (MMI). There are several relationships for converting PGA to MMI. The equation used here is developed by Trifunac and Brady (1975). The following heuristic rules are used to quantify the seismic hazard attributable to liquefaction:

For regions with liquefiable soils with high liquefaction potential

$$MMI_{LIQ} = MMI_{GS} + 2$$

For regions with liquefiable soils with moderate liquefaction potential

$$MMI_{LIQ} = MMI_{GS} + 1 \text{ and otherwise:}$$

$$MMI_{LIQ} = 0$$

The rules for combining the assorted hazards are based on expert opinion (after Stephanie and Kiremidjian, 1994) about the comparative precision of the hazard information and the behavior of the local geology. For this study, two potential combinations were considered and their assumed weights are shown in Table 3.3. The final combined hazard (MMI_F) is computed as a weighted sum of the various hazards. By over-laying the regional maps for each hazard as shown in Figures 3.5 and Figure 3.6 in GIS environment, the Dhaka City had been separated into four groups as areas of 1.8 times amplification, areas of 2.5 times amplification, areas of 1.8 times amplification plus liquefaction and areas of 2.5 times amplification plus liquefaction. And lastly, Figure 3.17, the regional distribution of the final combined seismic hazard (MMI_F) was produced.

107236

Table: 3.3 Quantification rules for seismic hazard (after Stephanie and Kiremidjian, 1994)

Rule	Possible hazards	Weighting scheme for Final combined hazard MMI_F
(a)	Ground shaking	$MMI_F = MMI_{GS}$
(b)	Ground shaking + Liquefaction	$MMI_F = .55 MMI_{GS} + .45 MMI_{LIQ} + .5$

Notes:

1. MMI_F = Final Combined Hazard
2. MMI_{GS} = Ground Shaking Hazard
3. MMI_{LIQ} = Liquefaction Hazard
4. MMI_F must be less than or equal 12

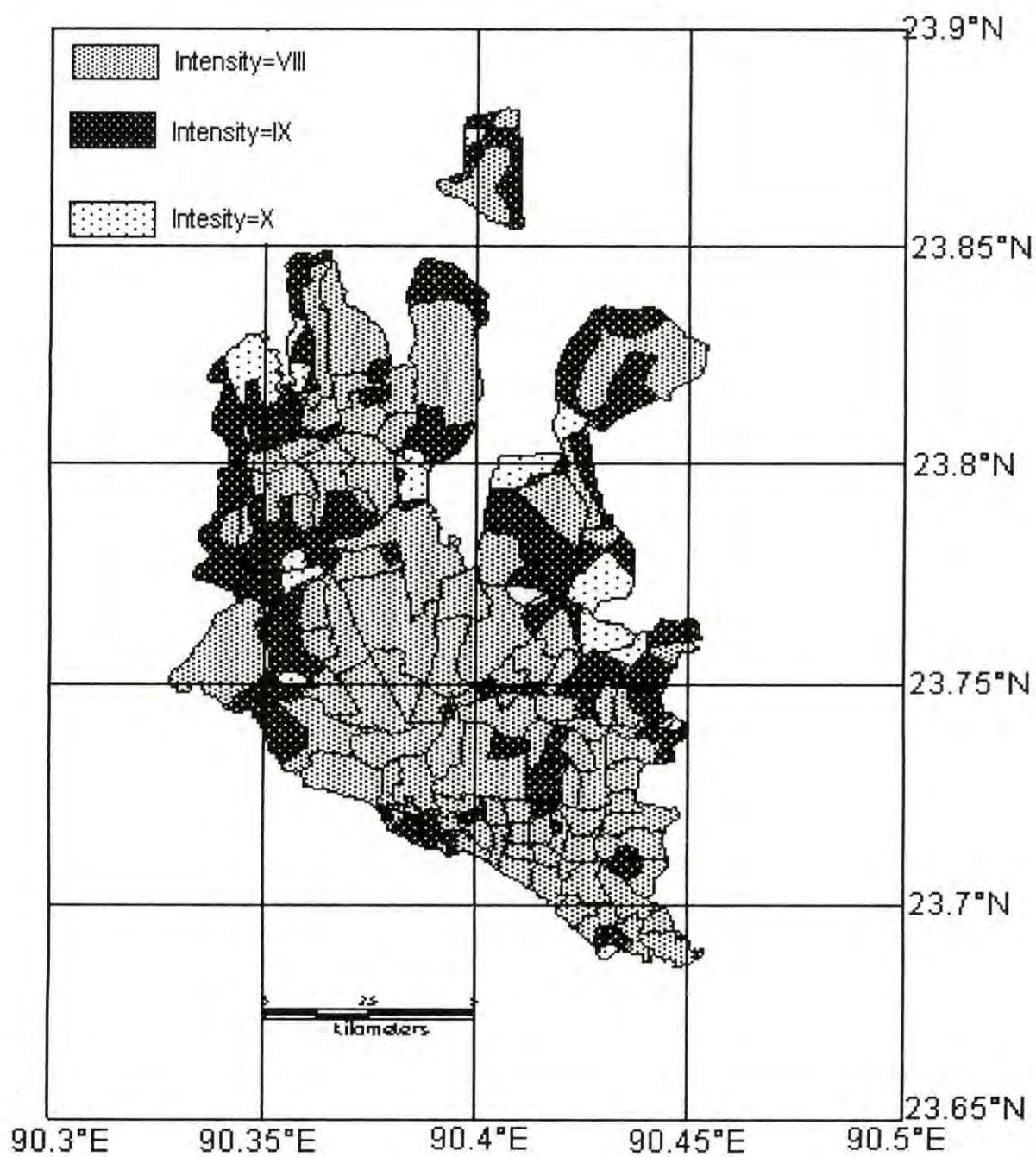


Figure 3.17: Combined hazard intensity map (after Rahman, 2004)

3.8 SUMMARY

The objective of this part of thesis was to introduce seismic microzonation of Dhaka city with a view to assessing regional multi-hazard seismic risk. In this work, the seismic risk analysis included consideration of primary hazards due to ground shaking and to local site effects such as soil amplification and liquefaction. A soil database of 253 boreholes (Rahman Gazi Md. Ferooz, 2000) were used to develop site amplification and soil liquefaction potential maps of the city. Both of these site effects are integrated in Geographical Information System (GIS) platform for combined hazard assessment. The GIS-based analysis is useful to engineers, planners, emergency personnel, government officials, and anyone else who may be concerned with the potential consequences of seismic activity in a given region. The results of a regional seismic hazard and risk analysis are usually presented in the form of microzone maps that serve as an effective means of transferring information from the scientific community to the professional community of decision makers involved in hazard and risk mitigation

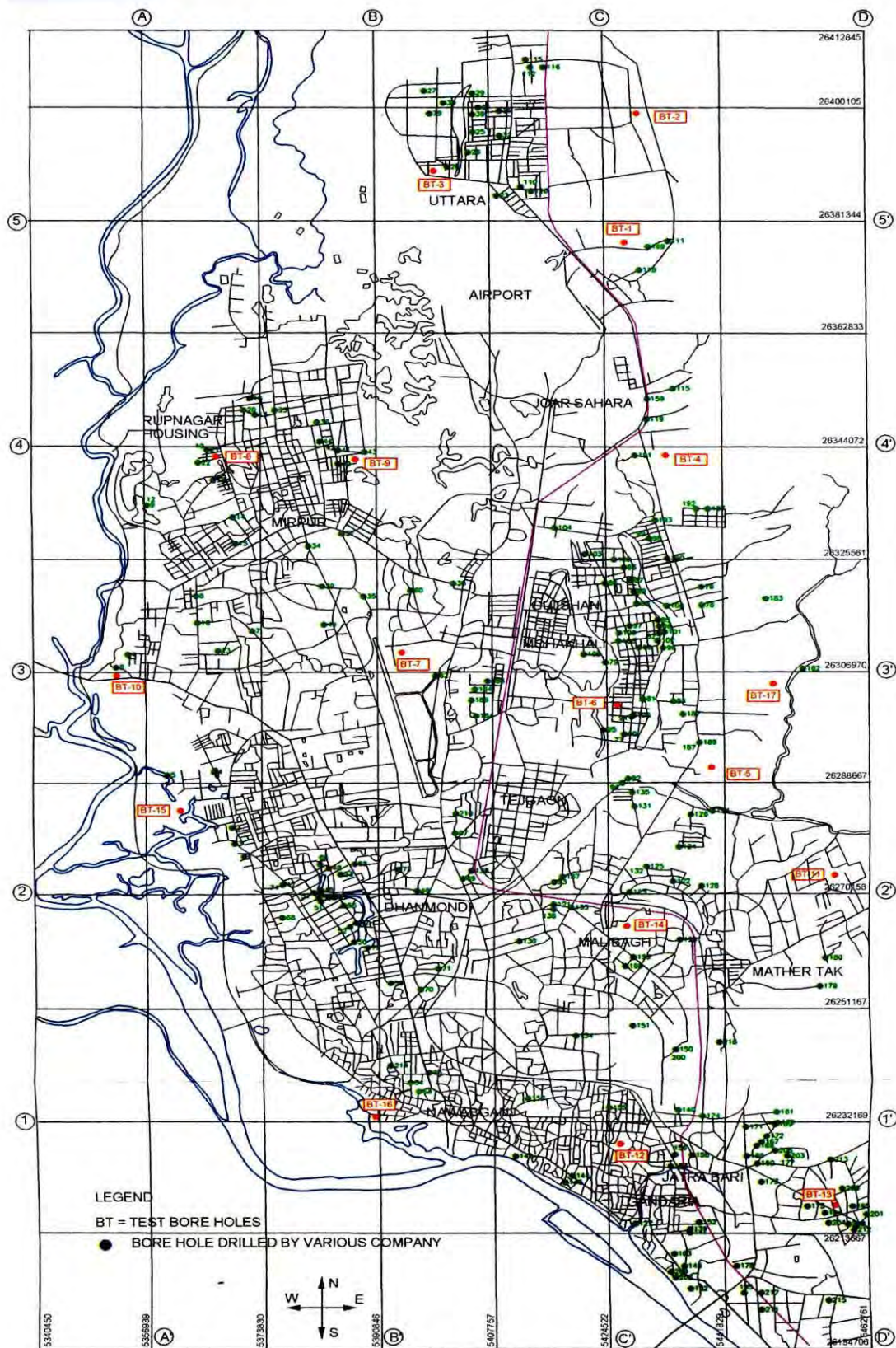


Figure 3.7 Map of Dhaka City Showing Borehole Locations (GRIDS ARE EXPRESSED IN KILOMETER) [after Bashar, 2004]

CLASS	SYMBOL	DESCRIPTION TERM	N-VALUE FROM SPT
S1		VERY LOOSE	0-4
S2		LOOSE	4-10
S3		MEDIUM DENSE	10-30
S4		DENSE	30-50
S5		VERY DENSE	>50

CLASS	SYMBOL	DESCRIPTION TERM	N-VALUE FROM SPT
C1		VERY SOFT	0-2
C2		SOFT	2-4
C3		MEDIUM STIFF	4-8
C4		STIFF	8-15
C5		VERY STIFF	15-30
C6		HARD	>30

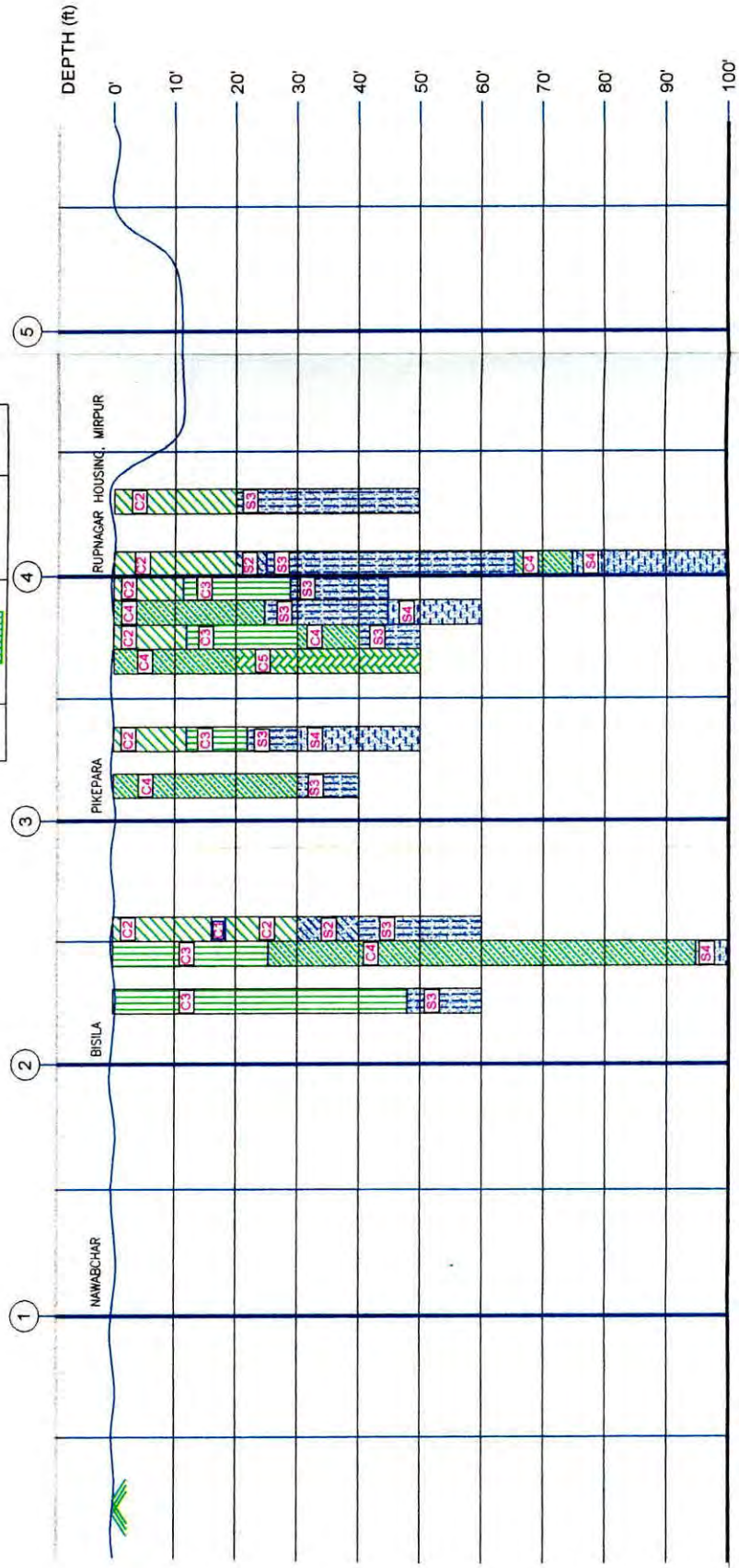


Figure 3.8 Soil Profile through grid A-A' (after Bashar, 2004)

CLASS	SYMBOL	DESCRIPTION TERM	N-VALUE FROM SPT
S1		VERY LOOSE	0-4
S2		LOOSE	4-10
S3		MEDIUM DENSE	10-30
S4		DENSE	30-50
S5		VERY DENSE	>50

CLASS	SYMBOL	DESCRIPTION TERM	N-VALUE FROM SPT
C1		VERY SOFT	0-2
C2		SOFT	2-4
C3		MEDIUM STIFF	4-8
C4		STIFF	8-15
C5		VERY STIFF	15-30
C6		HARD	>30

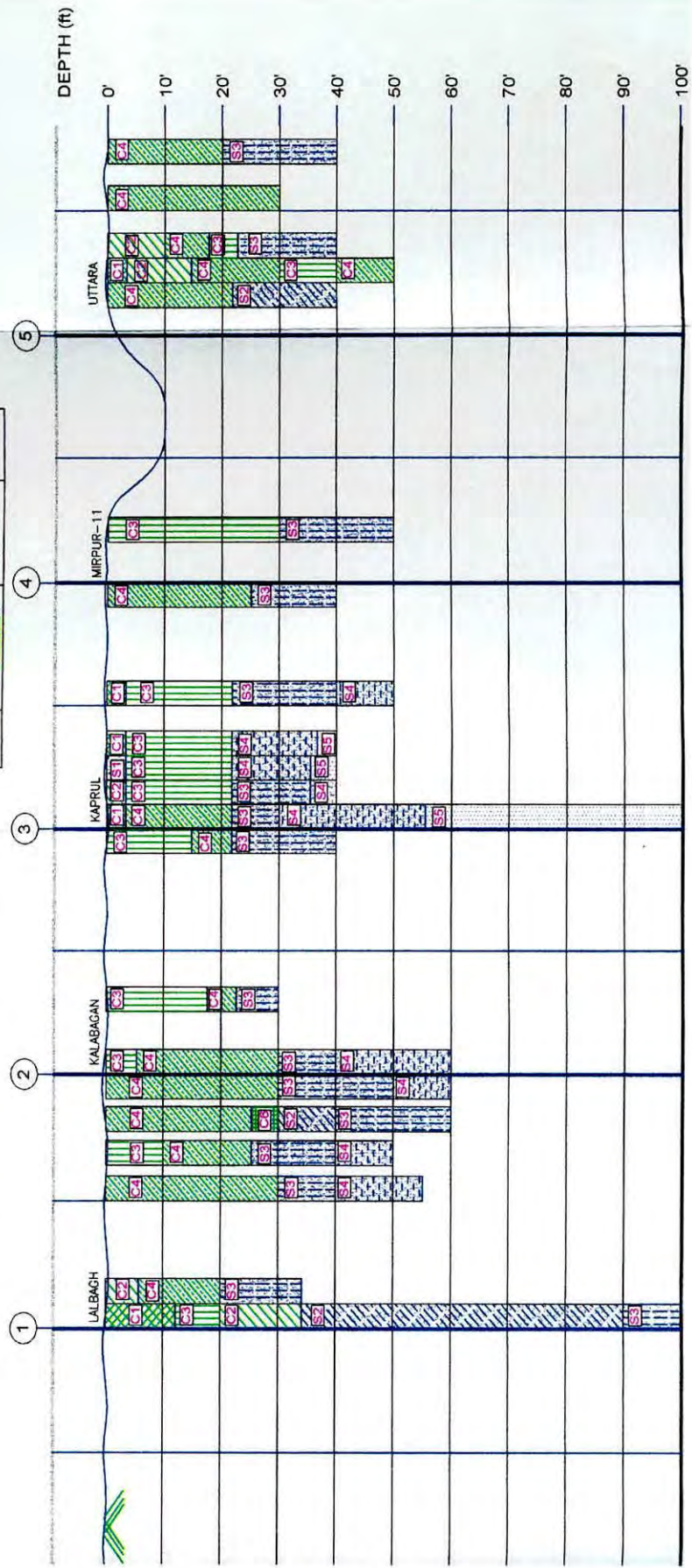


Figure 3.9 Soil Profile through grid B-B' (after Bashar, 2004)

CLASS	SYMBOL	DESCRIPTION TERM	N-VALUE FROM SPT
S1		VERY LOOSE	0-4
S2		LOOSE	4-10
S3		MEDIUM DENSE	10-30
S4		DENSE	30-50
S5		VERY DENSE	>50

CLASS	SYMBOL	DESCRIPTION TERM	N-VALUE FROM SPT
C1		VERY SOFT	0-2
C2		SOFT	2-4
C3		MEDIUM STIFF	4-8
C4		STIFF	8-15
C5		VERY STIFF	15-30
C6		HARD	>30

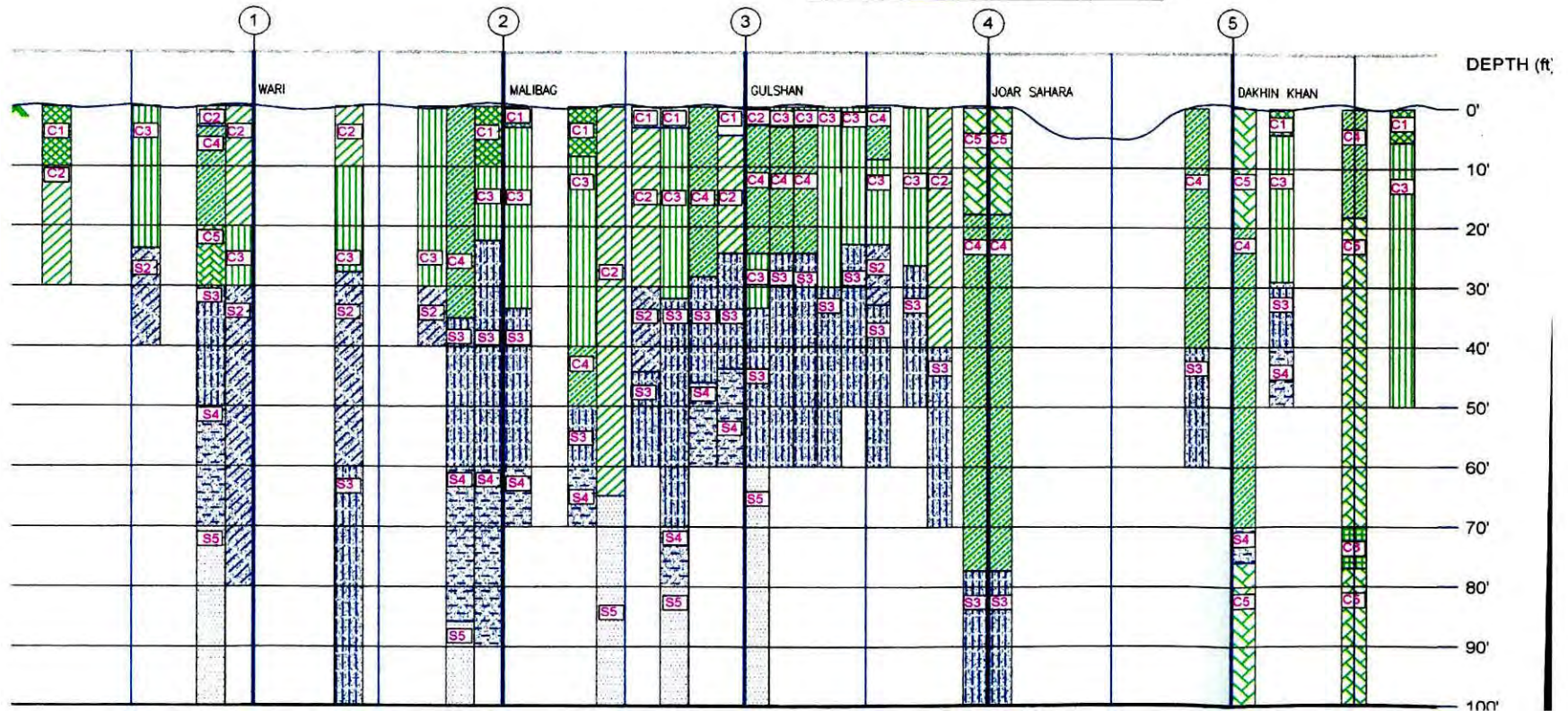


Figure 3.10 Soil Profile through grid C-C' (after Bashar, 2004)

CLASS	SYMBOL	DESCRIPTION TERM	N-VALUE FROM SPT
S1		VERY LOOSE	0-4
S2		LOOSE	4-10
S3		MEDIUM DENSE	10-30
S4		DENSE	30-50
S5		VERY DENSE	>50

CLASS	SYMBOL	DESCRIPTION TERM	N-VALUE FROM SPT
C1		VERY SOFT	0-2
C2		SOFT	2-4
C3		MEDIUM STIFF	4-8
C4		STIFF	8-15
C5		VERY STIFF	15-30
C6		HARD	>30

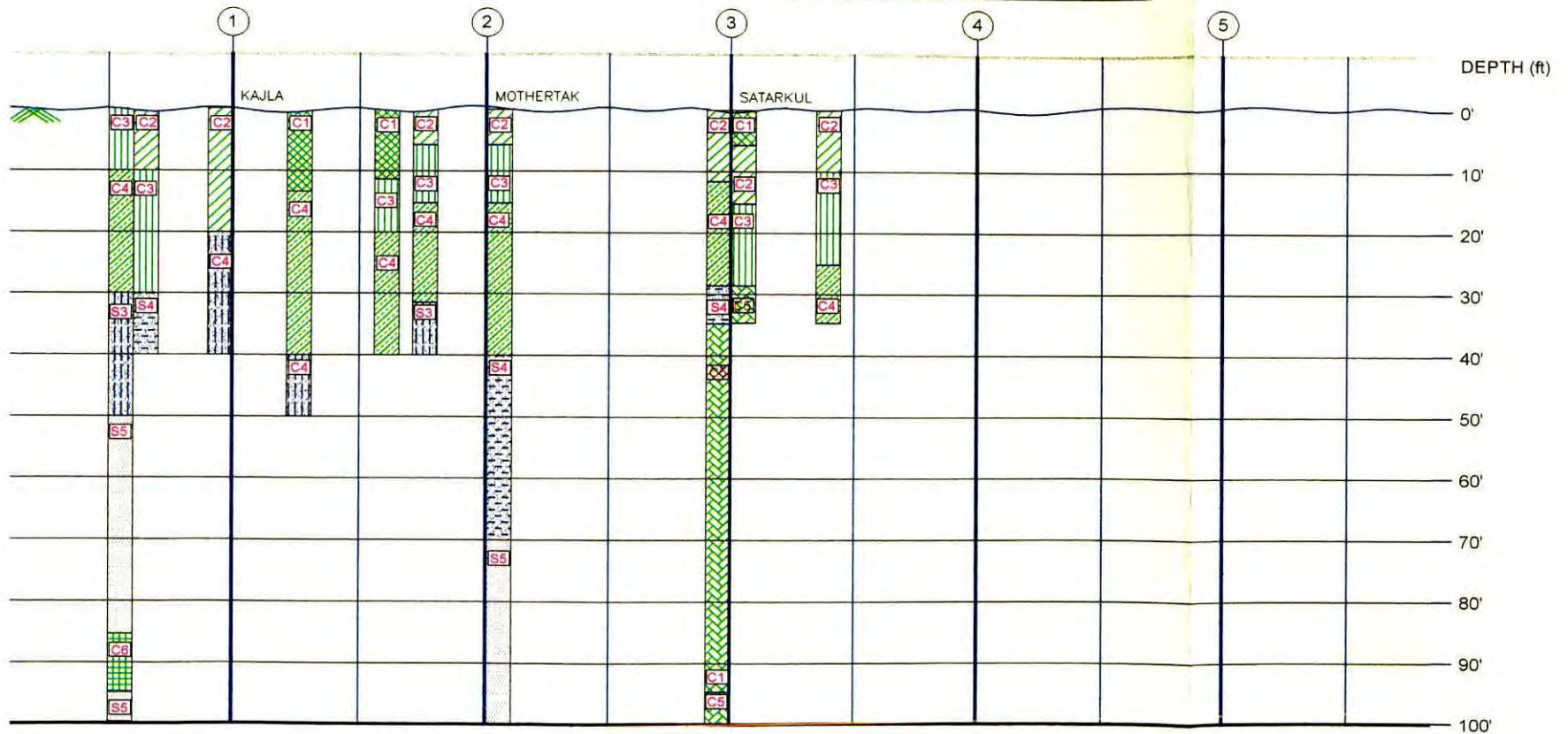


Figure 3.11 Soil Profile through grid D-D' (after Bashar, 2004)

CLASS	SYMBOL	DESCRIPTION TERM	N-VALUE FROM SPT
S1		VERY LOOSE	0-4
S2		LOOSE	4-10
S3		MEDIUM DENSE	10-30
S4		DENSE	30-50
S5		VERY DENSE	>50

CLASS	SYMBOL	DESCRIPTION TERM	N-VALUE FROM SPT
C1		VERY SOFT	0-2
C2		SOFT	2-4
C3		MEDIUM STIFF	4-8
C4		STIFF	8-15
C5		VERY STIFF	15-30
C6		HARD	>30



Figure 3.12 Soil Profile through grid 1-1' (after Bashar, 2004)

CLASS	SYMBOL	DESCRIPTION TERM	N-VALUE FROM SPT
S1		VERY LOOSE	0-4
S2		LOOSE	4-10
S3		MEDIUM DENSE	10-30
S4		DENSE	30-50
S5		VERY DENSE	>50

CLASS	SYMBOL	DESCRIPTION TERM	N-VALUE FROM SPT
C1		VERY SOFT	0-2
C2		SOFT	2-4
C3		MEDIUM STIFF	4-6
C4		STIFF	6-15
C5		VERY STIFF	15-30
C6		HARD	>30

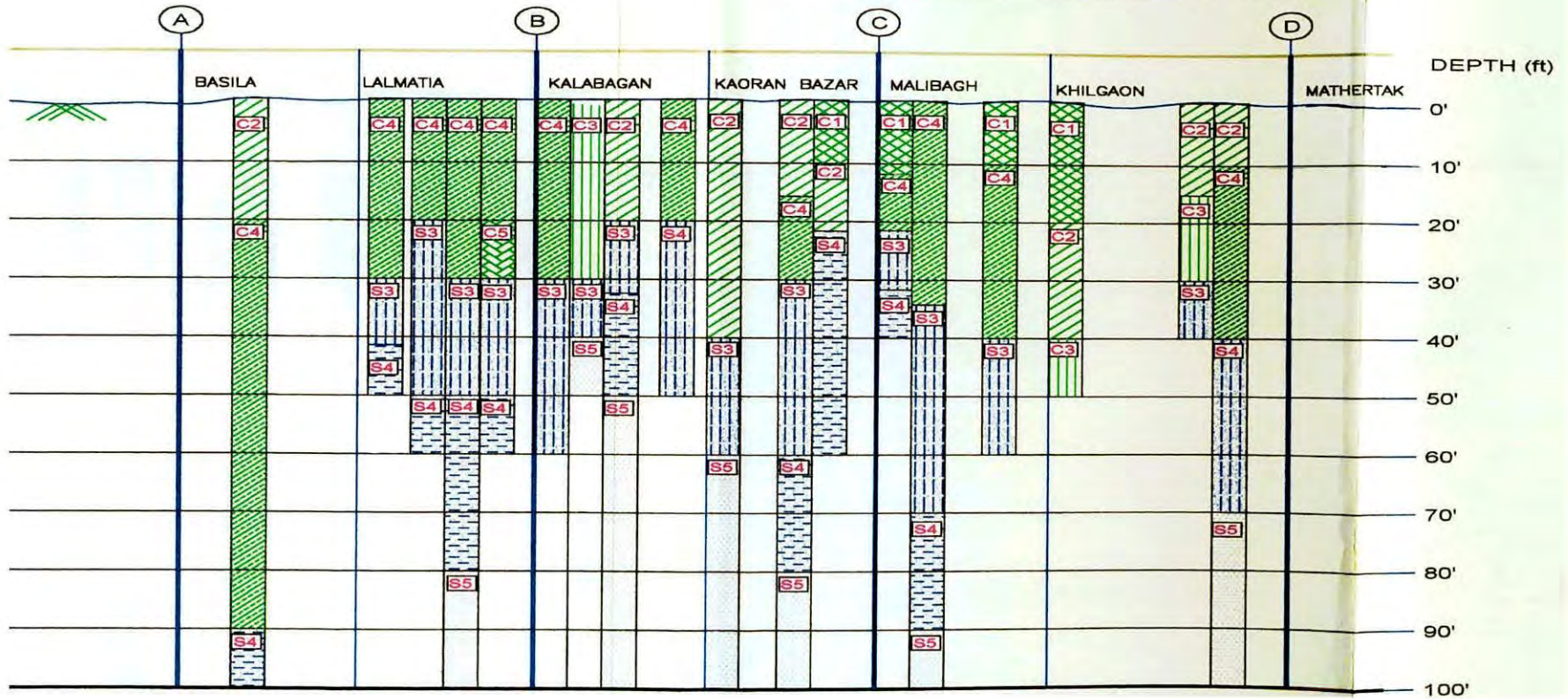


Figure 3.13 Soil Profile through grid 2-2' (after Bashar, 2004)

CLASS	SYMBOL	DESCRIPTION TERM	N-VALUE FROM SPT
S1		VERY LOOSE	0-4
S2		LOOSE	4-10
S3		MEDIUM DENSE	10-30
S4		DENSE	30-50
S5		VERY DENSE	>50

CLASS	SYMBOL	DESCRIPTION TERM	N-VALUE FROM SPT
C1		VERY SOFT	0-2
C2		SOFT	2-4
C3		MEDIUM STIFF	4-8
C4		STIFF	8-15
C5		VERY STIFF	15-30
C6		HARD	>30

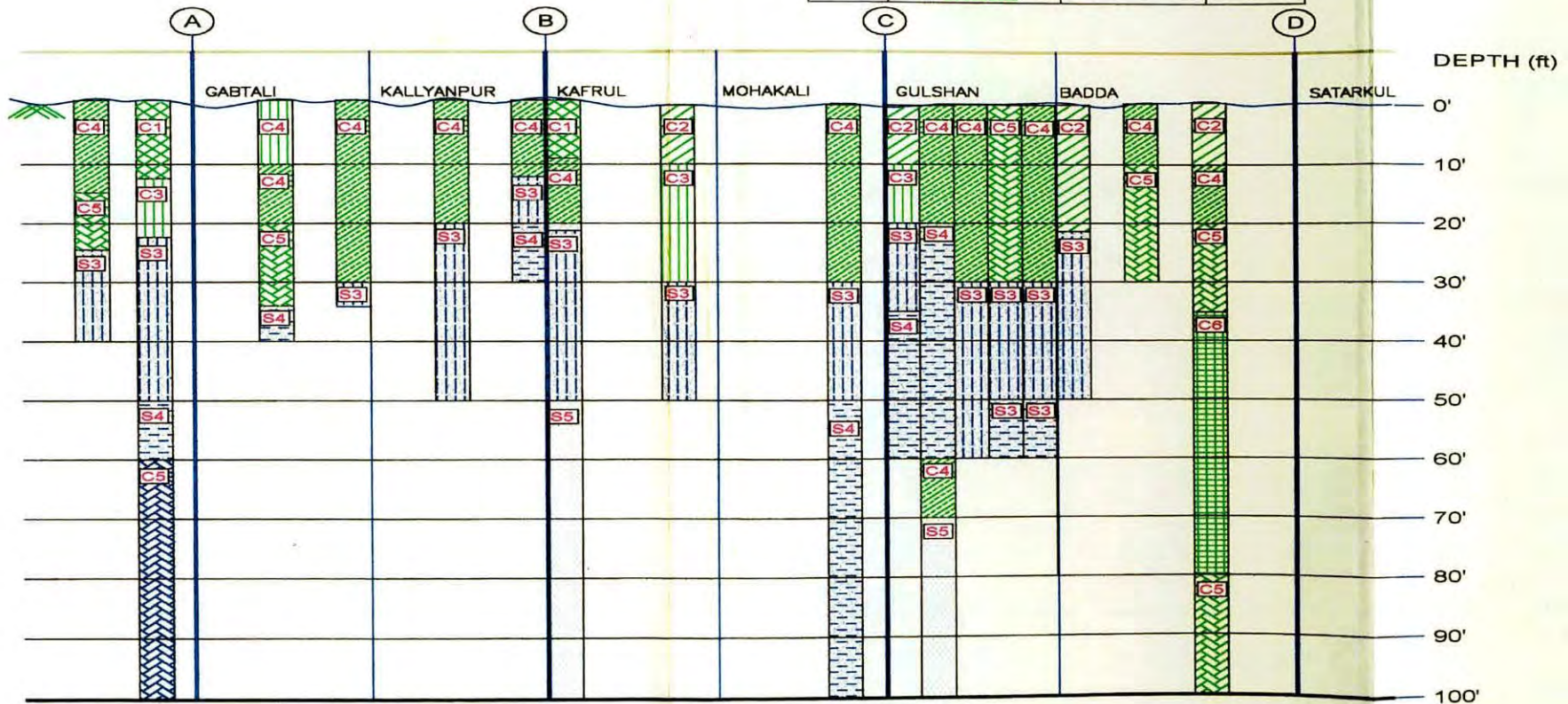


Figure 3.14 Soil Profile through grid 3-3' (after Bashar, 2004)

CLASS	SYMBOL	DESCRIPTION TERM	N-VALUE FROM SPT
S1		VERY LOOSE	0-4
S2		LOOSE	4-10
S3		MEDIUM DENSE	10-30
S4		DENSE	30-50
S5		VERY DENSE	>50

CLASS	SYMBOL	DESCRIPTION TERM	N-VALUE FROM SPT
C1		VERY SOFT	0-2
C2		SOFT	2-4
C3		MEDIUM STIFF	4-8
C4		STIFF	8-15
C5		VERY STIFF	15-30
C6		HARD	>30

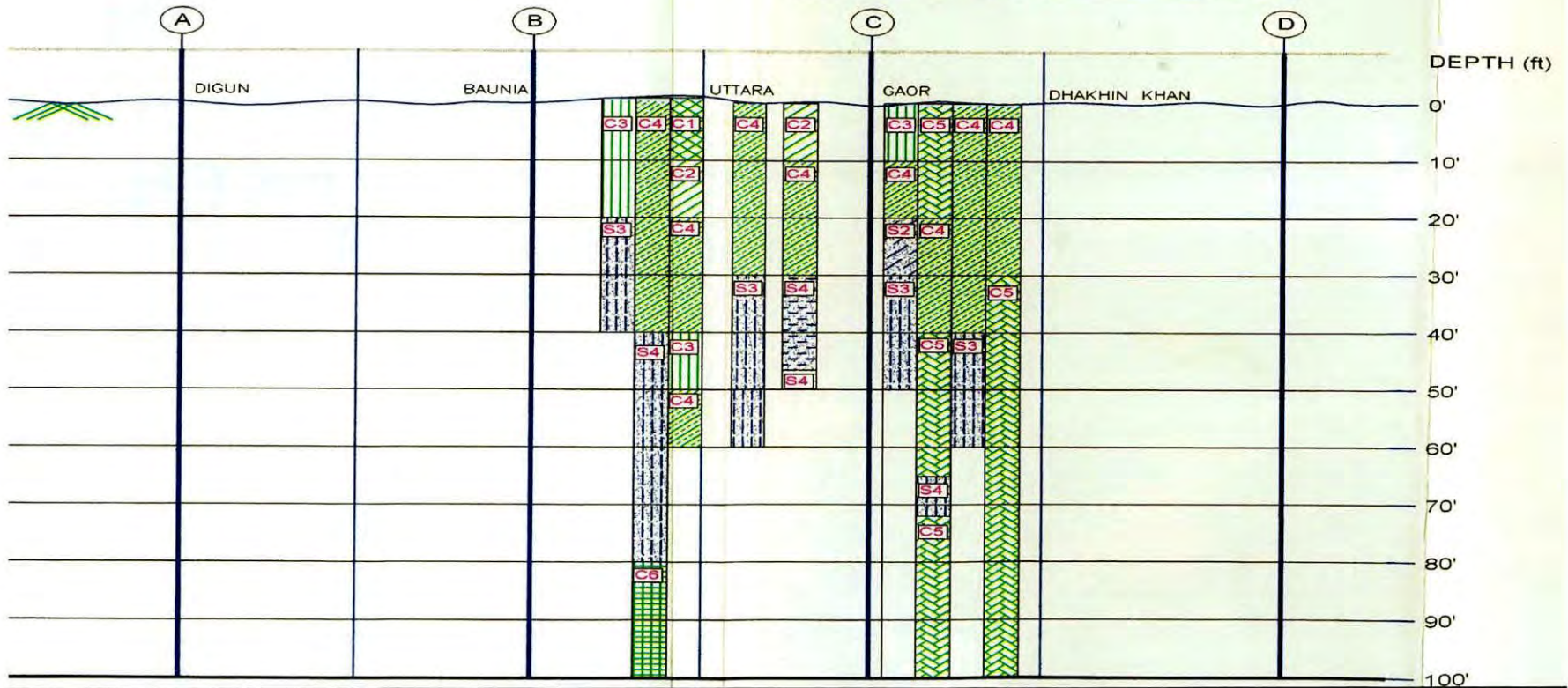


Figure 3.15 Soil Profile through grid 4-4' (after Bashar, 2004)

CLASS	SYMBOL	DESCRIPTION TERM	N-VALUE FROM SPT
S1		VERY LOOSE	0-4
S2		LOOSE	4-10
S3		MEDIUM DENSE	10-30
S4		DENSE	30-50
S5		VERY DENSE	>50

CLASS	SYMBOL	DESCRIPTION TERM	N-VALUE FROM SPT
C1		VERY SOFT	0-2
C2		SOFT	2-4
C3		MEDIUM STIFF	4-8
C4		STIFF	8-15
C5		VERY STIFF	15-30
C6		HARD	>30

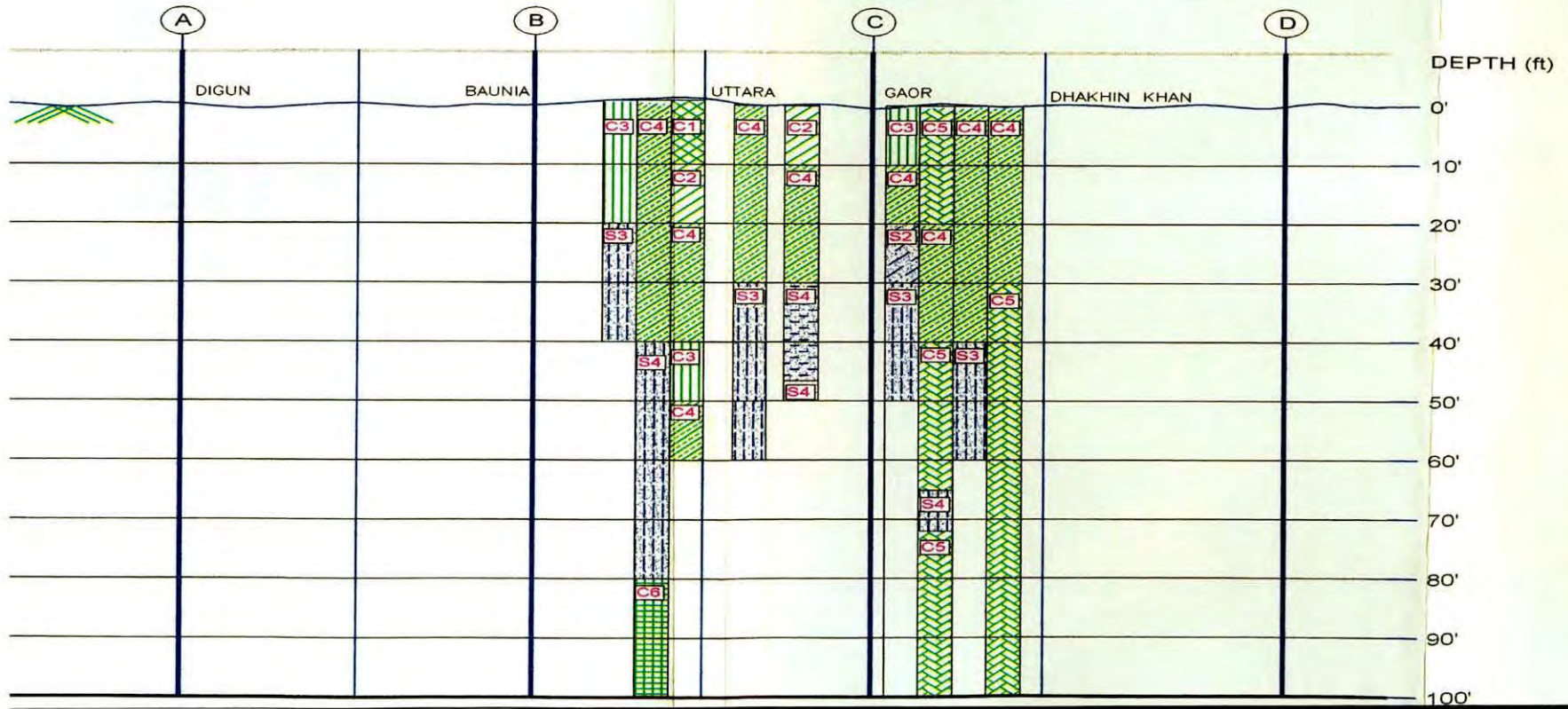


Figure 3.16 Soil Profile through grid 5-5' (after Bashar, 2004)

CHAPTER FOUR

BURIED WATER PIPELINE DAMAGE ANALYSIS

4.0 GENERAL

The damageability of buried water supply pipelines in seismic zones can be very serious and it is necessary to take preventive measures that eliminate, or at least decrease, that damageability. Pipelines that are the main source of water distribution for important cities in seismic zones should be investigated and analyzed in terms of vulnerability to earthquakes. Institutions and authorities responsible for the design, construction and operation of buried pipelines located in seismic zones should demand that the seismic effects are correctly taken into consideration in order to assure the good behavior of such pipelines during their working life.

The damage produced by breakage or disconnection of pipelines is quite variable, and can be related to technical, economical and social aspects. The breakage of gas pipelines, for instance, besides representing a health hazard and fire risk, causes leakage and the repairs in the pipeline represent an important cost. The most dramatic damage due to pipeline failure usually occurs when a pipeline carries drinking water. It means the interruption of water supply to several sectors and developments near the site where the failure occurred, and second, there will be no water available for putting out any fires that might arise due to electrical or gas leakage problems. On the other hand, social pressure might be very important if water supply is not promptly restored.

Distribution pipelines are typically in networks. Failure of a single distribution pipeline will not fail the entire network (once that pipe is valved out), but the customers on that failed distribution pipeline will have no water service until the pipe is repaired. No single distribution pipeline, will in general, be as important as a transmission pipeline, the large quantity of damage can lead to rapid system-wide depressurization, loss of fire fighting capability, and long outage times due to the great amount of repair work needed.

The damage algorithm for buried pipe is expressed as a repair rate per unit length of pipe, as a function of ground shaking or ground failure. The development of damage algorithms for

buried pipe is primarily based on empirical evidence, tempered with engineering judgment and sometimes by analytical formulations. Empirical evidence means the following: after an earthquake, data is collected about how many miles of buried pipe experienced what levels of shaking, and how many pipes were broken or leaking because of that level of shaking.

Repair rate of pipelines due to earthquake is related to peak ground acceleration. There exist a good number empirical relations such as Katayama (1975), O'Rourke (1982), Isoyama & Katayama (1998) and Isoyama (2000) for the prediction of earthquake-induced pipeline damage analysis which are presented in chapter two. In this study O'Rourke (1982) and Isoyama (2000) relations are used to predict the damage rate of pipelines and an estimation of financial loss is presented.

4.1 PIPELINE DATABASE DEVELOPMENT

GIS provides an ideal tool for analyzing relationships amongst spatial datasets. GIS is increasingly used in lifeline engineering for post earthquake investigation of damage and for risk assessment.

The history of water supply system of Dhaka city is very long. The only known maps available are those created by Dhaka Water Supply System, DWASA which has been responsible for design, finance and construction of Dhaka Water Supply System. A copy of map of DWASA water supply network of 1993 covering the whole Dhaka city at a scale of 1:25000 is collected for this study. This map is scanned at first and then the whole water pipeline networks are digitized which is illustrated in Figure 4.1.

No distinction is made between different pipe materials or diameters as this information was not available, although it is known from the authority that most of the network consists of PVC pipes with diameter up to 300mm and DI pipes with diameter larger than 300mm and with the help of another map (1991) of water supply pipeline network, pipeline networks of diameter 100mm, 200mm, 300mm and 450mm are distinguished. Appendices C and D show scanned maps of Dhaka WASA.



Figure 4.1 Full digitized map of whole pipeline networks of DWASA (1993)

Microzonation maps of different intensities are grouped presented in chapter three. and pipeline networks of different diameter are laid in these maps on GIS platform which are shown in Figures 4.2 to 4.6. Finally, the lengths of pipelines are calculated according to intensity from these digitized intensity-pipe maps for analysis which are shown in Table 4.1.

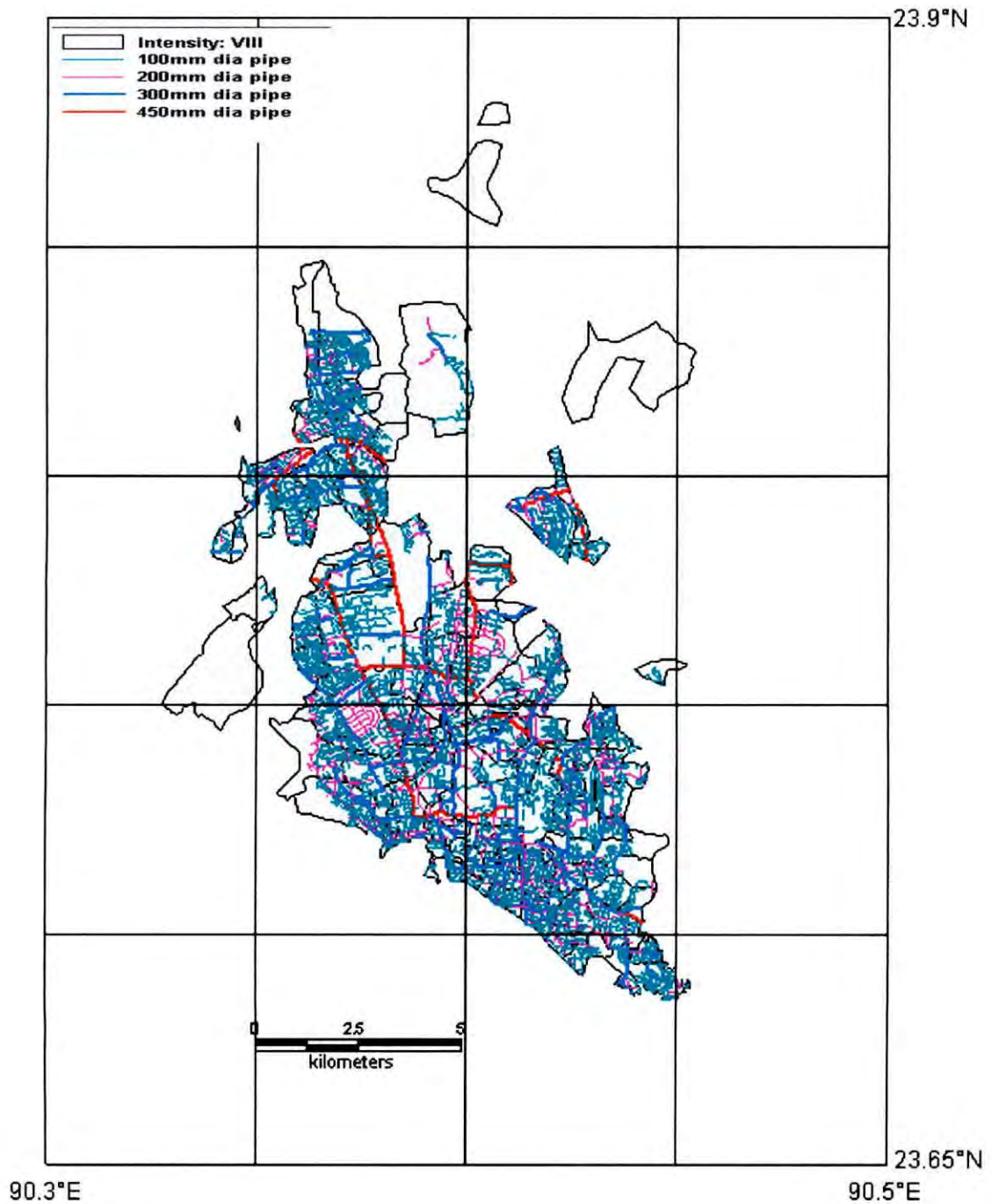


Figure 4.2 Lay-out of 100mm, 200mm, 300mm and 450mm diameter pipe on Microzonation map of intensity-8

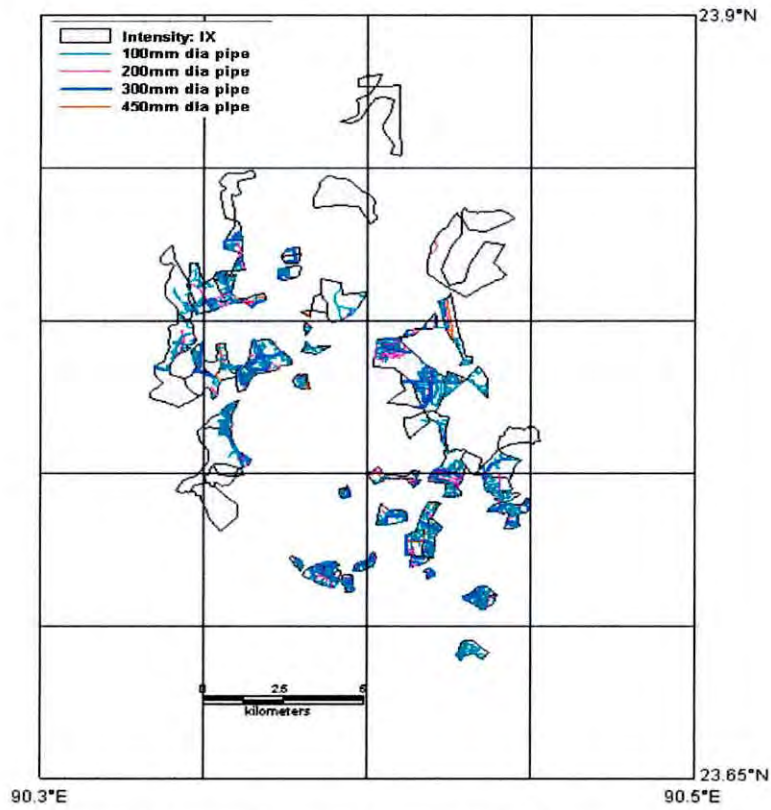


Figure 4.3 Lay-out of 100mm, 200mm, 300mm and 450mm diameter pipe on Microzonation map of intensity-9

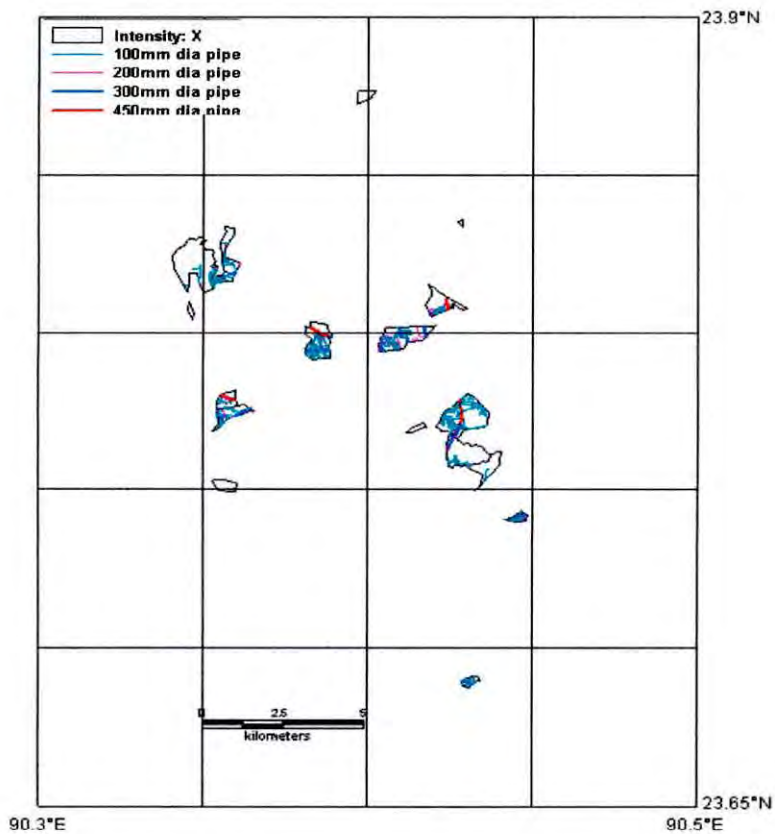


Figure 4.4 Lay-out of 100mm, 200mm, 300mm and 450mm diameter pipe on Microzonation map on intensity-10

Table 4.1 Pipeline lengths according to intensity

Intensity (MMI)	Pipe Length (km) in Respect of Diameter (mm)				Total Length (km)
	100mm	200mm	300mm	450mm	
8	683	198	122	40	1043
9	178	45	42	9	274
10	55	16	6	4	81
Total Length:	916 km	259 km	170 km	53 km	1398 km

From the digitized pipeline network, the length of 100mm, 200mm, 300mm and 450mm diameter pipe is found to be 916 km, 259 km, 170 km and 53 km respectively. But these lengths according to DWASA (2008) are 1693 km, 419 km, 190 km and 54 km for 100mm, 200mm, 300mm and 450mm diameter pipe respectively.

4.2 SELECTION OF PEAK GROUND ACCELERATION (PGA) VALUES FROM INTENSITY

In studies related to earthquake damage estimation and earthquake insurance, it has been observed that the Modified Mercalli intensity scale is the easiest and most convenient to work with. Most of the available damage statistics are related to the MM intensity at a site. However, for the recent instrumentally recorded data, the information on ground motion is usually in the form of peak ground motion parameter such as the PGA. Again, many empirical data base relationships are available in the literature to relate the MM intensity with the PGA. Peak ground acceleration is an instrumentally recorded continuous variable whereas Modified Mercalli intensity is a subjectively assigned discrete integer variable. Thus, it should be expected that there will be a range of PGA values corresponding to a given intensity level.

In the past, a number of researchers have developed PGA-MMI relationships. In each of the relationships given below, I is Modified Mercalli intensity and A is peak ground acceleration in cm/sec².

Gutenber and Richter (1942)

$$\log A = -.05 + 0.33I$$

4.1

Hershberger (1956)	$\log A = -0.9 + 0.43I$	4.2
Ambraseys (1974)	$\log A = -0.16 + 0.36I$	4.3
Trifunac and Brady (1975)	$\log A = 0.014 + 0.3I$	4.4

All the above relationships are log-linear in format. Previous work by McCann and Shah (1979) has shown that the assumption of log-linear relationship between PGA and MMI may not be a reasonable one. McCann and Shah has given the following relationship:

McCann and Shah (1979)	$\log A = -0.024I^2 + 0.595I - 0.68$	4.5
------------------------	--------------------------------------	-----

In McCann and Shah relationship, it is assumed that a range of peak ground acceleration values are associated with each intensity level. Table 4.1 lists the range of PGA values associated with each MMI level.

Table 4.2 Correlation between peak ground acceleration (PGA) and modified Mercalli intensity (MMI)

MMI	PGA (g) Interval				
V	0.03	<	A	>	0.08
VI	0.08	<	A	>	0.15
VII	0.15	<	A	>	0.25
VIII	0.25	<	A	>	0.45
IX	0.45	<	A	>	0.60
X	0.60	<	A	>	0.80
XI	0.80	<	A	>	0.90
XII			A	>	0.90

Using the above relationships, different PGA values are calculated for different MM intensity and shown in Table 4.3

Table 4.3 PGA values based on different existing empirical relationships for different intensity

Intensity (MMI)	PGA (g)				
	Gutenberg and Richter (1942)	Hershberger (1956)	Ambraseys (1974)	Trifunac and Brady (1975)	McCann and Shah (1979)
V	0.014	0.018	0.044	0.033	0.051
VI	0.031	0.049	0.102	0.066	0.108
VII	0.066	0.131	0.234	0.133	0.208
VIII	0.141	0.353	0.535	0.264	0.357
IX	0.301	0.951	1.226	0.528	0.549
X	0.643	2.561	2.808	1.053	0.756
XI	1.375	6.892	6.432	2.101	0.932

MM intensity and PGA values from Table 4.2 and 4.3 have also been plotted in Figure 4.5 for comparison. It can be seen in the graph of Figure 4.5 that for a particular intensity, Abraseys relation shows higher value and Gutenberg & Richter curve shows lower value. All most all of the remaining curves lie in between these two. The curve from Trifunac & Brady is close to the median value. Henceforth intensity-PGA relationships given by Gutenberg-Richter and Trifunac-Brady are considered for our analysis, values in higher side are ignored.

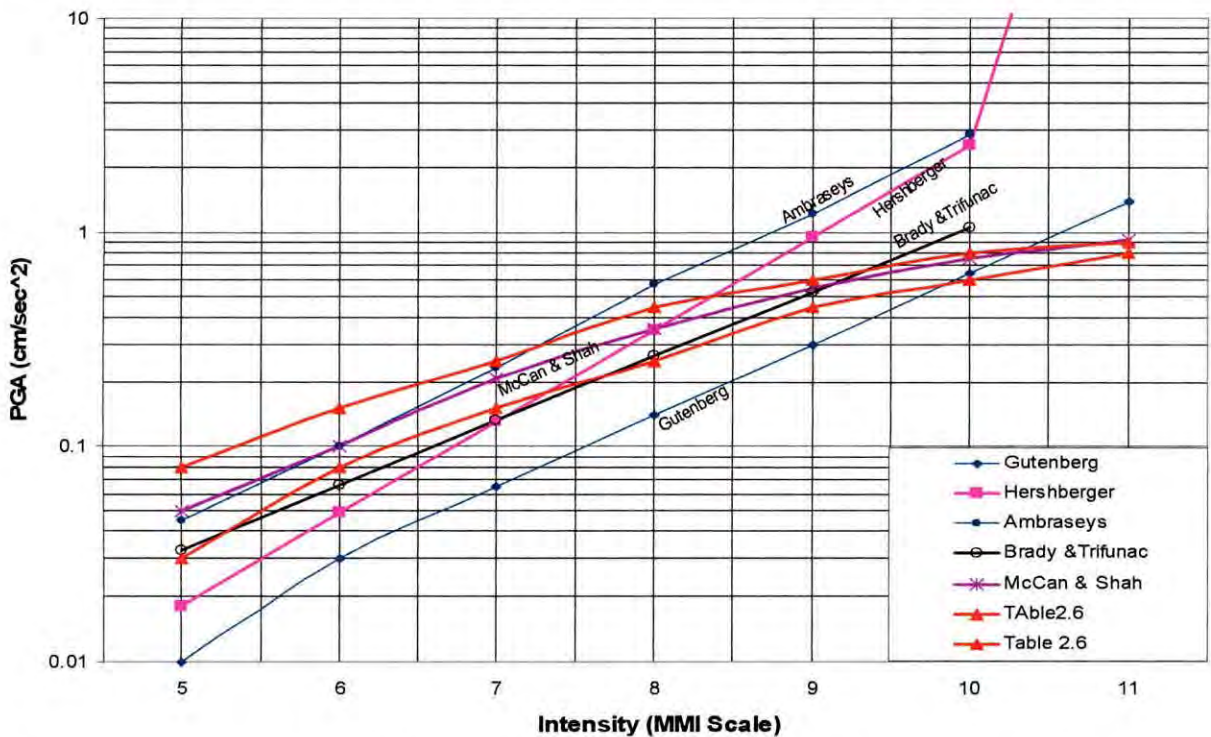


Figure 4.5 Comparison of PGA values derived from different modified Mercalli intensity (PGA-MMI) empirical relationships.

4.3 SELECTION OF DAMAGE ANALYSIS METHODS

Different pipeline fragility relations give very different predictions of pipeline damage rate for the same PGA value. The values calculated in Table 4.4 are from Katayama et al. (1975), Isoyama & Katayama (1982), O'Rourke et al. (1998) and Isoyama et al. (2000) fragility relations (Equations 2.9, 2.10, 2.11 and 2.12 respectively) and taking the values from this table a graph has been plotted which is shown in Figure 4.6. All these relations assume CI pipes irrespective of diameters.

Table 4.4 Pipeline repair rate from different fragility relations for PGA values based on Trifunac and Brady and Gutenberg and Richter relations

Eqn used	Intensity (MMI)	PGA (cm/s ²)	Repair Rate (R _R)			
			Katayama et al. (1975)	Isoyama and Katayama (1982)	O'Rourke et al. (1998)	Isoyama et al. (2000)
Trifunac and Brady	VII	130.473	0.010	0.000	0.019	0.000
	VIII	255.06	0.816	0.065	0.044	0.060
	IX	519.93	77.290	4.882	0.106	0.424
	X	1030.05	6100.980	307.510	0.249	2.029
Gutenberg and Richter	VII	64.746	0.000	0.000	0.008	0.000
	VIII	137.340	0.016	0.002	0.020	0.004
	IX	294.300	2.036	0.155	0.052	0.093
	X	627.840	257.923	15.307	0.134	0.665

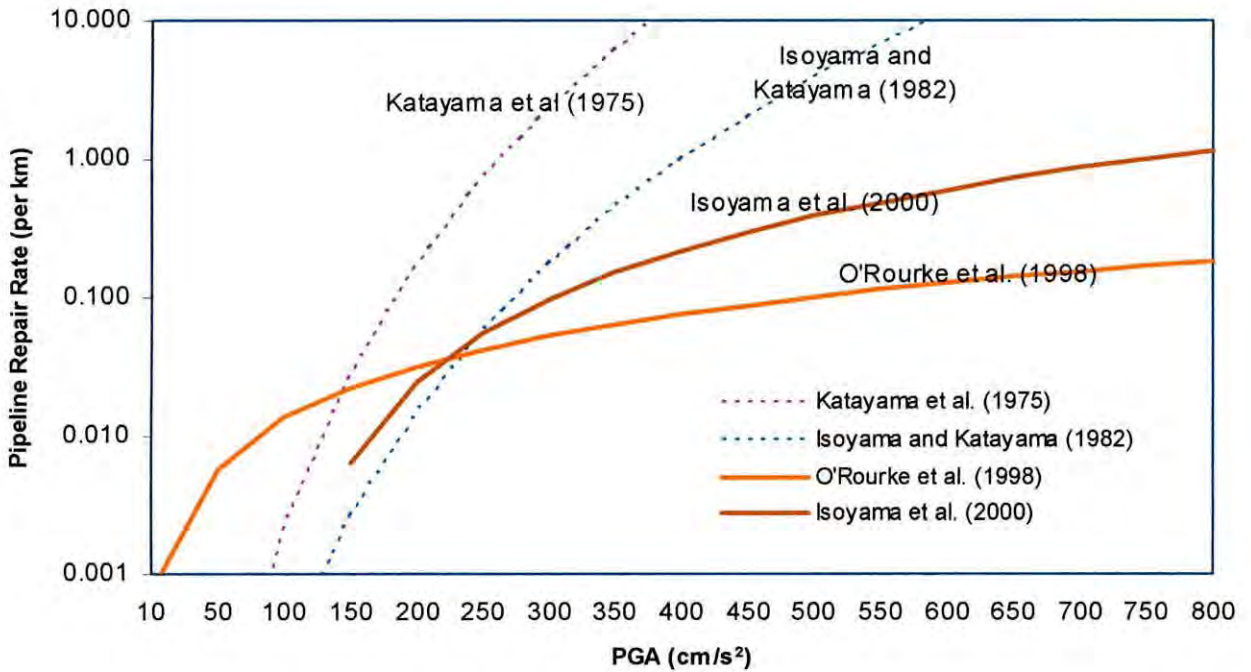


Figure 4.6 Comparison of the pipeline repair rate for different PGA values obtained from Trifunac and Brady PGA-MMI relation

It is observed from the Table 4.4 that the prediction of pipeline repair rate by Katayama significantly greater than any of the other predictions for PGA above about 200 cm/sec^2 particularly from 300 cm/sec^2 onward. It is also seen earlier that Isoyama and Katayama (1982) relation is suitable for prediction of pipeline repair rate for the PGA range of 170-330 cm/sec^2 . Beyond this, Isoyama and Katayama (1982) relation predicts significantly larger values of repair rate which can also be seen in the Table 4.4. Repair rates derived from O'Rourke et al. (1998) relation show relatively high values for low PGA whereas for PGA greater than around 220 cm/sec^2 the O'Rourke relation predicts lower repair rate values than any other relations. This study also reveals that in formulating the pipeline repair rate prediction Isoyama study is based on a much more reliable and comprehensive database than other studies. Moreover, it uses a wide range of PGA values. From Figure 4.6 it is seen that Isoyama (2000) relation is neither at lower end nor at higher end rather it lies somewhere in between two extremities. O'Rourke et al. (1998) and Isoyama (2000) fragility relations will be used in this study for damage analysis of pipelines.

From the selected peak ground acceleration (PGA) values and fragility relations, following four methods are used for damage analysis.

- Method 1: In this method, PGA and repair rate are based on Trifunac-Brady MMI-PGA relation and O'Rourke damage prediction relation.
- Method 2: This method is based on Gutenberg-Richter MMI-PGA relation and O'Rourke damage prediction relation.
- Method 3: This method involves Trifunac-Brad MMI-PGA relation and Isoyama damage prediction relation.
- Method 4: Where damage analysis is based on Gutenberg-Richter MMI-PGA relation and Isoyama damage prediction relation.

4.4 WATER PIPELINE DAMAGE ANALYSIS

Pipeline damage estimation is related to damage prediction relationship. Relative results of different damage prediction relationships are studied in the previous articles. Using the methods outlined in the preceding articles and pipeline lengths calculated from the digitized maps which are shown in Table 4.1, repair rates and number of repairs are worked out and presented in Table 4.5 to 4.8 and finally a different table, Table 4.9 is prepared for comparison of these repair rates which are also presented in graph of Figure 4.7.

The result presented in Table 4.5 shows pipeline length, repair rate and number of repairs based on O'Rourke damage prediction relation for different peak ground acceleration (PGA) derived from Trifunac and Brady PGA-MMI relation. The result presented in Table 4.6 shows pipeline length, repair rate and number of repairs based on O'Rourke damage prediction relation for different peak ground acceleration (PGA) derived from Gutenberg and Richter PGA-MMI relation. The result presented in Table 4.7 shows pipeline length, repair rate and number of repairs based on Isoyama damage prediction relation for different peak ground acceleration (PGA) derived from Trifunac & Brady PGA-MMI relation. The result presented in Table 4.8 shows pipeline length, repair rate and number of repairs based on

Isoyama damage prediction relation for different peak ground acceleration (PGA) derived from Gutenberg and Richter PGA-MMI relation.

Table 4.5 Intensity and number of repairs based on O'Rourke and Trifunac and Brady relation

Eqn used	Intensity (MMI)	PGA (cm/s ²)	Pipe Length (km) in Respect of Diameter (mm)				Total Length (km)	Repair Rate	Number Of Repairs
			100 mm	200 mm	300 mm	450 mm			
O'Rourke and Trifunac-Brady	8	255	683	198	122	40	1043	0.044	45
	9	520	178	45	42	9	274	0.106	29
	10	1030	55	16	6	4	81	0.249	20

Table 4.6 Intensity and number of repairs based on O'Rourke and Gutenberg and Richter relation

Eqn used	Intensity (MMI)	PGA (cm/s ²)	Pipe Length (km) in Respect of Diameter (mm)				Total Length (km)	Repair Rate	Number Of Repairs
			100 mm	200 mm	300 mm	450 mm			
O'Rourke and Gutenberg-Richter	8	100.06	683	198	122	40	1043	0.020	21
	9	137.34	178	45	42	9	274	0.052	14
	10	294.30	55	16	6	4	81	0.134	11

Table 4.7 Intensity and number of repairs based on Isoyama and Trifunac and Brady relation

Eqn used	Intensity (MMI)	PGA (cm/s ²)	Pipe Length (km) in Respect of Diameter (mm)				Total Length (km)	Repair Rate	Number Of Repairs
			100 mm	200 mm	300 mm	450 mm			
Isoyama and Trifunac-Brady	8	255	683	198	122	40	1043	0.060	62
	9	520	178	45	42	9	274	0.424	116
	10	1030	55	16	6	4	81	2.029	164

Table 4.8 Intensity and number of repairs based on Isoyama and Gutenberg and Richter relation

Eqn used	Intensity (MMI)	PGA (cm/s ²)	Pipe Length (km) in Respect of Diameter (mm)				Total Length (km)	Repair Rate	Number Of Repairs
			100 mm	200 mm	300 mm	450 mm			
Isoyama and Gutenberg-Richter	8	100.06	683	198	122	40	1043	0.004	4
	9	137.34	178	45	42	9	274	0.093	25
	10	294.30	55	16	6	4	81	0.665	54

Table 4.9 Pipeline repair rate for different intensity and fragility relation.

Intensity (MMI)	Pipeline Repair Rate (R _R) Based on Relations:			
	O'Rourke and Trifunac-Brady (OTB)	O'Rourke and Gutenberg-Richter (OGR)	Isoyama and Trifunac-Brady (ITB)	Isoyama and Gutenberg-Richter (IGR)
8	0.044	0.020	0.060	0.004
9	0.106	0.052	0.424	0.093
10	0.249	0.134	2.029	0.665

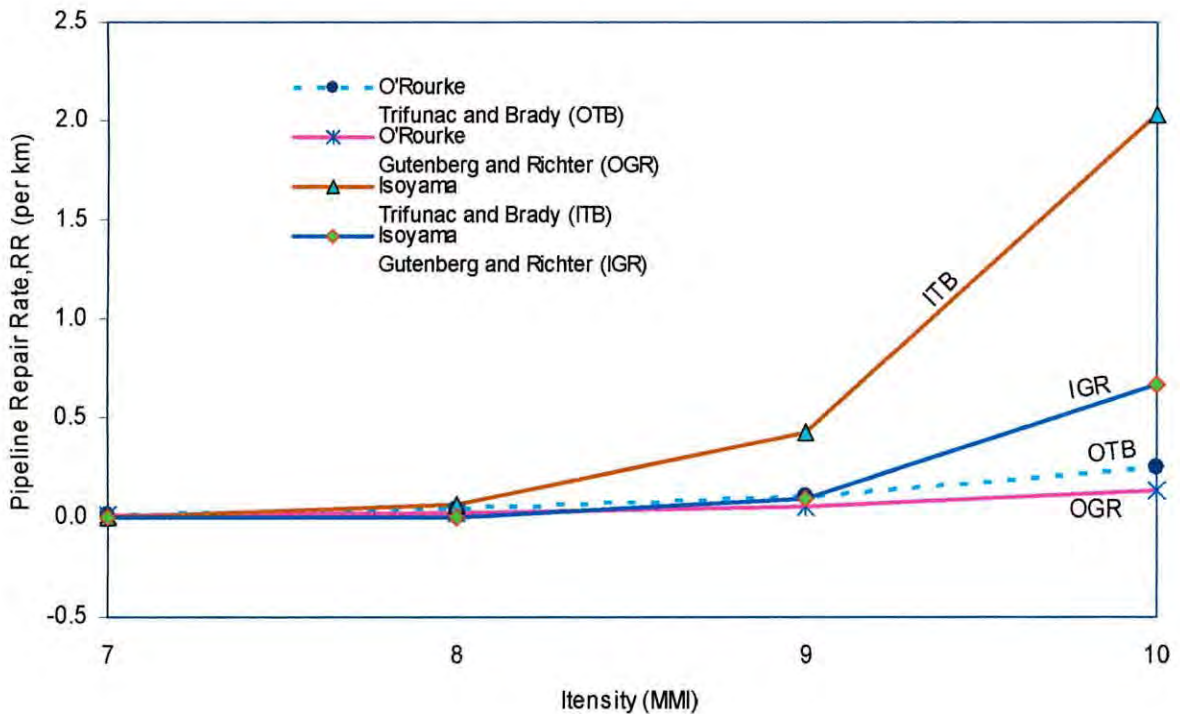


Figure 4.7 Comparison of the pipeline repair rate for different intensity and fragility relation.

From the Table 4.9 and Figure 4.7 it is seen that repair rates of O'Rourke and Trifunac and Brady relation are two times higher than those of O'Rourke and Gutenberg and Richter relation for all intensities. On the other hand Isoyama and Trifunac and Brady relation shows 15 times higher repair rate than the repair rate obtained from Isoyama and Gutenberg and Richter relation for intensity 8 while it is 5 times and 3 times higher for intensity 9 and 10 respectively. On the whole it is seen from these relations that repair rates vary from 0.004 to 0.06 for intensity 8, 0.052 to 0.424 for intensity 9 and 0.134 to 2.029 for intensity 10.

However due to absence of real repair rate data in Bangladesh, it is advisable to use a range of repair rates instead of a single value in the event of damage analysis of buried water supply pipelines due to earthquake.

4.5 Financial Loss Estimation

This study is not primarily intended to focus on the estimation of economic loss for the damage of pipelines due to earthquake. But loss estimation is a first step in the mitigation of earthquake risk and is a quantification of the problem of earthquake loss. For loss estimation a separate analysis is done for damage of pipelines which is shown in Table 4.10.

Table 4.10 Repair rate calculated for loss estimation

Eqn used	Intensity (MMI)	PGA (cm/s ²)	Pipe Length (km) in Respect of Diameter (mm)				Total Length (km)	Repair Rate	Number Of Repairs
			100 mm	200 mm	300 mm	450 mm			
Isoyama and Trifunac-Brady	8	255	683				683	0.060	41
				198	122	40	360	0.060	22
	9	520	178				178	0.424	76
				45	42	9	96	0.424	41
	10	1030	55				55	2.029	112
				16	6	4	26	2.029	53

Using the repair rates from Table 4.10 and taking the repair cost USD 250 per repair point based on some previous findings from damaging earthquake in India (Arya, 2000; Jain et al. 2002; Boomer et al. 2002) monetary loss is estimated and presented in the Table 4.11 to 4.13. From the digitized pipeline network it is found that the length of 100mm, 200mm, 300mm and 450mm diameter pipe is 916 km, 259 km, 170 km and 53 km respectively. But these

lengths DWASA (2008) are 1693 km, 419 km, 190 km and 54 km for 100mm, 200mm, 300mm and 450mm diameter pipe respectively. In estimating monetary loss for 100mm, 200mm, 300mm and 450mm diameter pipe, number of repairs are adjusted by multiplication factors of (1693/916), (419/259), (190/170) and (54/53) respectively.

Table 4.11 Repair cost for intensity 8

Intensity 8	Pipe Dia (mm)	Pipe Length (km)	Repair Rate	Number of Repairs	Adjusted Number of Repairs	Repair Cost (Million Tk.)	Total Cost (Million Tk.)
	100	683	0.06	41	75	1.32	1.87
	200	198	0.06	12	20	0.35	
	300	122	0.06	7	8	0.15	
	450	40	0.06	3	3	0.05	

Table 4.12 Repair cost for intensity 9

Intensity 9	Pipe Dia (mm)	Pipe Length (km)	Repair Rate	Number of Repairs	Adjusted Number of Repairs	Repair Cost (Million Tk.)	Total Cost (Million Tk.)
	100	178	0.424	76	140	2.46	3.43
	200	45	0.424	19	32	0.56	
	300	42	0.424	18	20	0.34	
	450	9	0.424	4	4	0.07	

Table 4.13 Repair cost for intensity 10

Intensity 10	Pipe Dia (mm)	Pipe Length (km)	Repair Rate	Number of Repairs	Adjusted Number of Repairs	Repair Cost (Million Tk.)	Total Cost (Million Tk.)
	100	55	2.029	112	206	3.60	5.00
	200	16	2.029	33	57	1.00	
	300	6	2.029	12	14	0.26	
	450	4	2.029	8	8	0.14	

Total Cost: Taka 10.30 million.

4.6 SUMMARY

The pipeline network is very important for daily life in Dhaka city like elsewhere. It must be kept well maintained, especially to the city. It offers basic need like water for urban area, but it can be greatly damaged by earthquake. In order to predict the damage of water pipeline network after earthquake, the fragility curves are very useful means to do so. Different available pipeline fragility relations such as Katayama (1975), O'Rourke (1982), Isoyama and Katayama (1998) and Isoyama (2000) are compared. Finally using two relations namely O'Rourke (1982) and Isoyama (2000), damage rate of pipelines is determined where PGA values obtained from Trifunac and Brady and Guutenberg and Richter MMI-PGA relations are used. After thorough investigation of these output it is deemed that Isoyama and Trifunac and Brady relation could be better pipeline damage analysis method.

Pipeline damage rate is expressed in number of repairs per unit length of pipe. The total number of repairs found for all intensities is 587 within a total pipe length of 2356 km. Out of which 421 number of repairs required for 1693 km pipelines of 100mm diameter, 109 number of repairs required for 419 km pipelines of 200mm diameter, 42 number of repairs for 190 km pipeline of 300mm diameter and 15 number of repairs for 54 km pipeline of 450mm diameter.

Any hazard especially earthquake hazard invokes financial involvement. So monetary loss estimation directly related to pipeline damage due to earthquake is a first step to mitigate the risk. This study also presented a picture of monetary loss due to earthquake damage of water pipeline network for different intensity. Total cost estimated for damage of pipeline is Tk.10.3 million. Out of which Tk.7.34 million requires to be spent for 1693 km pipe, Tk.2.06 for 419 km, Tk.0.62 million for 190 km and Tk.0.31 million for 54 km pipe. Though this figure of amount apparently is not large, secondary or indirect loss due to damage of buried water supply pipelines may be greater, such as interrupted water supply to business and industrial sectors cause reduction of output, reduced and sometimes contaminated water supplied to health service places such as hospital may cause health hazard resulting in extra life loss.

CHAPTER FIVE

CONCLUSIONS AND RECOMMENDATIONS

5.1 CONCLUSIONS

The main purpose of this project was to study the damage analysis of buried water supply pipelines of Dhaka city subject to earthquake and make an attempt for quantification of the problem in term of monetary loss. Although mechanical pipeline and soil models may be practical for site specific studies, it is not practical to use theoretical analysis techniques to assess the seismic vulnerability of pipeline networks.

Researchers have developed relationships between pipeline damage and various seismic and geotechnical parameters using empirical data. The seismic performance of buried water supply pipelines has been investigated by means of a detailed review of these existing empirical pipeline fragility relations such as Katayama (1975), O'Rourke (1982), Isoyama & Katayama (1998) and Isoyama (2000). In the process geographic information system (GIS) was used and several maps of pipeline networks were prepared to develop database on pipeline networks. These maps and database are shown at various stages of this study.

The major findings and conclusions drawn from various aspects of this study are summarized below:

- On the basis of intensity the whole Dhaka city has been divided into three different zones. Out of total area of 135 sq.km, 88 sq.km is (65%) of intensity VIII, 39 sq.km is (29%) of intensity IX and remaining 9 sq.km is (6%) of intensity X.
- The available empirical relationships between modified Mercalli intensity (MMI) and peak ground acceleration (PGA) have been studied and it is found that different relationships give different PGA values for the same intensity.
- Different pipeline fragility relations give different prediction of pipeline damage rate for the same PGA value.

- From the different relations it is seen that repair rates vary for different intensities, which are 0.044 to 0.06 for intensity 8, 0.052 to 0.0424 for intensity 9 and 0.134 to 2.029 for intensity 10.
- From the digitized pipeline network, based on 1993 DWASA data, the length of 100mm, 200mm, 300mm and 450mm diameter pipe is found to be 916 km, 259 km, 170 km and 53 km respectively. But these lengths according to DWASA 2008 data are 1693 km, 419 km, 190 km and 54 km for 100mm, 200mm, 300mm and 450mm diameter pipe respectively. Again from the intensity based pipeline network it is found that 1043 km pipe falls in the zone of intensity VIII, 274 km falls in the zone of intensity IX and 81 km falls in the zone of intensity X irrespective of pipe diameter.
- It is found that zone of intensity VIII contains 683 km of 100mm diameter pipe, 198 km of 200mm diameter pipe, 122 km of 300mm diameter pipe and 40 km of 450mm diameter pipe. Zone of intensity IX contains 178 km of 100mm diameter pipe, 45 km of 200mm diameter pipe, 42 km of 300mm diameter pipe and 9 km of 450mm diameter pipe. Zone of intensity X contains 55 km of 100mm diameter pipe, 16 km of 200mm diameter pipe, 6 km of 300mm diameter pipe and 4 km of 450mm diameter pipe.
- The total number of repairs found for all intensities is 587 within a total pipe length of 2356 km. Out of which 421 number of repairs required for 1693 km pipelines of 100mm diameter, 109 number of repairs required for 419 km pipelines of 200mm diameter, 42 number of repairs for 190 km pipeline of 300mm diameter and 15 number of repairs for 54 km pipeline of 450mm diameter.
- Direct loss due to damage of pipelines in term of money estimated is Tk.10.3 million. It is found that Tk.7.34 million requires to be spent for 1693 km pipe, Tk.2.06 for 419 km, Tk.0.62 million for 190 km and Tk.0.31million for 54 km pipe. Though this figure is not large, secondary or indirect loss due to damage of buried water supply pipelines may be greater, such as interrupted water supply to business and industrial sectors may cause reduction of output; reduced and sometimes contaminated water supplied to health service places such as hospital, clinics may cause health hazard resulting in extra life loss.

5.2 RECOMMENDATIONS

Lifeline earthquake engineering is relatively a new one especially in a country like Bangladesh. Damage analysis of buried water supply pipelines is also related to many other factors such as pipe material, different soil parameters, intensity of earthquake etc. In this study only few parameters are considered. To predict the agreeable damage of water pipeline due to earthquake the following recommendations can be made for further study:

1. For damage analysis, fragility relations are used based only on peak ground acceleration. So there is a wide scope of work with other earthquake parameters such as peak ground velocity (PGV) and permanent ground displacement (PGD).
2. Locating of active faults and its effects on vulnerability of buried pipelines may be the area of further study.
3. The effects of size, material, joint types and age of pipe on its damage should be considered in the future studies.
4. Routine pipeline repair data should be kept updated.
5. Shake table can be used in the future studies for understanding the behavior of pipes and for the analysis of damage to be incurred on the pipes of different diameter and material.

REFERENCES

- ALA (2001). Seismic fragility formulations for water systems, ALA,
- ANSARY, M.A. (2003). "Site Amplification Study of Dhaka City by Using Microtremor Observation", A Report submitted to CASR, BUET on April 2003.
- ARYA, A. (2000), Non-Engineered Construction in Developing countries- An approach toward Earthquake Risk Prediction, Proc. Of 20th WCEE, No.2824.
- AMBROSEYS, N.N. (2001). "Reassessment of earthquakes, 1900-1999, in the Eastern Mediterranean and the Middle East," Geophysical Journal International.
- AYALA, A.G. & O'ROURKE, M. J. (1989). "Effects of the 1985 Michoacan Earthquake on Water Systems in Mexico," Technical Report NCEER-89-0009, National Center for Earthquake Engineering Research, State University of New York at Buffalo, Buffalo, NY.
- BALLANTYNE, D. "Minimising earthquake damage," World Water and Environmental Engineering, September, 30-31
- BARD, P.-Y. & RIEPL-THOMAS, J. (2000). "Wave propagation in complex geological structures and their effects on strong motion." In: Kausel & Manolis (eds.) Wave Motion in Earthquake Engineering.
- BARENBERG, M.E. (1988). "Correlation of pipeline damage with ground motions." Journal of Geotechnical Engineering, ASCE, June.
- BILHAM, R., V.K.Gaur and P.Mohar (2001), Himalayan Seismic Hazard, SCIENCE Volume,6.
- BOLT, B.A. (1993). Earthquakes, W.H. Freeman and Company, New York.
- BOMMER, J.J. & MARTÍNEZ-PEREIRA, A. (2000). "Strong-motion parameters: definition, usefulness and predictability." Proceedings of the 12th World Conference on Earthquake Engineering, CD-ROM Paper No. 0206.
- BRESKO, D. (1980). "Seismic risk analysis of a water system," Research Report NSF-RANH,ENV-75-20977, Department of Civil Engineering, Carnegie-Mellon University – GAI Consultants Inc., Pittsburgh, PA, June 1980.
- DHAKA WATER SUPPLY AND SEWERAGE AUTHORITY (DWASA, 2008), personal communication.
- DUKE, C.M. & MATTHIESEN, R.B. (1973). "Earthquakes, lifelines and ASCE." Civil Engineering, ASCE, December 1973.
- DONALD BALLANTYNE and WILLIAN HEUBACH "Comparison of Mitigation Alternatives for Water Distribution Pipelines Installed in Liquefiable Soils."

EGUCHI, R.T. (1983). "Seismic vulnerability models for underground pipes," Proceedings of Earthquake Behavior and Safety of Oil and Gas Storage Facilities, Buried Pipelines and Equipment, PVP-77, ASME, New York, June.

EGUCHI, R.T. (1991). "Seismic hazard input for lifeline systems," Structural Safety.

EIDINGER, J. (1998). "Water distribution system." In: Anshel J. Schiff (ed.) The Loma Prieta, California, Earthquake of October 17, 1989 - Lifelines. USGS Professional Paper 1552-A, US Government Printing Office, Washington, A63-A78.

EIDINGER, J., MAISON, B, LEE, D. & LAU, B. (1995). "East Bay Municipal District water distribution damage in 1989 Loma Prieta earthquake". Proceedings of the Fourth US Conference on Lifeline Earthquake Engineering, ASCE, TCLEE, Monograph No. 6.

FEMA (1999). Earthquake Loss Estimation Methodology HAZUS 99 Service Release 2: Technical Manual, FEMA, Washington DC, <http://www.fema.gov/hazus>.

GELI, L., BARD, P.-Y. & JULIEN, B. (1988). "The effect of topography on earthquake ground motion: a review and new results." Bulletin of the Seismological Society of America.

GEOLOGICAL SURVEY OF BANGLADESH (GSB) (1990), Geological Map of Bangladesh

HAMADA, M., YASUDA, S., ISOYAMA, R. & EMOTO, K. (1986). "Study on liquefaction induced permanent ground displacements." Association for the Development of Earthquake Prediction in Japan, Tokyo, Japan.

HWANG, H. & LIN, H. (1997). "GIS-based evaluation of seismic performance of water delivery systems," Technical Report, CERl, the University of Memphis, Memphis, TN.

ISOYAMA, R., ISHIDA, E., YUNE, K. & SHIROZU, T. (2000). "Seismic damage estimation procedure for water supply pipelines," Proceedings of the Twelfth World Conference on Earthquake Engineering, CD-ROM Paper No. 1762.

ISOYAMA, R. & KATAYAMA, T. (1982). "Reliability evaluation of water supply systems during earthquakes," Report of the Institute of Industrial Science, University of Tokyo.

KACHADOORIAN, R. (1976). "Earthquake: correlation between pipeline damage and geologic environment." Journal of American Waterworks Association.

KATAYAMA, T. (1996). "Lessons from the 1995 Great Hanshin earthquake of Japan with emphasis on urban infrastructure systems." Proceedings of the 15th Congress on Structural Engineering in Consideration of Economy, Environment and Energy. Copenhagen, Denmark.

KATAYAMA, T., KUBO, K. & SATO, N. (1975). "Earthquake damage to water and gas distribution systems," Proceedings of the U.S. National Conference on Earthquake Engineering EERI, Oakland, CA.

KITaura, M. & MIYAJIMA, M. (1996). "Damage to water supply pipelines," Special Issue of Soils & Foundations, Japanese Geotechnical Society, Japan, January.

- LIANG, J. & SUN, S. (2000). "Site effects on seismic behaviour of pipelines: a review." *Journal of Pressure Vessel Technology*, ASME.
- MATSUSHITA, M., MORITA, S. & OGURA. (1998). "Post-earthquake reconstruction of Kobe water system based on the lessons from the 1995 Hanshin-Awaji (Kobe) earthquake." *Proceedings of the IWSA International Workshop on Anti-seismic Measures on Water Supply*, 'Water & Earthquake '98 Tokyo', Tokyo, Japan, 15-18 November.
- MIYAJIMA, M. & HASHIMOTO, T. (2001). "Damage to water supply system and surface rupture due to fault movement during the 1999 Ji-Ji earthquake in Taiwan." *Proceedings of the Fourth International Conference on Recent Advances in Geotechnical Earthquake Engineering and Soil Dynamics*. San Diego, California, CD-ROM Paper No. 1045.
- NAKAJIMA, T., IWAMOTO, T. & TOSHIMA, T. (1998). "Study on the anti-seismic countermeasures for ductile iron pipes," *Proceedings of the IWSA International Workshop on Antiseismic Measures on Water Supply*, 'Water & Earthquake '98 Tokyo', Tokyo, Japan, 15-18 November.
- NISHIO, N., HAMURA, A. & SASE, T. (1988). "Earthquake observation of a buried pipeline in a non-uniform ground," *Proceedings of the Ninth World Conference on Earthquake Engineering*, August 2-9, Tokyo-Kyoto, Japan.
- O'ROURKE, M.J. & AYALA, G. (1993). "Pipeline damage due to wave propagation." *Journal of Geotechnical Engineering*. ASCE.
- O'ROURKE, M.J. & LIU, X. (1999). *Response of Buried Pipelines Subject to Earthquake Effects*.
- O'ROURKE, T.D. (1998). "An overview of geotechnical and lifeline earthquake engineering." *Geotechnical Special Publication No. 75*, ASCE.
- O'ROURKE, T.D., BEAUJON, P.A. & SCAWTHORN, C.R. (1992). "Large ground deformations and their effects on lifeline facilities: 1906 San Francisco earthquake." In: O'Rourke, T.D. & Hamada, M. (eds.) *Case Studies of Liquefaction and Lifeline Performance During Past Earthquakes: Technical Report NCEER-92-0002*, 2. NCEER, Buffalo, New York.
- O'ROURKE, T.D., STEWART, H.E., GOWDY, T.E. & PEASE, J.W. (1991). "Lifeline and geotechnical aspects of the 1989 Loma Prieta earthquake," *Proceedings of the Second International Conference on Recent Advances in Geotechnical Earthquake Engineering and Soil Dynamics*, St. Louis, MO.
- O'ROURKE, T.D., STEWART, H.E. & JEON, S.-S. (2001). "Geotechnical aspects of lifeline engineering," *Proceedings of the Institution of Civil Engineers: Geotechnical Engineering*, 149, January 2001, Issue 1.
- O'ROURKE, T.D. & TOPRAK, S. (1997). "GIS assessment of water supply damage from the Northridge earthquake." In: David Frost, J. (ed.) *Spatial Analysis in Soil Dynamics and Earthquake Engineering: Geotechnical Special Publication No.67*. ASCE.

- RAHMAN, F. (2004), "Seismic Damage Scenario for Dhaka City", M.Sc. Engg. Thesis, BUET.
- REITER, L. (1990). *Earthquake Hazard Analysis: Issues and Insights*, Columbia University Press, New York.
- RICHTER, C.F. (1935). "An instrumental earthquake magnitude scale," *Bulletin of the Seismological Society of America*.
- SHARFUDDIN, M. (2001), *Earthquake Hazard Analysis for Bangladesh*. M.Sc. Engg. Thesis, BUET, Dhaka.
- SHIH, B.-J., CHEN, W.W., CHANG, T.-C. & LIU, S.-Y. (2000). "Water system damages in the Ji-Ji earthquake - a GIS application." *Proceedings of the Sixth International Conference on Seismic Zonation*. Palm Springs, California.
- SHIROZU, T., YUNE, S., ISOYAMA, R. & IWAMOTO, T. (1996). "Report on damage to water distribution pipes caused by the 1995 Hyogoken-Nanbu (Kobe) earthquake." *Proceedings from the 6th Japan-US Workshop on Earthquake Resistant Design of Lifeline Facilities and Countermeasures Against Soil Liquefaction*. Technical Report NCEER-96-0012.
- STEPHANIE, A. KING AND ANNE S. KIREMIDIJAN, (1994). *Regional Seismic Hazard and Risk Analysis through Geographic Information System*.
- STUART, R. et al. (1996). "Seismic and thermal analysis of buried piping," *Proceedings of the Eleventh World Conference on Earthquake Engineering*, CD-ROM Paper No. 1457.
- TAYLOR, C.L. & CLUFF, L.S. (1977). "Fault displacement and ground deformation associated with surface faulting." *The Current State of Knowledge of Lifeline Earthquake Engineering*, ASCE
- TRIFUNAC, M.D. & BRADY, A.G. (1975). "On the correlation of seismic intensity scales with peaks of recorded strong ground motion." *Bulletin of the Seismological Society of America*.
- TROMANS, LAIN (2004), "Behaviour of Buried Water Supply Pipelines in Earthquake Zones". A thesis submitted to the University of London for the degree of Doctor of Philosophy.
- WELLS, D.L. & COPPERSMITH, K.J. (1994). "New empirical relationships among magnitude, rupture length, rupture width, rupture area, and surface displacement." *Bulletin of the Seismological Society of America*.
- WENGSTROM, T.R. (1993). "Comparative analysis of pipe break rates: a literature review." *Chalmers Univ of Technology, Publication 2*.
- ZERVA, A. (2000). "Spatial variability of seismic motions recorded over extended ground surface areas," In: E. Kausel & G.D. Manolis (ed.) *Wave Motion in Earthquake Engineering: Advances in Earthquake Engineering*, MIT Press.

APPENDIX A

MODIFIED MERCALLI INTENSITY (MMI) SCALE AND EFFECTS ON WATER SUPPLY SYSTEMS

Levels in the MMI scale (Reiter, 1990) are defined partially in terms of the effects (both direct and indirect) of an earthquake on water supply systems, as highlighted below:

I. Not felt-or, except rarely under especially favourable circumstances. Under certain conditions, at and outside the boundary of the area in which a great shock is felt: sometimes birds, animals, reported uneasy or disturbed; sometimes dizziness or nausea experienced; *sometimes* trees, structures, *liquids, bodies of water, may sway*-doors may swing, very slowly.

II. Felt indoors by few, especially on upper floors, or by sensitive, or nervous persons. Also, as in grade I, but often more noticeably: sometimes hanging objects may swing, especially when delicately suspended; *sometimes* trees, structures, *liquids, bodies of water, may sway*, doors may swing, very slowly; sometimes birds, animals, reported uneasy or disturbed; sometimes dizziness or nausea experienced.

III. Felt indoors by several, motion usually rapid vibration. Sometimes not recognised to be an earthquake at first. Duration estimated in some cases. Vibration like that due to passing of light, or lightly loaded trucks, or heavy trucks some distance away. Hanging objects may swing slightly. Movements may be appreciable on upper levels of tall structures. Rocked standing motor cars slightly.

IV. Felt indoors by many, outdoors by few. Awakened few, especially light sleepers. Frightened no one, unless apprehensive from previous experience. Vibration like that due to passing of heavy or heavily loaded trucks. Sensation like heavy body striking building or falling of heavy objects inside. Rattling of dishes, windows, doors; glassware and crockery clink and clash. Creaking of walls, frame, especially in the upper range of this grade. Hanging objects swung, in numerous instances. *Disturbed liquids in open vessels slightly*. Rocked standing motor cars noticeably.

V. Felt indoors by practically all, outdoors by many or most: outdoors direction estimated. Awakened many, or most. Frightened few-slight excitement, a few ran outdoors. Buildings trembled throughout. Broke dishes, glassware, to some extent. Cracked windows-in some cases, but not generally. Overturned vases, small or unstable objects, in many instances, with occasional fall. Hanging objects, doors, swing generally or considerably. Knocked pictures against walls, or swung them out of place. Opened, or closed, doors, shutters, abruptly. Pendulum clocks stopped, started, or ran fast, or slow. Moved small objects, furnishings, the latter to slight extent. *Spilled liquids in small amounts from well-filled open containers*. Trees, bushes, shaken slightly.

VI. Felt by all, indoors and outdoors. Frightened many, excitement general, some alarm, many ran outdoors. Awakened all. Persons made to move unsteadily. Trees, bushes, shaken slightly to moderately. *Liquid set in strong motion*. Small bells rang-church, chapel, school, etc. Damage slight in poorly built buildings. Fall of plaster in small amount. Cracked plaster somewhat, especially fine cracks, chimneys in some instances. Broke dishes, glassware, in considerable quantity, also some windows. Fall of knickknacks, books, pictures. Overturned furniture in many instances. Moved furnishings of moderately heavy kind.

VII. Frightened all-general alarm, all ran outdoors. Some, or many, found it difficult to stand. Noticed by persons driving motor cars. Trees and bushes shaken moderately to strongly. *Waves on ponds, lakes, and running water. Water turbid from mud stirred up. In caving to some extent of sand or gravel stream banks.* Rang large church bells, etc. Suspended objects made to quiver. Damage negligible in buildings of good design and built or badly designed buildings, adobe houses, old walls (especially where laid up without mortar), spires, etc. Cracked chimneys to considerable extent, walls to some extent. Fall of plaster in considerable to large amount, also some stucco. Broke numerous windows, furniture to some extent. Shook down loosened brickwork and tiles. Broke weak chimneys at the roof-line (sometimes damaging roofs). Fall of cornices from towers and high buildings. Dislodged bricks and stones. Overturned heavy furniture, with damage from breaking. *Damage considerable to concrete irrigation ditches.*

VIII. Fright general-alarm approaches panic. Disturbed persons driving motor cars. Trees shaken strongly-branches, trunks, broken off, especially palm trees. Ejected sand and mud in small amounts. *Changes: temporary, permanent; in flow of springs and wells; dry wells renewed flow; in temperature of spring and well waters.* Damage slight in structures (brick) built especially to withstand earthquakes. Considerable in ordinary substantial buildings, partial collapse: racked, tumbled down, wooden houses in some cases; threw out panel walls in frame structures, broke off decayed piling. Fall of walls. Cracked, broke, solid stone walls seriously. Wet ground to some extent, also ground on steep slopes. Twisting, fall, of chimneys, columns, monuments, also factory stacks, towers. Moved conspicuously, overturned, very heavy furniture.

IX. Panic general. Cracked ground conspicuously. Damage considerable in (masonry) structures built especially to withstand earthquakes: threw out of plumb some wood-frame houses built especially to withstand earthquakes; great in substantial (masonry) buildings, some collapse in large part; or wholly shifted frame buildings off foundations, racked frames; *serious to reservoirs; underground pipes sometimes broken.*

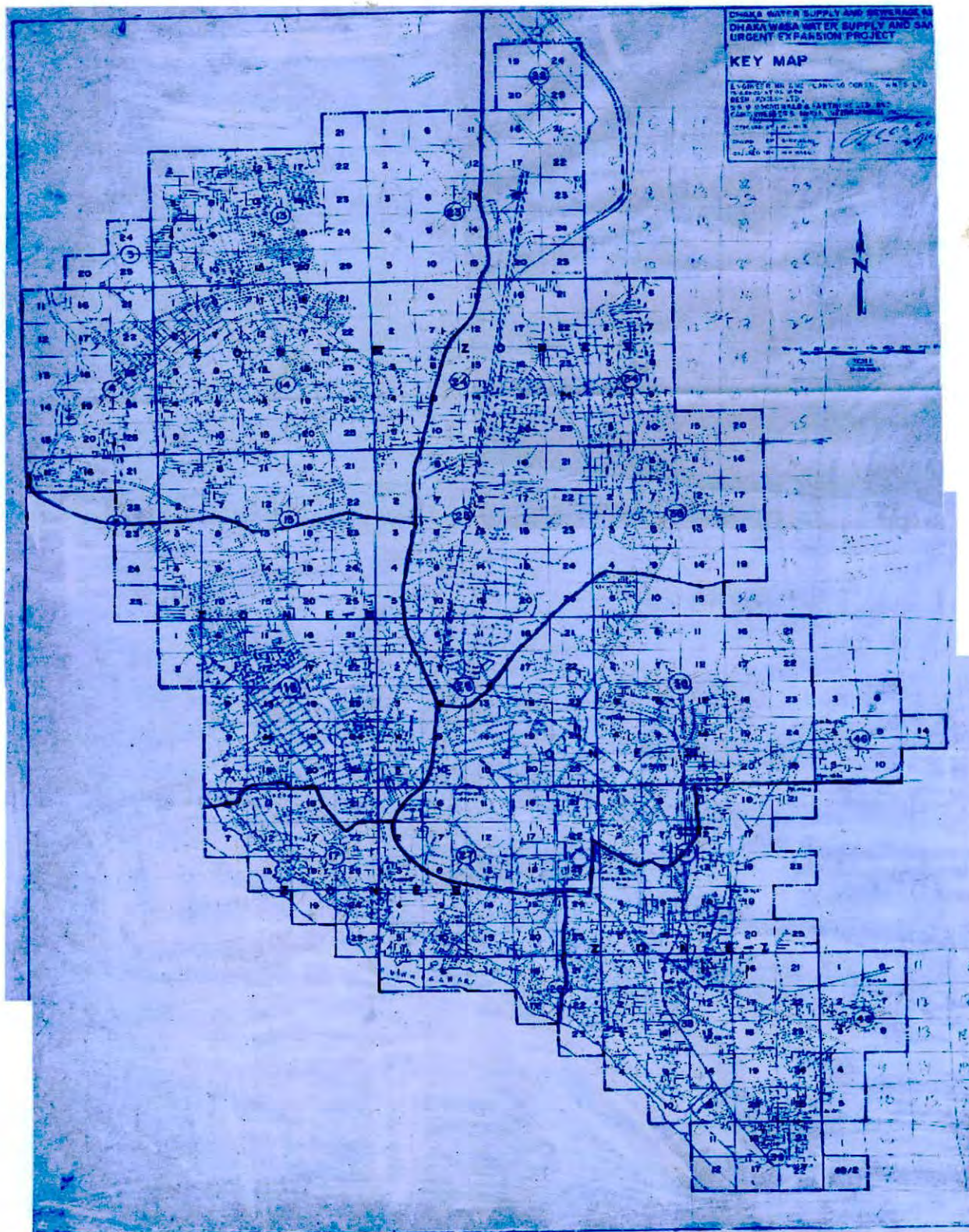
X. Cracked ground, especially when loose and wet, up to widths of several inches; *fissures upto a yard in width ran parallel to canal and stream banks. Landslides considerable from river banks and steep coasts.* Shifted sand and mud horizontally on beaches and flat land. Changed level of water in wells. *Threw water on banks of canals, lakes, rivers, etc.* *Damage serious to dams, dikes, embankments.* Severe to well-built wooden structures and bridges, some destroyed. Developed dangerous cracks in excellent brick walls. Destroyed most masonry and frame structures, also their foundations. Bent railroad rails slightly. *Tore apart, or crushed endwise, pipelines buried in earth.* Open cracks and broad wavy folds in cement pavements and asphalt road surfaces.

XI. Disturbances in ground many and widespread, varying with ground material. Broad fissures, earth slumps, and land slips in soft wet ground. Ejected water in large amounts charged with sand and mud. Caused sea waves ("tidal" waves) of significant magnitude. Damage severe to wood frame structures, especially near shock centres. *Great to dams, dikes, embankments often for long distances.* Few, if any (masonry) structures remained standing. Destroyed large well-built bridges by the wrecking of supporting piers, or pillars. Affected yielding wooden bridges less. Bent railroad rails greatly, and thrust them endwise. *Put pipelines buried in earth completely out of service.*

XII. Damage total-practically all works of construction damaged greatly or destroyed. Disturbances in ground great and varied, numerous shearing cracks. Landslides, falls of rock of significant character, slumping of riverbanks, etc., numerous and extensive. Wrenched loose, tore off, large rock masses. Fault slips in firm rock, with notable horizontal and vertical offset displacements. *Water channels, surface and underground, disturbed and modified greatly. Dammed lakes, produced waterfalls, deflected rivers, etc.* Waves seen on ground surfaces (actually seen, probably, in some cases). Distorted lines of sight and level. Threw objects upward into the air.

Appendix B

Water pipeline networks of Dhaka city (after DWASA, 1993)



Appendix C

Water pipeline networks of Dhaka city (after DWASA, 1991)

